Kawasaki disease related coronary artery aneurysms:

Structural and hemodynamic factors associated

with thrombosis, stenosis and failure to achieve

dimensional normalization

By

Mathew Mathew

A thesis submitted in conformity with the requirements
for a *Master of Science* degree from
The Institute of Medical Science,
The University of Toronto (2020)

Mathew Mathew
Master of Science thesis, 2020

The University of Toronto
Institute of Medical Science

Thesis Title: Kawasaki disease related coronary artery aneurysms: Structural and hemodynamic factors associated with thrombosis, stenosis and failure to achieve dimensional normalization

Abstract

Coronary artery (CA) aneurysms are potential sequelae of Kawasaki Disease (KD) that may require long-term follow-up and medical management. Current KD clinical guidelines calibrate treatments based on risk stratification criteria that consider patients' maximum and current CA aneurysm dimensions. Despite these criteria, patient outcomes at the highest risk-strata are variable, and multiple management strategies may be considered. This study evaluates structural and hemodynamic features of CA aneurysms for associations with thrombosis, stenosis and failure to achieve dimensional normalization using epidemiological data and computational fluid dynamic simulations. Findings suggest greater risk for negative outcomes in CA aneurysms of the right main and left anterior descending coronary arteries; of saccular shape, larger cross-sectional area and lower wall-shear stress; with branches involving the left main bifurcation, multiple CA aneurysms and higher recirculation times. Current risk stratification criteria may benefit from considering these features secondarily to CA aneurysm z-scores.

Contributions

Overarching

Mathew Mathew │ The Hospital for Sick Children │ M.Sc. Candidate

- Literature review
- Project planning and management
- Writing protocol, funding, REB applications, and thesis
- Negotiations with intra- and inter- hospital staff for training and data acquisition

Brian McCrindle │ The Hospital for Sick Children │ Supervisor

- Provided guidance for all aspects of the project.

Cedric Manlhiot │ The Hospital for Sick Children

- Provided statistical advice as well as feedback for the project protocol, feasibility and grant applications.

Sunita O'Shea │ The Hospital for Sick Children

- Helped with Research Ethics Board (REB) application and approval process.
- Helped obtain access to numerous SickKids patient data systems.

David Steinman │ The University of Toronto │ Advisory Committee Member

- Provided feedback on the final thesis and the thesis defence presentation.
- Facilitated the introduction between SickKids and Stanford collaborators.

Rae Yeung │ The Hospital for Sick Children │ Advisory Committee Member

- Provided feedback on the final thesis and the thesis defence presentation.

Objective 1

Mathew Mathew │ The Hospital for Sick Children │ M.Sc. Candidate

- Contributed to IKDR database design
- Managed and adjudicated IKDR data
- Trained and supervised summer students on data collection
- Validated echocardiography data from reports
- Screened and defined study cohort

- Characterization of aneurysm structural features from imaging data

- Data interpretation

- Data preparation for statistical analyses

- Simple statistical analyses

Brian McCrindle │ The Hospital for Sick Children │ Supervisor

- Provided access to the International Kawasaki Disease Registry (IKDR) and facilitated data collection and validation by providing access to summer students and endorsing contact with IKDR primary investigators.

Cedric Manlhiot │ The Hospital for Sick Children

- Conducted the complicated statistical testing required for this project objective.

- Provided feedback on data quality issues.

Pedrom Farid, Christian Delayun, Justin Kritzinger, Georgina Eagleson, and Shaili Perez.

- Summer students who worked on extracting and transcribing the majority of the data from over 10,000 echocardiogram reports.

Objective 2

Mathew Mathew │ The Hospital for Sick Children │ M.Sc. Candidate

- Screened and defined study cohort

- Obtained funding for

- Obtained imaging and clinical data from various databases

- Helped with 3D anatomic modeling

- Data interpretation

- Simple statistical analyses

Noelia Gutierrez │ Stanford University │ Collaborator

- Provided training on using the SimVascular image processing software and guidance for 3D anatomic modeling.

- Conducted the hemodynamic simulations and post processing from provided data to obtain measures for the hemodynamic variables of interest.

- Provided education on the computational fluid dynamic methodologies used by Stanford collaborators.

Alison Marsden │ Stanford University │ Collaborator

- Provided oversight for the hemodynamic simulations.
- Provided the computational resources required to conduct the simulations.

Prashob Porayette │ The Hospital for Sick Children

- Provided training on navigating and interpreting cardiac MRIs, Cardiac CTs, Echocardiograms and conventional angiograms as well as the respective SickKids hospital systems.

Sunder Devadas│ The Hospital for Sick Children

- Facilitated MRI, CT and angiographic data acquisition.

Sunita O'Shea│ The Hospital for Sick Children

- Negotiated contracts between Stanford University and SickKids.

David Steinman │ The University of Toronto │ Advisory Committee Member

- Provided education on computational fluid dynamics
- Provided statistical advice for objective 2.

Acknowledgments

Table of contents   Page

Chapter 4: Conclusions

List of Abbreviations

AR	Aortic Valve Regurgitation
ASA	Acetylsalicylic Acid (Aspirin)
A$_{WSS1}$	Area with Wall Shear Stress less than 1 Dyne/Cm^2
BSA	Body Surface Area
CA	Coronary Artery
CABG	Coronary Artery Bypass Graft
CFD	Computational Fluid Dynamics
CMRI	Cardiac Magnetic Resonance Imaging
CRP	C-Reactive Protein
CTA	Computed Tomography Angiography
DN	Dimensional Normalization
HDL	High Density Lipoprotein
IVIG	Intravenous Immunoglobulin
IVMP	Intravenous Methyl Prednisone
IVUS	Intravascular Ultrasound
KD	Kawasaki Disease
LAD	Left Anterior Descending Coronary Artery
LCA	Left Main Coronary Artery
LCX	Circumflex Coronary Artery
LDL	Low Density Lipoprotein
LMP	Luminal Myofibroblastic Proliferation
LMWH	Low Molecular Weight Heparin
LPN	Lumped Parameter Network
MACE	Major Adverse Cardiac Event
MI	Myocardial Infarction
NA	Necrotizing Arteritis
IKDR	International Kawasaki Disease Registry
OSI	Oscillatory Shear Index

PCI	Percutaneous Coronary Intervention
RBC	Red Blood Cell Count
RCA	Right Main Coronary Artery
RT$_{branch}$	Coronary Artery Branch Recirculation Time
SA/C	Subacute/Chronic Vasculitis
SickKids	The Hospital for Sick Children
TAWSS	Time Averaged Wall Shear Stress
TEE	Transesophageal Echocardiography
VSMC	Vascular Smooth Muscle Cell
vWF	Von Willebrand Factor
WBC	White Blood Cell Count
WSS	Wall Shear Stress

List of figures   Page

List of tables

Chapter 1: Background

1.1 Overview

Kawasaki disease is a self-limited, febrile vasculitis of unknown etiology that predominantly affects children >5 years of age. Due to the lack of definitive tests, diagnosis relies on identifying a constellation of clinical findings, while excluding clinically similar diagnoses with known causes. Unfortunately, this can result in delayed treatment or missed diagnosis, increasing the risk for coronary artery aneurysms (CA aneurysms), the primary adverse outcome of KD. In fact, the illness is considered the leading cause of acquired heart disease in children of the developed world. A subset of patients with CA aneurysms could experience further morbidity or mortality due to myocardial ischemia or infarcts resulting from coronary artery (CA) thrombosis or stenosis. Consequently, the recently published American Heart Association guidelines for the diagnosis, treatment and long-term management of KD includes algorithms for increased accuracy and reliability of KD diagnosis; additional therapies for IVIG-refractory patients; and better stratification of long-term risk using body-surface area (BSA) adjusted Z-scores of maximum CA lumen diameter. These Z-scores allow us to contrast a patient's CA diameters with the CA diameters of a normal patient of similar body size. The long-term thromboprophylactic management of patients with CA aneurysm's following KD is based on a patient's maximum and current CA Z-scores with specific medical recommendations for instances of thrombosis and stenosis. These criteria are mostly based on expert clinical opinion and empirical evidence. Recent collaborative efforts such as the International Kawasaki Disease Registry (IKDR), as well as advances in computational fluid dynamic technologies afford clinical researchers novel avenues to broaden current understanding of negative outcomes in patients with CA aneurysms post KD. Such studies could help refine risk stratification and long-term medical management strategies for these patients. The current study aims to correlate the structural and hemodynamic features of coronary arteries and aneurysms with risk for negative outcomes such as thrombosis, stenosis and failure to achieve dimensional normalization in patients with persisting CA aneurysms post KD.

1.2   Epidemiology of Kawasaki Disease

1.2.1 History

In 1967, Tomisaku Kawasaki first described a constellation of symptoms associated with a "unique clinical entity" that he dubbed Mucocutaneous Lymph Node Syndrome[1]. During the early 1970's, a link between this syndrome and coronary artery vasculitis was well established and the disease became commonly known as Kawasaki disease (KD)[2]. The earliest suspected case of KD occurred in 1871, confirmed by an autopsy report revealing thrombosed CA aneurysms in a 7-year-old boy diagnosed with "scarlatinal dropsy"[3]. Since then, good clinical records consistently described incidences of systemic vasculitis resulting in death via thrombosed CA aneurysms, the classic pathology of fatal KD [4, 5]. Kushner *et al.* described how KD had masqueraded as atypical cases of illnesses involving a fever or rash such as acrodynia, Steven-Johnson syndrome, scarlet fever, acute rheumatic fever or infantile polyarteritis nodosa[5].

1.2.2 Incidence and Genetic Susceptibility

Presently, the diagnosis for KD has been reliably described, and its incidence noted worldwide, where affected males outnumber females by ~1.5:1[6-12]. In Japan, KD affects 308.0 per 100,000 children <5 years old[13], a markedly higher incidence compared to other developed countries like South Korea[14], Taiwan[15], the United States[16], Canada[17] or Europe[10] (199.7, 82.8, 20.8, 19.6 and 4.9-15.2 per 100,000 children <5 years old respectively). Epidemiological data from Hawaii also suggest that children of Japanese ancestry are more susceptible to KD when compared to Caucasians of similar age (210.5 vs. 13.7 per 100,000 children <5 years old) [18]. A similar trend is noted when comparing KD recurrence rates using surveillance data from the United States (1984 – 2008) and Japan (2001 – 2002). The rate of recurrent KD in the US was 1.7%, but increased to 3.5% in Asian and Pacific Islander patients; the same rate observed in Japan (3.5%)[19]. Nakamura *et al.* reported that the risk of developing CA sequelae was higher for a recurrent case of KD when compared to the patient's index case, regardless of prior CA aneurysms. The above studies suggest a strong genetic predilection for Kawasaki disease.

Surveillance data from Japan (1995 – 1996) revealed that ~1% of KD patients had a positive family history[20]. During the epidemic year of 1982, the overall incidence for children <4 years of age was 0.19%, but the incidence for second-case onset in families with more than one child was 2.1%, a ~11-fold increase in relative risk[21]. More than half of these second cases occurred within 10 days of the index case, while all occurred within a year. Furthermore, various twin studies have a demonstrated that twins can have very similar progression of KD with the risk of concordance (temporal and clinical) being as high as 14%[22-25]. These studies support the notion that the pathogenesis of KD involves genetic susceptibility and an environmental trigger.

1.2.3 Environmental Trigger

There have been multiple epidemiological studies aimed at elucidating this environmental trigger which has predominantly been hypothesized as being of infectious nature. This hypothesis is supported by multiple spatial and temporal clustering analyses[26-28] as well the common co-occurrence of KD and infectious symptomology[29, 30]. At the global level, incidence rates of KD in the extratropical regions of the northern hemisphere demonstrate a bimodal seasonality which peaks in the winter and drops in the late summer and fall[31]. Although this pattern is consistent with various pediatric bacterial and viral infections, it has not been noted in the tropics or the southern hemisphere. Furthermore, temporal clustering of geographically unrelated cases does not reflect the person-to-person spread that is typical of infectious diseases[28]. Viral and bacterial cultures from KD patients have failed to identify a consistent infectious entity[32, 33] and there is no known agent with a global distribution pattern similar to KD[34]. These inconsistencies suggest that KD could be triggered by multiple infectious agents[27, 30, 35].

An alternative hypothesis suggests that infectious agents and environmental factors influence, over time, a child's susceptibility to develop KD when encountering the disease trigger[36]. The concept is supported by noted consistencies between risk factors for KD and the *hygiene hypothesis*[37], where lack of early-life exposure to microbial agents can increase the risk of allergic disease[38], which in turn is also associated with

increased risk of Kawasaki disease[39, 40]. Additionally, epidemiological analyses correlating tropospheric wind currents originating from north-eastern China with incidence of KD in Japan, Hawaii and San Diego suggest a wind-borne trigger[41, 42].

1.2.4 Epidemiology of Clinical Outcomes

On the outcomes side of the KD discussion, a case fatality rate of 0.015% was noted in Japan between 2011 and 2012[43]. Peak mortality occurs at 15 to 45 days post fever onset, possibly due to the concomitant CA vasculitis, elevated platelet count and hypercoagulable state[44]. In the long-term, Japanese patients with CA sequelae were determined to have an increased risk of mortality when compared to the general Japanese population (Standardized Mortality Ratio, 1.86; 95% CI, 1.02-3.13)[45] and virtually all KD related deaths are due to CA aneurysms[46, 47]. These studies highlight the importance of long-term follow-up of patients who develop cardiac sequelae post KD. This is further emphasized when considering that many cases of myocardial ischemia and infarctions in young adults have been attributed to "missed" episodes of childhood KD[48]. In San Diego, ~5% of all adults <40 years of age, with suspected myocardial ischemia, were confirmed to have KD related coronary artery lesions[49].

1.3   Pathology of Kawasaki Disease

1.3.1 Pathogenesis

Over 50 years since its first description, the etiology of KD is still debated. Early studies suggested that a bacterial superantigen was responsible for the triggered immune cascade associated with KD[50, 51], but a related prospective multicenter study did not support this hypothesis[32]. Subsequent studies describe an oligoclonal response to a classic antigen, with immunoglobulin A (IgA) playing a critical role[52, 53]. Fanco *et al.* suggest that the classic antigen conveys a protective effect against future exposure to the pathogen in most cases[54], hence the low rates of recurrence and the self-limiting nature of KD. A more recent hypothesis suggests infection via a novel RNA virus that enters through the upper respiratory tract[55, 56]. It is possible that all of the above finding are

associated with the KD pathogen, which may also be influenced by environmental effects and genetic susceptibility, contributing to the difficulty of identification.

1.3.2 Vasculitis and the Coronary Arteries

Kawasaki disease is characterized by a self-limited, systemic vasculitis: inflammation of all medium sized arteries, affecting multiple tissues and organs during the acute phase. Systemic clinical findings include: Joints (arthritis), liver (hepatitis), lungs (interstitial pneumonitis), gastrointestinal tract (abdominal pain, vomiting, diarrhea, gallbladder hydrops), meninges (aseptic meningitis, irritability), heart (myocarditis, pericarditis, valvulitis), urinary tract (pyuria), pancreas (pancreatitis) and lymph nodes (lymphadenopathy)[47]. Nevertheless, inflammation predominantly affects the coronary arteries and results in some of the most important clinical outcomes, CA aneurysms. Aneurysms refer to the ballooning of a segment of a vessel that leads to abnormal function and flow within that segment. The formation of any aneurysm involves the damaging or weakening of the vessel wall. Arterial vessel walls consist of multiple layers that enclose the "lumen", the space where blood flows. The outermost layer is the adventitia followed in order by the external elastic lamina, media, internal elastic lamina, intima and the innermost endothelium. Predominantly, the adventitia is composed of collagen; the media of vascular smooth muscle cells (VSMC); the intima and endothelium of endothelial cells. The external and internal lamina are of elastic fibers collectively known as the elastica.

1.3.3 Pathology of Coronary Artery Aneurysms

Orenstein *et al.* described a model of KD arteriopathy that has important implications for the long-term management of patients with CA sequelae following KD[57]. They developed their model from histological analysis of 48 KD related CA aneurysm samples studied under light and transmission electron microscopy. The model consists of 3 distinct pathological processes. The first, Necrotizing Arteritis (NA), is an acute self-limiting process that is completed within 2 weeks of fever onset. A synchronized

neutrophilic process of the luminal endothelium, NA progressively destroys the arterial wall into the adventitia resulting in acute phase CA aneurysms. The second process is a subacute/chronic vasculitis (SA/C) beginning within 2 weeks of fever onset, but can continue for months to years. Infiltration of macrophages, eosinophils, lymphocytes and plasma cells commenced in the adventitial vaso vasorum and progressed luminally. The accompanying tissue damage is highly variable and dependent on the degree of SA/C inflammation. The process is responsible for the continued progression of CA aneurysms and likely causes the transition of medial and adventitial smooth muscle cells into classic myofibroblasts giving rise to the third process called Luminal Myofibroblastic Proliferation (LMP). Subacute/chronic vasculitis coupled LMP (an intra-luminal process) may result in luminal stenosis due to the inflammation and various matrix products associated with myofibroblasts, whose circulating factors might cause remote LMP. Neither granulomatous inflammation nor granulomas were detected. There was no smooth muscle cell hyperplasia and minimal medial fibrosis.

1.3.4 Pathology and Primary Outcomes

Pathological outcomes for coronary artery sequelae are dependent on the severity of the damage caused to the arterial wall and the impact of hydrostatic forces, influencing the diameter of the aneurysms formed. From a hemodynamics perspective, CA aneurysms with larger vessel diameters have decreased flow velocity as predicted by the calculation of Reynolds number. This results in areas with a lower wall-shear stress and increased turbulent flow regardless of any other structural features associated with the aneurysm. The implications of these abnormal hemodynamics will be explored in later sections. With regards to the CA vessel wall, larger more saccular aneurysms usually result from significant NA that has destroyed the intima, media and elastica interna, sometimes with extension into the adventitia[57]. These layers of the vessel wall may not be regenerated to be physiologically normal. As such, one may speculate that these CA aneurysms may undergo a less significant LMP process due to the lack of medial SMCs. Large fusiform aneurysms could represent a less severe acute NA with substantial SA/C. These CA

aneurysms could have a partially preserved media that could undergo a more significant LMP process. Small CA aneurysms and dilated arteries nearly always resolve with time. Large CA aneurysms may appear to be "resolving" or "regressing" as the size of their lumen decreases. This decrease is not likely a result of regeneration or remodelling of the vessel wall, rather, it may be due to the LMP process or organized thrombosis, both of which will be discussed in the CA aneurysm focused section of this thesis. Consequently, a distinction should be made between true versus apparent regression or resolution of a CA aneurysm. These terms should only refer to aneurysms or dilations whose vessel wall functions were preserved or restored following the KD related arteriopathic processes described above. This thesis postulates the use of a new term, "Dimensional Normalization", to address the incidence of a CA aneurysm's luminal diameter returning within range of normal parameters. Dimensionally normalized CA aneurysms, or those in the process of dimensional normalization, may have persistent vessel wall dysfunction, such as the continuation of the LMP process which could result in progressive stenosis. It is possible that dimensionally normalized CA aneurysms pose additional long-term risks that are presently unknown[58, 59]. Figure 1, taken from the 2017 American Heart Association guidelines[47] succinctly summarizes the pathology and outcomes of KD related coronary artery aneurysms.
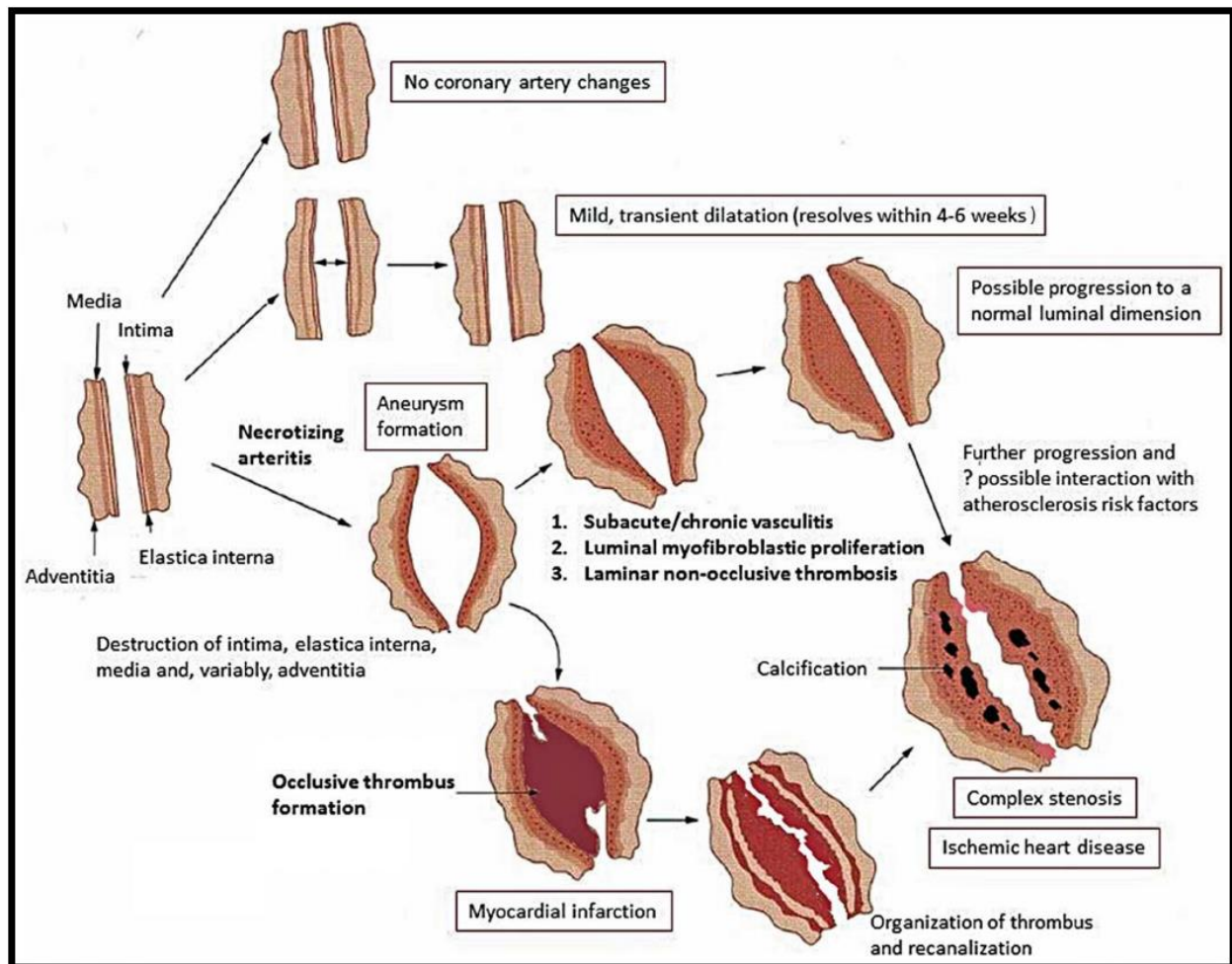
Figure 1. Natural history of KD related coronary artery abnormalities. Taken from the 2017 American Heart Association guidelines[47, 60]

1.4   Diagnosis

1.4.1 Complete and incomplete Kawasaki Disease[47, 61]

Kawasaki disease is diagnosed via a constellation of signs and symptoms. Principal clinical findings based on epidemiological case definition include fever (temperature > 38⁰C), rash (maculopapular, diffuse erythroderma, or erythema multiform-like), conjunctivitis (bilateral, bulbar and without exudate), cervical lymphadenopathy (≥1.5cm diameter), oral changes (Erythema and cracking of lips, strawberry tongue, and/or erythema of oral and pharyngeal mucosa) and extremity changes (Erythema and edema of the hands and feet in acute phase, and/or erythema of oral and pharyngeal mucosa). Complete KD (also referred to as classic or Typical KD) is diagnosed in patients who meet the case definition based on sufficient principal clinical findings. The classic case definition requires ≥5 day's history of fever and the presence of ≥4 of the 5 other principal clinical findings. Experienced physicians who have treated multiple KD patients may make the diagnosis in as little as 3 days from fever onset. However, an early diagnosis is not always possible since not all the clinical features present at a single time point, but may manifest over time. Conversely, some clinical features may have abated early and careful review is required to establish a diagnosis, particularly in patients who present with ≥1 week's history of fever. Due to the lack of pathognomonic tests, patients who do not meet the requirements for the case definition may still be diagnosed with Incomplete KD. Other clinical, laboratory and imaging findings may also support a diagnosis of incomplete KD.

1.4.2 Cardiovascular findings

Cardiovascular complications are the major cause of morbidity and mortality in patients with KD. Inflammation of the pericardium, myocardium, endocardium and coronary arteries can be prominent during the acute phase. At this time, electrocardiography may show arrhythmia and functional abnormalities involving the atrioventricular and sinus nodes, suggesting myocardial or pericardial involvement[62]. Malignant arrhythmias are rare, but may be indicative of myocarditis or myocardial

ischemia[63, 64]. Conversely, myocarditis occurs frequently in acute KD and is extensively appreciated on reports of acute phase myocardial biopsies[65]. In fact, a recent histopathological investigation by Harada *et al.* demonstrated that myocarditis develops before coronary artery abnormalities, and was not associated with ischemic damage[66]. Kawasaki disease-related acute myocarditis readily responds to steroid treatment, and any associated acute left ventricular (LV) dysfunction is transient, unlike late onset LV dysfunction that may result from coronary insufficiency and/or myocardial fibrosis[67]. McCrindle *et al.* suggest that KD associated myocarditis responds as such because it is limited to interstitial edema and inflammation, and not myocyte necrosis[47].

The exception to this mild, short-term myocardial dysfunction is the KD shock syndrome which is often misdiagnosed as toxic or septic shock[68]. KD shock syndrome is associated with cardiovascular collapse and hypotension, affecting ~7% of KD patients[69]. On presentation, a diagnosis of KD may be considered for all such cases, if fever persists despite negative bacterial cultures[47]. KD shock syndrome is also associated with IVIG resistance, more-severe laboratory markers of inflammation, coronary artery aneurysms and mitral regurgitation[69]. Kawasaki disease-related acute mitral regurgitation was shown to have a consistent incidence rate of ~25%, with mostly mild to rarely moderate severity that did not persist on follow-up, according to a large multicenter American study[67]. Aortic regurgitation was much less common, affecting ~1% of patients, however, it was also associated with coronary artery dilation.

Clinically, CA involvement is defined based on the maximal luminal dimensions of the 4 main branches as determined by echocardiogram assessment. Muniz *et al.* found that the mean acute CA dimensions in children with KD were greater than those of patients with other febrile illnesses, while both were increased compared to normative afebrile controls[70]. As such, CA abnormalities are considered a key finding for the diagnosis of KD, especially for clarifying a diagnosis of incomplete KD. Newburger *et al.* determined that the prevalence of CA aneurysms appears to be a little over 20%, which can be reduced to 4% with prompt IVIG treatment[71, 72]. Evidence also suggests that CA abnormalities detected on baseline echocardiograms obtained within 10 days of illness,

predict further CA involvement in ~80% of patients with significant findings[73]. Patients with severe coronary artery involvement may develop aneurysms in other medium sized arteries as well, including the axillary, subclavian, brachial, femoral, iliac, splanchnic and mesenteric arteries; especially around the branching points[47]. The pathology of these arteries is probably similar to that of the CAs and can progress towards similar outcomes of rupture, thrombosis or stenosis. However, such outcomes are rare at these sites, and not usually associated with clinical signs, symptoms or sequelae because collateralization is common[47].

1.5   Coronary Artery Aneurysm Assessment

1.5.1 Anatomy of Coronary Arteries

The CAs are an epicardial vascular system of small and medium vessels responsible for supplying the heart muscle with oxygenated blood. Their ostia (origin) stem from the left and right sinuses of Valsalva at the aortic valve, giving rise to a left and right system. The right main (RCA), left main LCA), left anterior descending (LAD) and circumflex (LCX) coronary arteries are medium vessels considered to be the most important of the coronaries, as they serve as the ostia for a host of other vessels. In some instances, a third coronary artery arises from the aortic valve, while there also exist rare instances of 4 coronary arteries[74]. The right system consists of the RCA and its associated vessels, while the left system begins with the LCA that bifurcates into the LAD and LCX. Trifurcation of LCA is noted in ~20% of the population, giving rise to the ramus intermedius branch of the left coronary system[75]. The patient-specific CA anatomy can affect coronary circulation and residual blood-flow through collaterals, serving as a prime determinant for myocardial ischaemic/reperfusion injury and cardio-protection[76].

The posterior descending artery is another important vessel that supplies the posterior third of the interventricular septum and is used to determine coronary dominance. Approximately 70% of people have a right dominant system, where the posterior descending artery is supplied by the RCA[77]. In left dominant systems (10% of population) the posterior descending artery is supplied by the LCX while in co-dominant

systems (20% of population) it is supplied by both the RCA and the LCX. A CA branch that supplies the posterior descending artery will have larger luminal diameters than normal to accommodate increased blood-flow and volume. Figure 2 provides a schematic summary of the general coronary artery anatomy, but it is important to keep in mind that there are a number of other congenital CA abnormalities, defined with regards to their anomalous anatomy, histology and pathology[78].
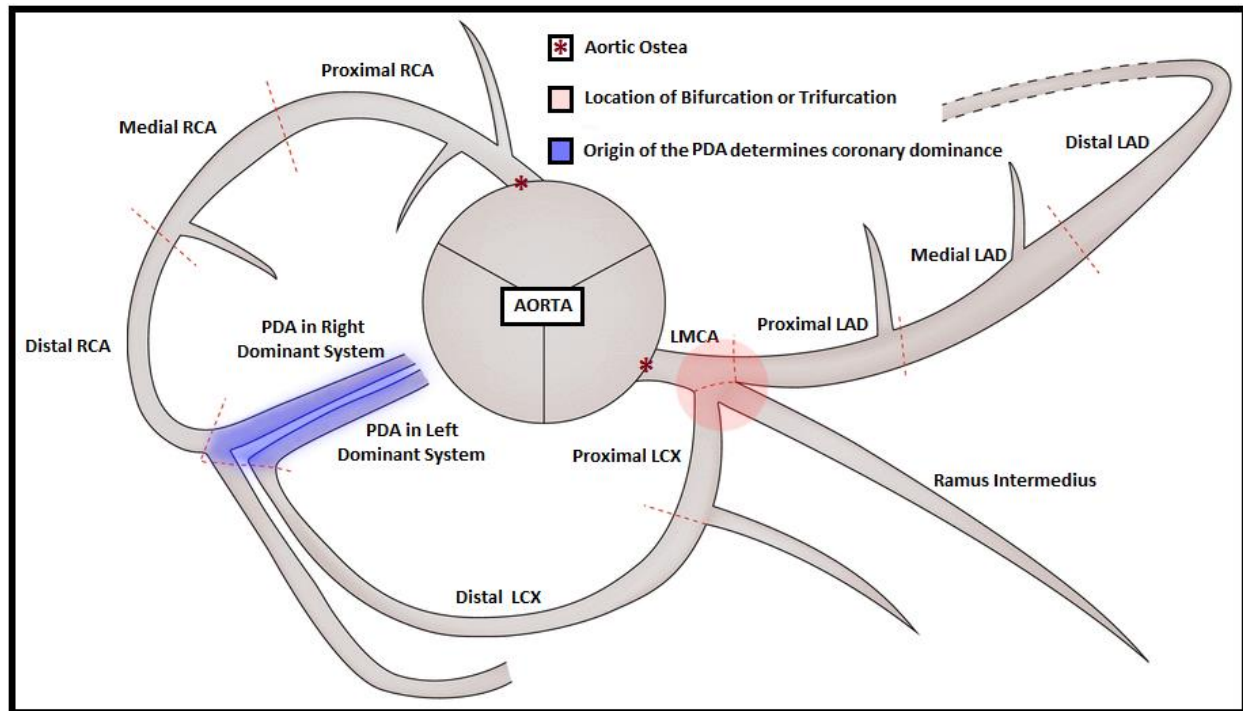
Figure 2. Axial view schematic of the typical coronary artery anatomy. Modified from Seon *et al.* [79]

Figure 3. Average median Wall Shear Stress (WSS) value per coronary artery segment – Modified from Starikov *et al.*[80]

Figure 2: PDA = Posterior Descending Coronary Artery
Figure 3: LMCA, LAD, LCX, RCA = 4 main coronary arteries; Suffix = Proximal, Medial and Distal segments

P a g e | 12
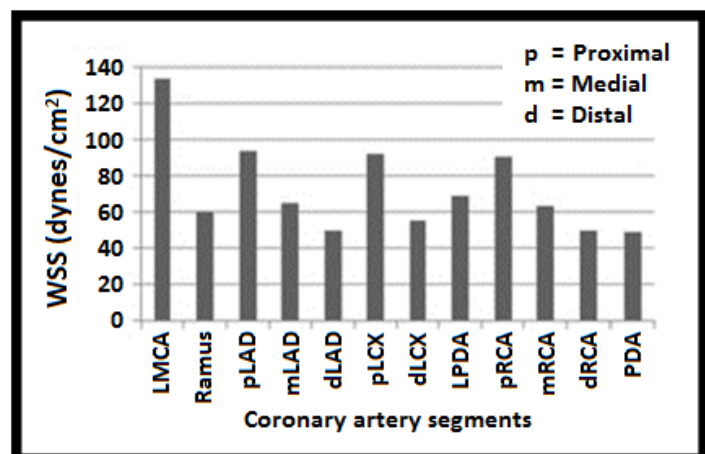
Coronary artery hemodynamics have been evaluated for the standard Left-dominant system. Wall-shear stress (WSS) is a hemodynamic vector that measures the force acting on a point on the vessel wall, by the blood, in the direction of blood-flow. For cardiology purposes, the WSS vectors are usually surmised over a cardiac cycle and presented in the form of a "time-averaged" WSS (TAWSS). In the case of laminar blood-flow of the coronary arteries, the WSS vectors are aligned with the TAWSS vectors throughout the cardiac cycle. This alignment is characterized by a dimensionless measure called the Oscillatory Shear Index (OSI). An OSI at or very close to zero indicates laminar blood flow, while a value of 0.5 represents purely oscillatory flow. With respect to coronary anatomy and function, a higher OSI (more oscillatory flow) may be considered a surrogate, albeit imperfect, measure for turbulent blood-flow within these arteries[81]. Particle recirculation time, is a measure of how much time a particle of interest spends within a particular circuit. For the coronary arteries, the 4 main branches serve as 4 circuits for particles of blood, where the particle residence time is measured in number of cardiac cycles. Longer particle residence times can serve as a surrogate measure of blood-flow stasis and pooling.

The WSS is highly variable based on the coronary artery branch and the distance from their respective ostia, but generally decreases distally while being significantly higher in the LCA than the RCA, LAD or LCX (Fig.3)[80]. Wall-shear stress can also spike around the bifurcations of the different arteries, especially where the LCA bifurcates into the LAD and LCX[82]. Flow velocities can also differ between the different coronary arteries. The LCA has the highest flow velocity with the RCA being the lowest and the LAD and LCX being equivalent[83, 84]. The above variations have considerable implications for perfusion defects and outcomes involving pathological obstruction of the coronaries arteries, as well as for systems that attempt to define CA anatomy in the general population such as normalized values for luminal dimension. These implications will be explored in later sections.

1.5.2 Prevalence of Coronary Artery Aneurysms

Early reports on the incidence of KD related CA aneurysms varied greatly due to the subjectivity of assessments predating standard echocardiography and IVIG treatment[47]. In 1984, the Japanese Ministry of Health released criteria for the quantitative definition of coronary artery aneurysms based on the maximum luminal diameter of the 4 major CAs. A strict clinical trial was developed based on these criteria, and revealed that 23% of patients with complete KD, who only receive aspirin; and 8% with aspirin and 4-day low-dose IVIG developed coronary artery abnormalities at 2 weeks[71]. A follow up trial showed that the 2-week prevalence of KD related CA abnormalities could be reduced to ~4% if patients were promptly treated with a single high dose (2gm/kg) of IVIG. Newer criteria for CA aneurysm assessments use BSA-adjusted Z-scores for the maximal luminal diameters and define thresholds that also capture most dilations, increasing the apparent prevalence of CA aneurysms. This is demonstrated in a later trial that defined CA aneurysms based on the minimum cut-off values from the Japanese Ministry of Health and Z-score criteria (Table 2 and Table 3 respectively). The study evaluated the use of single-dose methylprednisolone in addition to high-dose IVIG and showed that the 1-week prevalence of CA aneurysms was 30% regardless of treatment group. The prevalence of CA aneurysms further increases if one considers dilations under the minimum cut-off values, whose maximum luminal dimension significantly decreased on follow-up[85]. The above studies describe the incidence of KD related CA aneurysms in strictly defined study populations. However, late presentations, missed diagnoses, delayed treatment, IVIG resistance and could all increase the risk and severity of KD related CA abnormalities[47].

1.5.3 Risk Stratification

Presently, there exist two separate systems for stratification of clinical management and risk of negative outcomes in patients with coronary artery aneurysms following acute Kawasaki disease. Both criteria are applicable to echocardiographic measurements and use maximum luminal dimension to define CA aneurysms as one of 3 categories: small, medium or large aneurysms. They differ in their use of luminal dimensions where one system uses absolute measurements while the other uses BSA-adjusted standard scores. Current American Heart Association guidelines stratify medical management and risk using both absolute measures and Z-scores as shown in Table 1.

Table 1. Risk stratification of coronary artery abnormalities during follow-up Taken from 2017 AHA guidelines[42]

Classification	Description
1	No involvement at any timepoint (Z score always <2)
2	Dilation only (Z score 2 to <2.5)
3	Small aneurysm (Z score ≥2.5 to <5)
3.1	Current or persistent
3.2	Decreased to dilation only or normal luminal dimension
4	Medium aneurysm (Z score ≥5 to <10, and absolute dimension <8 mm)
4.1	Current or persistent
4.2	Decreased to small aneurysm
4.3	Decreased to dilation only or normal luminal dimension
5	Large and giant aneurysm (Z score ≥10, or absolute dimension ≥8 mm)
5.1	Current or persistent
5.2	Decreased to medium aneurysm
5.3	Decreased to small aneurysm
5.4	Decreased to dilation only or normal luminal dimension

The Japanese Ministry of Health first published guidelines for the classification of coronary artery aneurysms over 30 years ago. Since then, there has been little change in their definitions regarding aneurysms, with a continued focus on thresholds of absolute luminal dimension using different criteria based on patient age (Table 2)[86]. Currently, this system is used to define most KD related CA aneurysm statistics in Japanese studies, although it is difficult to track progression over time due to the lack of a continuous measure that is not adjusted for patient size. Furthermore, the inclusion of age does not completely account for the fact that coronary artery dimensions naturally increase with body size. A 3-month-old patient with a 5mm CA aneurysm has a much higher thrombotic risk than a 14-year-old patient with the same dimensions[47].

Table 2. Japanese ministry of health criteria for CA aneurysm

Small aneurysms or dilations
Maximum luminal diameter ≤4 mm.
In patients ≥5 years of age, a maximum luminal diameter of <1.5 times that of an adjacent segment.
Medium aneurysms
Maximum luminal diameter from >4 mm to <8 mm.
In patients ≥5 years of age, a maximum luminal diameter between 1.5 and 4 times that of an adjacent segment.
Giant aneurysms
Maximum luminal diameter ≥8 mm.
In patients ≥5 years of age, a maximum luminal diameter >4 times that of an adjacent segment.

In 1998, De Zorzi *et al.* showed that the body surface area (BSA) adjusted coronary artery luminal dimensions for some patients considered "normal" under Japanese Ministry of Health criteria, were actually larger than expected for the acute, convalescent and late phases when compared to established references for body size[87]. This raised concerns that use of Japanese Ministry of Health criteria may result in underdiagnoses and underestimation of the true prevalence of KD related CA aneurysms[88]. Ensuing studies demonstrated similar results in a Japanese and Singaporean patient cohorts[89, 90], spurring the development Z-score methods for normalizing coronary artery luminal dimension in KD patients. Standard scores (Z-scores) are statistical constructs used to define observed values with respect to their expected values in the general standardized population where the scores represent the number of standard deviations from the mean. A Z-score of ≥2.5 in any coronary artery branch would be expected to occur in ~0.6% of the general population, while a similar Z-score in 2 coronary artery branches would be expecting in ~0.1%, implying a threshold for sensitivity and specificity of CA aneurysm discernment. After adjusting for BSA based on regression models, such methods allow for standardization as a continuous measure[91] within a classification scheme[92], facilitating temporal and geographical comparisons[93]. However, these studies were based on a limited number of patients, and did not provide normative values for the left circumflex coronary artery. Kobayashi *et al.* were the first to develop a rigorous methodology using a different but larger patient population and a lambda-mu-sigma regression analysis that allowed calculation of values for all 4 main CA branches. Dallaire *et al.* developed an

equally rigorous system using a square-root function to fit BSA[94]. The 2017 American Heart Association guidelines for the diagnosis, treatment and long-term management of Kawasaki disease does a good job of summarizing the key differences between these different systems (Table 3).

Table 3. **Z-score methods for normalizing coronary artery lumen dimensions – Modified from the 2017 American heart Association guidelines[47]**

	De Zorzi et al	McCrindle et al	Olivieri et al	Kobayashi et al	Dallaire et al
Year of publication	1998	2007	2009	2009	2011
Number of subjects	89	221	432	5344	1036
Country	USA	USA	USA	Japan	Canada
Regression method for fitting BSA	Linear	Exponential	Logarithmic	LMS	Square root
BSA calculation method	N/a	N/a	Duboi	Dubois	Haycock
Values for the left circumflex	No	No	No	Yes	Yes

A 2018 study by Ogata *et al.* was conducted on ~1000 patients from American and Japanese hospitals that allows for a comparison of the Kobayashi and Dallaire Z-scores [93]. The Dallaire equations identified CA aneurysms in a greater number of patients than the Kobayashi ones. The study also showed that CA aneurysms Japanese children were more likely to develop CA aneurysms from KD when compared to their American peers regardless of controls for young age, male sex, late treatment and IVIG resistance. These results, when taken in conjunction with previously described variations in coronary artery anatomy, suggests that there are various factors and considerations that need to be accounted for with regards to defining CA aneurysms and their prevalence.

1.5.4 Echocardiographic Assessment

Echocardiography is the primary imaging modality used to assess the cardiac sequelae of Kawasaki disease[47], demonstrating a high sensitivity and specificity for the detection of abnormalities in the proximal segments of the coronary arteries[95]. An initial echocardiogram is recommended as soon as a diagnosis of KD is suspected, as it establishes the baseline for longitudinal follow-up and monitoring of CA aneurysms. Normal findings may be appreciated on echocardiograms within the first week of fever onset and would not be valid rationale for dismissal of a KD diagnosis or delayed treatment. Approximately 80% of patients with significant coronary artery involvement noted on follow-up echocardiograms, were found to have some form of CA abnormality on their baseline echocardiogram taken within 10 days of illness[73].

High-resolution echocardiographic evaluation of the coronary arteries is possible with the use of a high-frequency transducer. Most echocardiography protocols for KD recommend that the evaluations focus on the RCA, LCA, LAD, LCX and posterior descending artery using quantitative and qualitative assessments. Quantitative measurements of luminal diameter should be made between the inner edges of the coronary lumen, and the maximal dimensions of apparent aneurysms and dilations should be included[47]. Points of branching should be excluded in most assessments due to naturally occurring focal dilations. However, small aneurysms at the bifurcation or trifurcation of the LCA should be included.

Qualitative definitions of aneurysm shape and location may also be obtained from echocardiography assessment. Aneurysm shape may be defined as either saccular or fusiform. Saccular aneurysms have similar axial and lateral diameters, where fusiform aneurysms are symmetrical with proximal and distal tapering as highlighted in Figure 4. Proximal and distal CA aneurysms are defined based on their respective segmental proximity to the aortic ostia. Distal involvement is rare in the absence of preceding or co-occurring proximal abnormalities[47]. Coronary arteries are considered ectatic if they are diffusely dilated with no aneurysms.

Figure 4. Saccular and Fusiform coronary artery aneurysms seen on CT angiogram
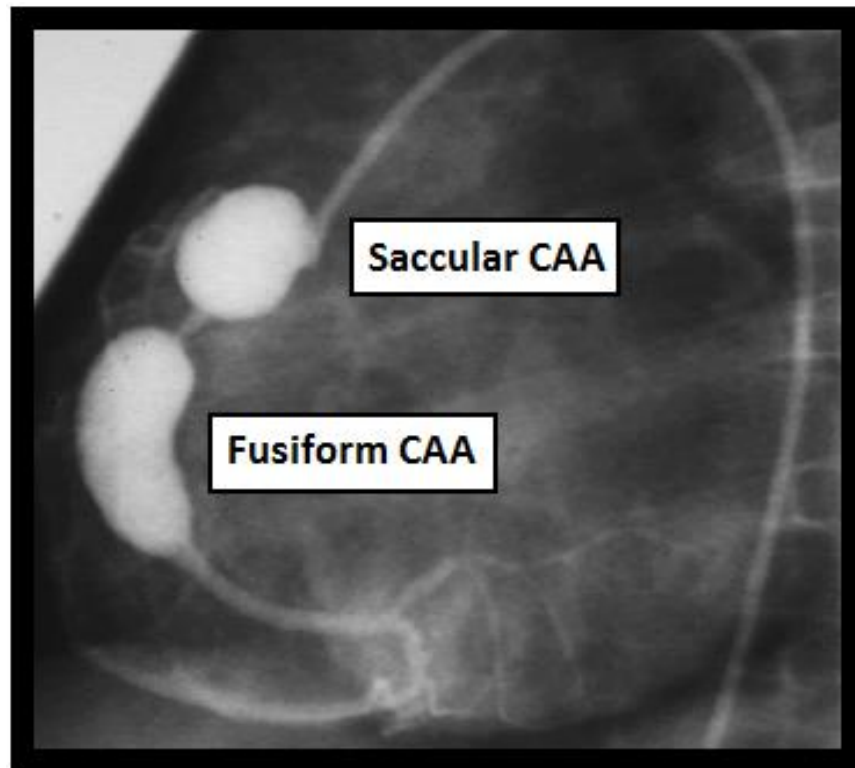
1.5.5 Echocardiographic Limitations

Although echocardiograms are the gold standard for acute and long-term assessment of coronary artery abnormalities[47], one must keep in mind the limitations associated with their use. Firstly, measuring the parameters for CA anatomy is a skill dependent task of the echocardiographer. Measures for luminal dimensions may be taken at locations within a CA aneurysm that do not represent its maximum diameter. This is an important issue when considering that small changes in luminal dimensions can result in large changes for calculated Z-score and resultant risk stratification. Furthermore, some regions with dilations or small CA aneurysms may be mistaken for having normal luminal dimensions. These are referred to as occult aneurysms whose maximum luminal Z-scores fall within normal ranges, while their normal CA diameters are much smaller than normal for their size. Proximity to the aortic ostia may also be subjective, with some

aneurysms classified as being medial when unclear as to whether they are closer to the proximal or distal segment of the artery. It can also be hard to visualize the distal portions of the coronary arteries, especially in the LAD and LCX, resulting in an underrepresentation of distal aneurysms in studies that use echocardiograms to describe the incidence of CA aneurysms in patients with KD. Accordingly, limitations exist for Z-score based criteria, which only reflect normal values for proximal coronary artery segments. The issue is exacerbated in older children, since visualization of the coronary arteries becomes progressively more difficult with increasing body size. Transesophageal echocardiography (TEE), cardiac magnetic resonance imaging (CMRI) and computed tomography angiograms (CTA) may be used to visualize the coronary arteries in older patients[47]. Conventional invasive angiography may also be used in instances of complex CA involvement and provides greater accuracy of assessment as compared to its non-invasive counterparts. Classification of aneurysm shape is the most subjective of all these measures, where patient specific longitudinal echo reports may constantly fluctuate between a saccular and fusiform definition of an observed aneurysm. Finally, although echocardiographic assessment of coronary artery thrombosis and stenosis have been reported, the sensitivity and specificity of detecting these outcomes via echocardiograms has not been well established[47].

1.6   CAA related outcomes

1.6.1 Overview

The majority of long-term cardiac sequelae related to Kawasaki disease stem from the development of coronary artery aneurysms that are defined by their maximum luminal dimensions[47]. Manlhiot *et al.* reviewed 1,356 patients diagnosed with KD between 1990 and 2007, with follow-up including serial echocardiograms for up to 15.7 years. Their investigation revealed that major adverse cardiac events (MACE; MI, thrombosis, stenosis, intervention and death) occurred in 1% of patients with Z-score <10 and absolute dimension <8mm; in 29% of patients with Z-score ≥10 and absolute dimension <8mm, and in 48% of patients with Z-score ≥10 and absolute dimension

≥8mm[92]. Long-term MI, interventions and death in KD are secondary to thrombosis and stenosis. The Kawasaki disease guidelines published by the American Heart Association in 2017 summarize the progression and pathology of myocardial ischemia (MI), thrombosis, stenosis, dimensional normalization and resolution(Fig.1)[47, 60]. This section will further elaborate on the various events that lead to or result from these outcomes.

1.6.2 Myocardial Ischemia and Infarction

The most serious complication related to Kawasaki disease is the rupture of a coronary artery aneurysm which may result in a cardiac tamponade. However, CA aneurysm rupture is a rare event that occurs in rapidly expanding large aneurysms in the first 2 to 3 weeks post fever onset, while an MI can occur during any phase of the disease[57]. Myocardial ischemia usually develops due to disrupted blood-flow to the heart and can result in infarctions, sudden death or myocardial dysfunction that may be progressive. The high risk of MI during the acute phase mirrors that of acute thrombosis, while patients with severe coronary artery involvement also poses a long-term risk for MI related to thrombosis or stenosis. In fact, patients with severe coronary artery involvement do not have any cardiac symptoms unless MI develops[47]. The signs and symptoms of KD related MI may be atypical and non-specific, especially in young children[96]. Prompt management for acute infarctions or ischemia can improve patient outcomes[97], but resultant long-term myocardial dysfunction can occur independent of coronary artery involvement[47]. Patients who have had extensive myocardial damage following an MI may develop adverse ventricular remodelling and myocardial aneurysms[98]. Myocardial dysfunction in these patients may also present in the form arrhythmia such as ventricular tachycardia, a potential predicator for long-term consequences such as sudden death[99]. Patients who develop MI are at further risk for subsequent MI[47]. However, instances of gradually progressive stenosis may be accompanied by cardio-protective collateralization regardless of prior MIs, especially in younger patients[100]. Tsuda *et al.* reported on outcomes for 60 patients who survived KD

related MIs, describing a 30-year survival rate of 63%, where 29% of the cohort were free of ventricular tachycardia after 25 years[101].

1.6.3 Thrombosis

Thrombosis refers to the deleterious formation of blood clots within the vasculature, that may impede circulation and precipitate further sequelae such as MIs. The process may stem from any combination of endothelial dysfunction, abnormal blood-flow or hypercoagulability that may be secondary to other pathological processes.

Coagulation is a hemostatic process that normatively prevents excessive bleeding following vascular injury and facilitates wound healing. The process involves *primary* and *secondary hemostasis,* both of which occur simultaneously. When the vascular endothelium is damaged, it exposes its underlying collagen and becomes activated, releasing von Willebrand factor (vWF) from its endothelial cells. Circulating platelets weakly bind to the exposed collagen while vWF strengthens the adhesion. Von Willebrand factor is also found in blood plasma and the α-granules of platelets. Platelet adhesion causes them to become activated, resulting in tighter binding and the release of biomolecules that trigger further platelet activation and adhesion. This cascade of events is called *primary hemostasis* and results in the formation of a platelet plug. *Secondary hemostasis* may be initiated through an intrinsic or extrinsic pathway, both of which involve a cascade of coagulation factors that circulate in the blood plasma. The two pathways merge into a common pathway that eventually results in the formation of a strong fibrin clot.

Dysfunctional coagulopathy, increased platelet activation and thrombocytosis (elevated platelet count) are characteristic of acute phase KD, and are associated with the arterial vasculitis. Burns *et al.* first described the extent of the associated characteristics, noting increases in coagulation factors, fibrinogen, platelet count and beta-thromboglobulin (a pro-platelet protein), with lowered levels of antithrombin III, although these features return to normal parameter following the subacute stage of the disease[102]. Recent findings also describe concomitant hyperlipidemia during the acute

phase of KD with significantly increased triglyceride levels compared to febrile and healthy controls, which further contributes to the hypercoagulable profile of these patients[103-105]. Consequently, KD related peak mortality occurs within 15 to 45 days of fever onset[47].

After the initial acute phase, CA aneurysm related hemodynamics and endothelial dysfunction would likely have a significant role in long-term thrombotic risk. The pro-thrombotic effects of endothelial activation have previously been described; and it has been noted that large aneurysms have lost their intima, media and elastica which may not regenerate[47, 57]. This is important when considering the antiplatelet, anticoagulation and pro-fibrinolytic signaling and processes associated with a healthy endothelial layer, all of which contribute to thrombosis prevention and resolution[106]. Regardless, systemic endothelial dysfunction is present many years after the resolution of acute KD, even in patients with little CA involvement[107]. Dietz and colleagues conducted a large systematic review of studies examining Kawasaki disease related endothelial dysfunction in 2015. Their meta-analysis revealed that most surrogate markers of cardiovascular disease risk and endothelial dysfunction were significantly higher in KD patients than normal controls. These results accounted for the heterogeneity of the outcomes of the investigations considered (I^2). Specifically, 11 of 13 studies ($I^2 = 89\%$) showed significantly decreased flow-mediated dilation in KD patients; 10 of 11 ($I^2 = 89\%$) studies showed significantly decreased flow-mediated dilation in KD patients with CA aneurysms than in KD patients with normal coronary arteries[108]. Decreased flow-mediated dilation is related to decreased endothelial secretion of Nitric Oxide, a potent inhibitor of platelet adhesion. Nitric oxide and prostacyclin (platelet inhibitor) are also affected by hemodynamics where healthy shear stress contributes to endothelial signaling for these molecules[109]. Additionally, a higher OSI (more turbulent flow) is known to induce a pro-coagulant phenotype in endothelial cells, resulting in increased expression of tissue factor[110]. Hemodynamic parameters may also contribute to increased thrombotic risk independent of the endothelium, by acting on circulating blood factors.

Coronary regions with lower time-averaged WSS (TAWSS) values may represent areas where the shear force is insufficient, providing a stable environment for pro-thrombotic cell-cell or cell-endothelium pathogenic adhesions that are not disrupted[111]. Furthermore, regions with a higher OSI may have a greater number of blood particle collisions, thereby facilitating these interactions. Increased local blood viscosity can be appreciated in such areas, which can further impede blood-flow and reduce shear stress[112]. Lower shear stress results in lowered shear-induced diffusion which increases the duration that blood particles, such as platelets, stay within an associated region[113]. In the case of platelets, this may further facilitate their deposition and adhesion to the luminal wall[114]. All of the above are compounded in larger aneurysms, known to have recirculation zones where blood particles may become "stuck" for extended periods[114]. However, high shear stress is also known to increase thrombotic risk by increasing platelet adhesion to circulating vWF[113]. Unlike endothelial vWF, circulating vWF occurs in a globular form that inhibit platelet binding. This globular vWF suddenly elongates under high shear stress, allowing platelet binding while providing a greater surface area for vWF-platelet collisons[113]. This is not usually a problem because high shear flows imply a higher shear-induced diffusion which would wash away activated vWF-platelet molecules before aggregation can occur; but has implications for CA branches with aneurysmal and stenotic regions, as will be explained in the following section.

1.6.4 Stenosis and atherosclerosis

Stenosis refers to the pathological, progressive narrowing of a vessel, resulting in impaired flow. Coronary artery stenosis in adults usually occurs due to an atherosclerotic process that results in plaque buildup on the luminal walls of the artery, eventually impairing blood flow which may result in an MI. While the relationship between Kawasaki disease and atherosclerosis remains elusive to this day, there are multiple studies on KD related stenosis, that suggest that it may be characteristically different from atherosclerotic stenosis. Arterial wall stiffness is one of the manifestations of atherosclerosis and is usually assessed via measures of pulse wave velocity (rate at which

pressure waves move down a vessel). In 2016, Iwazu *et al.* conducted a systematic review of 8 major studies with a focus on pulse wave velocity in KD patients. The review suggested that patients with KD have increased pulse wave velocity regardless of antecedent CA involvement when compared to the normal population and controlling for blood pressure[115]. Additionally, reduced high-density lipoprotein (HDL) and increased triglycerides levels[116] as well as markers for ongoing low-grade inflammation[117] are reported years after the resolution of KD. The above pulse wave velocity, lipid and inflammation patterns suggests that KD patients may have a predisposition for developing early onset atherosclerosis. However, no further evidence supports this hypothesis as evaluated in a study involving KD patients with even longer follow-up (7-20 years) while controlling for age, sex, body mass index, waist-to-hip ratio, blood pressure, cigarette smoking, family history, diet, glucose level, insulin level, Carotid Intima-Media Thickness Test, high-density lipoprotein cholesterol level, lipoprotein (a) level, homocysteine level, arterial stiffness, C-reactive protein level, and inflammatory cytokine level[118]. It should also be noted that patients with significant CA involvement are managed with thromboprophylactic therapies that limit physical activities and may consequently have higher levels of adiposity[47].

Kawasaki disease related stenosis, may be better associated with the previously described luminal myofibroblastic proliferative (LMP) process, or progressive mural thrombosis[47]. The relationship between hemodynamics and thrombosis have been previously explained, but hemodynamics may also have a role to play in the LMP process since it is known to affect the vascular smooth muscle cells (VSMC) from which the myofibroblasts are derived. Ueba *et al.* first described the inhibitory effect of higher WSS on VSMC proliferation mediated by transforming growth factor-beta 1 in an autocrine manner[119]. More recently, Fitzgerald *et al.* demonstrated that the Akt pathway is also involved in reduced VSMC proliferation and increased apoptosis when exposed to normal WSS[120]. Finally, Haga *et al.* showed that VSMC proliferation and survival was increased in response to a higher OSI[121]. These findings must be regarded with caution since myofibroblasts may not necessarily respond in the same manner as their progenitors. It

should also be noted that besides forming the neointima, myofibroblasts also induce thickening of the tunica media, adventitial fibrosis, and remodelling of the extracellular matrix, a process that can contribute to late lumen loss after vascular injury[122]. These events are significant when considering aneurysm resolution, as will be discussed shortly.

Once stenosis does occur, there can be a significant increase in the regional WSS. If the lesion leads into an aneurysm, there can be a jetting effect that further decreases WSS within the aneurysm while increasing blood particle residence time[113]. Any stenotic lesion that occurs proximal to an aneurysm, theoretically compounds thrombotic risk since high WSS would allow plasma vWF to activate circulating platelets that will then be transferred to an aneurysmal region with low WSS and higher particle residence times. High WSS is also known to increase the sensitivity of platelets to low WSS[123].

1.6.5 CA aneurysm resolution vs. normalization

The dimensional normalization of a coronary artery aneurysm or dilation does not equate resolution of the coronary artery sequelae. This thesis uses the term " dimensional normalization" to describe the event where CA aneurysm dimensions return within normal parameters, regardless of the means by which they do so. The term "resolution" or "regression" should only refer to instances of normalization where the various layers of the vessel wall demonstrate natural physiology and function. As of yet, resolution has only been demonstrated for small CA aneurysms and regions of transient dilation in which the luminal wall "recoils" after the resolution of KD related inflammation[57]. The intima, media, elastic and adventitia are all preserved in this situation, and their physiology and function is normative. However, as previously described, larger aneurysms may dimensionally normalize over time via the LMP process, sequential calcification and progression of mural thrombi or recanalization of thrombotic occlusions[47, 57, 60]. In such cases, the hemodynamics within the aneurysm may return to normal, although endothelial dysfunction may persist. Pulse wave velocity abnormalities have already been described in the previous section as has the LMP associated thickening of the vessel wall. Intravascular ultrasound (IVUS) has shown that this thickening can be either symmetrical

or asymmetrical, and is most prominent in dimensionally normalized CA aneurysm segments[124]. The modality has also been used to virtually characterize the histology of CA aneurysms, normalized segments and stenosed segments. Fibrous and fibrofatty areas with necrotic cores and dense calcification were noted in normalized CA aneurysms, and especially in stenosed regions[125]. Functional abnormalities were also noted in patients with angiogram confirmed dimensional normalization of CA aneurysms[126]. Specifically, the normalized segments showed paradoxical vasoconstriction in response to acetylcholine and diminished vasodilation in response to nitroglycerine. Positron emission tomography analysis normalized regions (as per echocardiography and angiography) show reduced myocardial blood-flow and flow reserve, along with the impaired vasodilation regardless of location within the coronary artery or the severity of involvement[127-129]. These findings strongly support the idea that the endothelium has not truly recovered in these lesions. It is also understood that after normalization, aneurysms with a larger original diameter may have more abnormalities than smaller aneurysms[47]. Dimensional normalization is also more likely in the case of smaller original diameters.

Kato *et al.* reported luminal outcomes for 598 KD patients diagnosed between 1973 and 1983, who had angiographic follow-up for up to 21 years. In this cohort, 49% of all patients with CA aneurysms achieved dimensional normalization within 6 to 18 months after KD[96]. Normalization was only appreciated in patients whose aneurysms were originally small or medium in size. Furthermore, normalization complicates the debate on risk stratification using Z-scores vs absolute dimensions. Coronary artery dimensions increase with age and body size, which is part of the rationale for using BSA-adjusted Z-scores. However, herein lies the issue with regards to normalization. Young KD patients with CA aneurysms may achieve dimensional normalization with age, as the surrounding vessel diameter increases to match that of the aneurysm. In such cases, absolute dimensions would not change while BSA-adjusted Z-scores decrease. These normalized segments could potentially be missing their intima, media and elastica layers, differentiating them from LMP or thrombosis mediated normalization. The above

investigations and reasoning support the current KD guidelines that stratify risk based on both maximum and current CA aneurysm dimension.

1.6.6 Kawasaki disease and myocardial perfusion

Although it is well known that coronary artery thrombosis and stenosis may lead to myocardial ischemia or infarction, recent studies also highlight the role of coronary microvascular circulation on these negative outcomes that are related to decreased myocardial perfusion[130, 131]. The previous section briefly described how patients with KD related CA aneurysms that have dimensionally normalized over time may still have dysfunctional CA arteries and myocardial perfusion. However, there is decreased perfusion in all KD patients irrespective of CA status, suggesting significant myocardial microcirculatory dysfunction. The extent of this dysfunction is related to the severity of any upstream CA lesions[132][133]. The reduced perfusion may result in diffuse myocardial fibrosis that results in further loss of contractile function[132]. This brief summary of the myocardial perfusion defects associated with KD emphasizes the importance of protecting the cardiac microvasculature. It is also apparent that KD related myocardial hypoperfusion following acute convalescence is related to the structural and hemodynamic features of the macroscopic CAs as well as persisting microvascular dysfunction.

1.7   Patient Management

1.7.1 Acute phase treatment

The acute phase of KD is characterized by a systemic vasculitis that presents with fever and a host of other symptoms as described in the diagnosis section of this thesis. While optimal treatments await the discovery of the specific agent(s) or trigger(s) related to the pathogenesis of KD, current acute strategies aim for prompt resolution of the inflammation and related fever with the aim of reducing the risk of CA aneurysm formation. In this regard, IVIG is the treatment of choice that significantly reduces fever duration and decreases the incidence of CA aneurysms, as is well established[134, 135].

However, about 20% of children develop transient coronary artery dilation and 5% develop CA aneurysms (Z >2.5) despite timely treatment with the recommended high-dose IVIG[47]. There are also incidences of IVIG resistance where a secondary treatment needs to be administered. In the majority of cases this secondary treatment is a another high-dose of IVIG, but a other options exist based on empirical evidence and significant practice variation has been noted[47]. Adjunct therapy with high-dose acetylsalicylic acid (ASA; Aspirin) is considered the standard of care due to its anti-inflammatory and anti-platelet activity. However, ASA does not appear to lower the incidence of CA abnormalities[136] and there is a high practice variability for its acute phase dosing (low vs medium vs high dose) and duration of use post discharge[47]. Corticosteroids, Infliximab and Etanercept may also be considered as adjunct therapies for children deemed to have a higher risk for CA abnormalities, as outlined in the current KD guidelines.

1.7.2 Long-term treatment

Coronary artery aneurysms pose a chronic risk for thrombosis and stenosis, which can lead to more serious adverse events such as MIs; thereby necessitating long-term follow-up for affected patients. Long-term medical management focuses on thromboprophylaxis since thrombosis can pose an immediate risk to the patient's wellbeing, while non-occlusive mural thrombi can progress to form stenotic lesions. Arterial thrombosis is usually initiated by platelet activation, as described previously. Consequently, patients with coronary artery involvement are prescribed low-dose aspirin on discharge, which allows for antiplatelet activity with no anti-inflammatory effects. Following the acute phase, these patients may remain on the low-dose ASA for as long as the CA aneurysms persist, regardless of luminal dimension[47]. Larger CA aneurysms may have an increased thrombotic risk due to reduced WSS coupled with increased OSI and flow stasis as shown in rheological[137, 138] and simulation[139, 140] based studies. The relationship between these hemodynamic parameters and thrombotic risk has been previously described in the thrombosis section of this thesis, and is closely related to increased platelet activation and aggregation as well as coagulation. As such, patients

with larger CA aneurysms may be placed on additional anticoagulation medications such as low molecular-weight heparin (LMWH; Enoxaparin, Tinzaparin) or Warfarin (Coumadin). This strategy was shown to be effective in a study by Sugahara and colleagues, where 1 of 19 patients treated with Warfarin and ASA developed MI's compared to 16 of 49 patients treated with ASA alone[141]. Additionally, there were 7 sudden deaths associated with the ASA-only group, but none for the anticoagulation group. Regardless, in the case of medium CA aneurysms or large CA aneurysms that have reduced in size, a dual antiplatelet strategy may be preferred over the addition of anticoagulants[47]. This is achieved by prescribing Clopidogrel (Plavix) in addition to ASA to bolster the antiplatelet effects, as Clopidogrel inhibits platelet aggregation via a different mechanism from ASA (ASA inhibits cyclooxygenase and thromboxane A2; Clopidogrel blocks ADP receptors). Although not specific to KD, patients at risk for thrombosis related cardiac events were shown to have a lower incidence of such events when prescribed dual antiplatelet therapy compared to ASA alone (OR: 0.87, $P<0.01$)[142]. Kawasaki disease patients with extremely large, and multiple, CA aneurysms that are at a very high risk for thrombosis, or patients who thrombosed despite anticoagulation, may be prescribed "triple therapy" (dual antiplatelet therapy + anticoagulation)[47]. However robust, empirical evidence does not yet exist for such therapy, although it is a common notion that the benefits outweigh the risks.

The 2017 Kawasaki disease guidelines support the use of β-blockers for long-term medical management of patients with persisting large CA aneurysms that are at high risk for myocardial ischemia, unless contraindications exist[47]. β-blockers reduce myocardial oxygen demand by decreasing a patient's heart-rate. As such, they can reduce the risk of MI and death, should a coronary artery occlusion occur, as well as a lower mortality risk following MI[143]. They may be prescribed for KD patients at a significant risk of CA occlusions or in patients with a history of thrombosis or MI[47].

The guidelines also support the empirical use of statins (hydroxymethylglutaryl coenzyme-A reductase inhibitors) for KD patients with persisting coronary artery aneurysms of any size[47]. Statins help regulate cholesterol by decreasing levels of low-

density lipoprotein (LDL), and are routinely used for the prevention of atherosclerotic progression and events[144]. As such, they may help address the issue of lowered high-density lipoprotein (HDL) in patients following acute KD, although with minimal effect. Statins also have anti-inflammatory[145], anti-platelet[146], anti-coagulant[147], anti-elastolytic[148] and fibrinolytic[149] pleiotropic effects that would be beneficial for thromboprophylaxis in KD patients with coronary artery sequelae. Amelioration of endothelial dysfunction, as well as endothelium regeneration may also be possible with extended use of statins[150-153]. Statins have also been shown to have a dose-dependent bi-phasic effect on angiogenesis, with low-dose therapy being angiogenic and high-dose therapy being angiostatic[154]. Furthermore, they can inhibit smooth muscle cell proliferation, migration and invasion[155], which could have overlapping effects on LMP related myofibroblasts. Investigations on the effects of statins on aneurysms have demonstrated conflicting results. Some studies have shown that statins reduces the rate of aneurysm progression[156]; others claim the drug has no effect[157] and a third claim suggests that the drug accelerates aneurysm progression and increases the chance of rupture[158].

It should be noted that the above mentioned studies do not all deal with aneurysms in the same vascular location or organ, which may explain differential findings and their empirical use in KD. Niedra *et al.* reviewed 20 KD patients as young as 8 months of age, who developed CA aneurysms and were empirically treated with statins for a median of 2.5 years. There was no effect on growth for any of the children, and only transient laboratory abnormalities were appreciated[159].

1.7.3 Other Long-term Considerations

Clotting and coagulation are physiological processes that help maintain hemostasis. Medications that treat thrombosis decrease the activity of these processes and pose a risk for abnormal bleeding in patients, especially the anticoagulants taken in combination with ASA. Low-dose aspirin on its own may rarely have very mild side-effects, the worst of which include bruising, confusion, vertigo, nausea, vomiting,

tinnitus, abdominal pain, cramping, fatigue and minor bleeding. Reye's syndrome poses the greatest concern for patients on aspirin and the drug should be discontinued should the patient develop chicken pox or influenza. Patients who require adjunct treatment with LMWH or Warfarin face an even greater bleeding risk due to the interaction between anti-platelets and anti-coagulants. Furthermore, LMWH needs to be administered every 12 (Enoxaparin) to 24 (Tinzaparin) hours via subcutaneous injections that can be very uncomfortable for children. Consequently, most patients or their parents prefer the use of Warfarin which can be taken orally, but comes with the risk of additional side-effects such as tracheal calcification, hair loss and decreased bone-mineral density. Dosing and maintenance of Warfarin is much harder than for LMWH, which is why LMWH is often the preferred alternative when a stable level of anticoagulation is necessary, as during the early course of the disease and in very young patients[160]. Both medications also require persistent monitoring to maintain optimal dosing[47]. For these reasons, if appropriate, dual anti-platelet therapy with Clopidogrel may be preferred since it requires less monitoring. That being said, the rate of bleeding complication in KD patients who receive anticoagulation therapy in addition to aspirin was relatively low, at about 0.39 to 0.52 episodes/patient year[160]. Statin use may pose an additional risk for side-effects such as muscle pain and liver damage. However, these effects are rare, especially in light of the very low dose prescribed to children; and are reversible with cessation of medication.

Besides the side-effects, inconveniences and costs associated with medication use, children taking anticoagulants in addition to Aspirin are restricted from activities that involve bodily contact with risk of injury or trauma[47]. Patients at risk for myocardial ischemia may be further restricted from highly dynamic or physically taxing activities. Generally, KD patients perform <50% as much moderate-to-vigorous activity as their healthy peers, regardless of the presence or extent of CA sequelae[161]. This phenomena was associated with lower self-efficacy for physical activity and affected females to greater extent than males.

From a family-centered psychosocial perspective, children with KD related CA aneurysms face a plethora of challenges related to their chronic condition that can have important health and life-style implications, and require consistent medication, follow-up and medical testing in some circumstances[47]. The uncertain long-term prognosis for these patients may also pose a coping challenge for the individual and their family[160]. All the above issues highlight the importance of educating parents and developing a better understanding of the long-term outcomes associated with KD. Current risk stratification criteria should also be refined to increase their specificity for thrombotic risk, thereby reducing the number of patients who receive medication unnecessarily.

1.7.4 The Challenges of KD Aneurysm Research

The relatively low incidence rate of Kawasaki disease, and even lower rate of CA sequelae, have been previously described in the epidemiology section of this thesis. While these are desirable statistics from a public health perspective, the low incidence rates pose a challenge for KD CA aneurysm related research efforts. Empirical investigation of KD related CA aneurysms is difficult when considering the small number of CA aneurysm patients that would be treated at any single medical institution. This challenge has often inspired collaborative efforts between multiple institutions. One such effort resulted in the creation of the International Kawasaki Disease Registry (IKDR) in 2013.

The primary goal of the IKDR is to investigate the incidence of outcomes of KD related CA aneurysms as well as their associated clinical and management factors. The registry is based on a secure REDCap data entry platform hosted and maintained by the cardiovascular clinical research unit and the cardiovascular data management center at the Hospital for Sick Children (SickKids) in Toronto, Canada. The registry only includes patients diagnosed with KD after January 1st 1999, who have echocardiogram confirmed CA aneurysms of Z-score ≥ 2.5 in at least one of the main coronary artery branches[162]. In 2018, the registry boasted a cohort of almost 2,000 KD patients from over 35 hospitals across Canada and the United States.

While this is an impressive number, preliminary research suggests significant variability in the long-term management of KD patients with persisting CA aneurysms across different institutions[163]. This may pose limitations for certain studies, such as those investigating thrombosis, since not all patients in the cohort may receive the same thromboprophylactic treatment. Furthermore, the exclusion of all patients with Z-scores < 2.5, eliminates the opportunity for studies to investigate outcomes for patients with CA aneurysms compared to those without them. Nonetheless, the IKDR can serve as a springboard for investigations on CA aneurysms, while facilitating further collaboration that could enable novel studies.

1.7.5 Computational Fluid Dynamics

While the IKDR represents collaborative efforts between medical experts, multidisciplinary collaborative efforts may present alternative avenues for further advancement in the field. Such efforts between physicians, surgeons and biomechanical engineers have been tremendously successful in recent decades. Particularly, the steady development of supercomputers coupled with the exponential rise of computational processing power has allowed for significant advancements and applications for the field of computational fluid dynamics (CFD). Computational fluid dynamics is a branch of fluid mechanics that uses algorithms and computer based simulations to analyze and solve problems involving fluid flows. As such, CFD methodologies are very useful for cardiovascular investigations and applications, where hemodynamics can have significant implications. Analyses of flow features can provide quantitative measures of hemodynamic characteristics that cannot be obtained from standard imaging modalities. Furthermore, CFD techniques can use data obtained from other non-invasive imaging modalities that effectively adhere to the concept of *Primum non nocere*.

A number of research teams around the world have used patient-specific computational fluid dynamics in various vascular investigations on thrombosis, stenosis and aneurysms[114, 164-166]. Dr. Alison Marsden leads one such research team, affiliated with Stanford University in the United States. Their team refined a CFD protocol that allows

for quantitative analyses of flow features in coronary artery aneurysms[139]. A pilot study that applied their methods to 5 patients with persisting CA aneurysms and thrombotic events following KD, showed that the aneurysmal areas had a lower mean WSS with higher OSI and particle residence times (a measure of flow stasis) when compared to 1 patient with normal coronary artery anatomy[140]. Although these results were statistically underpowered due to the small sample size, they are qualitatively intuitive and support a methodological framework for future hemodynamic studies in KD patients.

1.8   Summary

Kawasaki disease is a self-limiting, systemic vasculitis that predominantly affects children under 5 years of age. The disease also has a genetic predilection for male sex and children of Japanese descent. The etiology of the disease is unknown, but believed to be an environmental trigger of infectious nature; although there are a lot of conflicting research findings in this regard. KD has a relatively low incidence rate and an very low recurrence rate, but is the leading cause of acquired heart disease in children of the developed world. The case fatality rate is also very low, with peak mortality occurring between 3 to 6 weeks following fever onset.

Long-term morbidity or mortality due to KD primarily occurs due to cardiac sequelae. The most significant of these sequelae are coronary artery aneurysms that can significantly increase a patient's risk for thrombosis or stenosis. Myocardial infarction is rare, but can occur secondarily to these adverse events. Currently, risk management strategies for patients with persisting CA aneurysms following KD are stratified using measures of absolute luminal dimension and BSA-adjusted Z-scores that haven't changed much in over a decade. Normal branches have a Z-score <2.5; small CA aneurysms, $2.5 \leq$ Z-score <5; medium CA aneurysms, $5 \leq$ Z-score <10; and large CA aneurysms, Z-score ≥ 10 or absolute diameter ≥ 8mm.

Necrotizing arteritis (NA), subacute/chronic vasculitis (SA/C) and luminal myofibroblastic proliferation (LMP) are the 3 main pathological processes associated with KD related CA aneurysms. NA causes the formation of acute large, saccular CA aneurysms; SA/C is responsible for CA aneurysm progression and is thought to result in

fusiform CA aneurysm formation; LMP leads to dimensional normalization or stenosis. Dimensional normalization refers to instances where the maximum luminal diameter of aneurysms with a Z-score ≥ 2.5 have decreased to levels below that threshold. While truly resolved CA aneurysms have normal luminal dimensions and function, dimensionally normalized CA aneurysms may have persisting endothelial dysfunction.

For all the above reasons, patients who develop CA aneurysms following Kawasaki disease require consistent follow-up and long-term management. Where resolution of the KD associated inflammation and fever is the primary goal of acute management, long-term management focuses on preventing adverse outcomes secondary to CA aneurysm formation, especially thromboprophylaxis. Thrombosis during acute KD and in small and medium CA aneurysms is thought to be more dependent on endothelial dysfunction and abnormal coagulation. In larger CA aneurysms, hemodynamic effects may play a more significant role in thrombus formation and stenotic progression.

CA hemodynamics are known to be influenced by anatomical features such as shape and location. Incorporating information on coronary artery anatomy and hemodynamics may help refine current risk stratification criteria for patients with persisting CA aneurysms following KD. This is important when considering the psychosocial, lifestyle and financial implications of long-term CA aneurysm management on patients and their families. The first step to such refinement would be to empirically evaluate measures of hemodynamics and CA anatomy for associations with outcomes of KD related CA aneurysms. However, such a task is difficult due to the small number of KD CA aneurysm patients available at any one institution. The International Kawasaki Disease Registry (IKDR), sought to address such issues through collaboration, and has established a sizeable cohort of patients with KD related CA aneurysms for use in research endeavors. Hemodynamic investigations could also benefit from collaboration, particularly between CFD focussed biomedical engineering teams and KD focused clinical research groups. This thesis aims to use such collaborative efforts to take the first steps towards refining the current risk stratification criteria for patients with coronary artery aneurysms following Kawasaki disease.

1.9   Aims, Hypotheses and Rationale.

1.9.1 Overview and Objectives

The overarching goal for this body of work, is to use novel technologies and collaborative efforts to empirically evaluate aspects of CA anatomy and hemodynamics for implications on long-term management of patients with coronary artery aneurysms following Kawasaki disease. The study has 2 major objectives with the first objective being divided into 5 aims and the second objective into an additional 2 aims. Aims 1 through 5 focus on relationships between the structural features of CA aneurysm and branch anatomy and the negative outcomes of thrombosis, stenosis and failure to achieve dimensional normalization. Aims 6 and 7 evaluate how hemodynamic parameters are associated with thrombotic risk, while qualifying the efficacy of their adjunct use in current risk stratification criteria. The specific objectives, aims, hypotheses and rationales are outlined and listed on the next page.

Objective 1:

Defining the associations between the structural features of CA branches and aneurysms versus the outcomes of thrombosis, stenosis and dimensional normalization:

Aim 1: Determine the relationship between CA aneurysm shape and outcomes.

Aim 2: Determine the relationship between CA aneurysm location and outcomes

Aim 3: Determine the relationship between CA aneurysm cross-sectional
area and outcomes

Aim 4: Determine the relationship between the 4 main CA branches and outcomes.

Aim 5: Determine the relationship between CA aneurysm branch anatomy and outcomes.

Objective 2:

Evaluating associations between CA aneurysm and branch hemodynamics versus thrombotic risk.

Aim 6: Determine the relationship between hemodynamic measures and thrombotic risk.

Aim 7: Evaluate the adjunct use of hemodynamic measures for risk stratification in patients with persisting large CA aneurysms following Kawasaki Disease

1.9.2 Specific Aims, Hypotheses and Rationales

1.9.2A   Aim 1: To determine the relationship between CA aneurysm shape and thrombosis, stenosis and dimensional normalization.
Hypothesis: Saccular CA aneurysms pose a greater thrombotic risk but fusiform aneurysms are more likely to achieve dimensional normalization or stenose.
Rationale: Saccular CA aneurysms could have a greater recirculation time than fusiform CA aneurysms, which is also associated with greater thrombotic risk. Furthermore, saccular CA aneurysms are thought to result from the acute KD related necrotizing arteritis (NA) process, while fusiform CA aneurysms are more likely associated with sub-acute/chronic vasculitis (SA/C). Generally, NA results in greater endothelial damage than SA/C, and greater endothelial damage is associated with higher thrombotic risk. Fusiform CA aneurysms may suffer less endothelial damage than saccular aneurysms and may preserve more of their medial layer as well. With a more preserved media, the SA/C vasculitis linked LMP process in fusiform aneurysms may cause the transition of a greater number of SMCs to myofibroblasts, facilitating the LMP process. A healthier vessel wall and/or a more prominent LMP process would increase the speed and incidence of dimensional normalization. However, the LMP process is also thought to be associated with KD related stenosis and the same factors that increase its chances of dimensional normalization may also increase risk for stenosis.

1.9.2B   Aim 2: To determine the relationship between CA aneurysm location and thrombosis, stenosis and dimensional normalization.
Hypothesis: Distal CA aneurysms are more likely to thrombose, stenose and dimensionally normalize when compared to proximal CA aneurysms.

Rationale: Flow velocity and volume are lower in the distal portions of coronary arteries when compared to proximal portions. Low flow velocity and volume are also associated with increased thrombotic risk. Furthermore, distal CA aneurysms are difficult to appreciate on echocardiograms, and even more difficult in the presence of mural thrombi. As such, it is entirely possible for thromboprophylactic treatment to be delayed or missed in patients with large distal but small proximal coronary artery aneurysms. Lower flow velocity is also linked to lower WSS; which has been associated with increased risk for atherosclerotic stenosis and increased proliferation of myofibroblasts. Accordingly, it is plausible that lower WSS would result in a more prominent LMP process. As previously mentioned, a more prominent LMP process would increase the chance of dimensional normalization in a patient, but also increase the risk of stenosis.

1.9.2C Aim 3: To determine the relationship between CA aneurysm cross-sectional area and thrombosis, stenosis and dimensional normalization.

Hypothesis: CA aneurysm cross-sectional area will be positively correlated with thrombosis and stenosis, but negatively correlated to dimensional normalization.

Rationale: The flow velocity and wall shear stress of CA aneurysms is lower when compared to normal vessels. Coronary artery aneurysms with greater cross-sectional area will have even lower flow velocities and wall shear stress, with greater luminal surface area exposed to endothelial damage. Blood pooling and residence time within an aneurysm may also be increased in CA aneurysms with greater cross-sectional area. All these factors would suggest an increased risk for thrombosis and stenosis. A greater luminal surface area exposed to endothelial damage allows the LMP process to affect more of the vessel wall, potentially increasing the rate of myofibroblastic proliferation, further increasing the risk for stenosis in the long run. However, it is assumed that the effect of aneurysm diameter will overshadow any effect of aneurysm length with regards

to dimensional normalization, where CA aneurysms with larger diameters are less likely to return to normal dimensions.

1.9.2D **Aim 4:** To determine the relationship between the 4 main CA branches and thrombosis, stenosis and dimensional normalization.

Hypothesis: CA aneurysm thrombosis, stenosis and dimensional normalization is most likely in the RCA and least likely in the LCA.

Rationale: The RCA has the lowest flow velocity, while the LCA has the highest. Lower blood flow velocities are associated with lower wall shear stress which in turn is thought to be associated with increased risk for thrombosis and stenosis as well as increased chance for dimensional normalization.

1.9.2E **Aim 5:** To determine the relationship between CA aneurysm branch anatomy and thrombosis, stenosis and dimensional normalization.

Hypothesis: The occurrence of CA aneurysm thrombosis and stenosis will be higher in CA branches with greater anatomical complexity. However, the chance for dimensional normalization will be less for these branches.

Rationale: Coronary artery branches with greater anatomical complexity may compound the hemodynamic and endothelial effects of multiple CA aneurysms or dilations, thereby increasing the amount of circulating pro-thrombotic factors and effects within the branch. This also applies to circulating factors that may be responsible for remote LMP events whose compounding effects may also increase the chance for stenosis. Regardless, CA branches with greater anatomical complexity represent a more severe episode of acute KD with more aneurysms that need to be resolved for a branch to achieve dimensional normalization.

1.9.2F   **Aim 6:** To determine the relationship between hemodynamic measures of CA branches and aneurysms versus thrombotic risk.

Hypothesis: Aneurysms with a lower wall shear stress or higher oscillatory shear index, and CA branches with higher residence time or greater area exposed to very low wall shear stress will be more likely to thrombose.

Rationale: There has been prior evidence describing the association between these hemodynamic parameters and thrombotic risk in other types of aneurysms. However, there has been little indication that the same holds true for KD related CA aneurysms.

1.9.2G   **Aim 7:** To evaluate the adjunct use of hemodynamic measures for risk stratification in patients with persisting large CA aneurysms following KD.

Hypothesis: If hemodynamic measures are associated with thrombotic risk (evaluated in aim 6), then their adjunct consideration with CA aneurysms Z-scores and diameter could potentially improve the specificity of current risk stratification criteria, especially in patients with large CA aneurysms.

Rationale: If hemodynamic measures are associated with thrombotic risk, it may be possible to set thresholds for the measures, which could further advise medical management of patients with large CA aneurysms. The high-sensitivity of current risk stratification criteria has already been established; where patients with small (2.5≤ Z-score >5) and medium (5≤ Z-score >10; Diameter >8mm) CA aneurysms very rarely develop adverse outcomes. However, thromboprophylactic management in patients with large CA aneurysms is empiric and variable, often requiring the occurrence of an adverse event before more aggressive management is considered. This is partly due to the extensive range of Z-scores for patients with large CA aneurysms (anywhere between 10 and 70). Hemodynamic thresholds could further stratify this risk level, advising the aggressiveness of long-term medical management.

Chapter 2: Methods

2.1 Overview

This body of work was divided into two related parts that use distinct methodologies to individually address the anatomic and hemodynamic aims. The first part was a retrospective cohort based investigation that used echocardiogram reports to address major aims #1 through #3. The second part was a retrospective case-control based investigation that used computational fluid dynamics to address major aim #4. The two parts also used different patient cohorts with regards to data source, availability, acquisition and quality. The specific methodologies are discussed below.

2.2 Part 1: Coronary artery anatomy based investigations

2.2.1 Objective 1:

Defining the associations between the structural features of CA branches and aneurysms versus the outcomes of thrombosis, stenosis and dimensional normalization:

Aim 1: Determine the relationship between CA aneurysm shape and outcomes.

Aim 2: Determine the relationship between CA aneurysm location and outcomes

Aim 3: Determine the relationship between CA aneurysm cross-sectional
  area and outcomes

Aim 4: Determine the relationship between the 4 main CA branches and outcomes.

Aim 5: Determine the relationship between CA aneurysm branch anatomy and outcomes.

2.2.2 Collaboration

The primary cohort for study part 1 was established through collaboration with the International Kawasaki Disease Registry and its data management center located at the Hospital for Sick Children in Toronto, Canada. It is important to disclose that the author of this thesis is also a part of the IKDR data management center. Project proposals were presented to the IKDR members, and de-identified data were made available for accepted proposals. All post-processed data was made available to the IKDR for potential future studies.

2.2.3 Cohort

Study part 1 established a cohort of patients with coronary artery aneurysms and consistent echocardiology follow-up after Kawasaki disease. Each of the specific aims had additional exclusion criteria, and represented a smaller portion of the primary cohort to better facilitate the individual analyses. As discussed previously, no single institution has access to the large number of KD patients with coronary artery aneurysms, required to empirically investigate their possible outcomes. This was especially true when considering the investigations involved with study part 1 of this thesis, that required detailed data about the patients' coronary artery anatomy. As such, the primary cohort for study part 1 was established using data from the International Kawasaki Disease Registry (IKDR).

Inclusion criteria encompassed all patients who developed coronary artery aneurysms with Z-scores ≥ 2.5 following a diagnosis of Kawasaki disease after January 1st, 1999. Included patients must have had a normal cardiovascular system except for KD related abnormalities. Patients with comorbidities that affect thrombosis and hemostasis were excluded. Patients were also excluded if they did not have any echocardiographic reports available for the first year following diagnosis.

2.2.4 Echocardiogram reports

Echocardiographic evaluation of coronary artery aneurysms is the primary and most commonly used method of assessment, with persistent follow-up. The current and previous Kawasaki disease guidelines recommend that an echocardiographic assessment be done at least once a year for all patients with coronary artery aneurysms[47, 88]. Sub-acutely, patients are recommended to have an echocardiogram done every 3 months until 1 year of follow-up. After that, patients with small or medium CA aneurysms are recommended to have an echocardiographic assessment done every year, while patients with large CA aneurysms have one done at least bi-annually. Consequently, echocardiograms are the best available means of retrospectively evaluating coronary artery aneurysm and branch anatomy.

All the patient data and imaging reports were obtained from the hospitals affiliated with the IKDR. As part of enrollment in the IKDR, participating sites had to provide de-identified copies of all the echo, cardiac magnetic resonance imaging (CMRI), computed tomography (CT) and angiographic imaging reports for each individual patient[162]. While providing the copies of the actual files themselves would have been ideal, it was highly unfeasible. Consequently, data from these reports were extracted, and the information was standardized for all patients across all sites.

2.2.5 Data collection, storage and extraction

Imaging reports were obtained as either hard copies, digital file transfers or uploads on to the secure IKDR REDCap server. Hard copies are stored in a locked file cabinet that lies in a secure office space at SickKids. Digital file transfers were uploaded onto the REDCap platform before being stored on a secure network drive at SickKids. All data extracted from the imaging reports was made available to the IKDR management team for use in other related projects.

Data extraction was a two part process. A dedicated team of summer students were responsible for transcribing dates as well as measures of height, weight and absolute luminal dimensions from each echo report onto an excel file. This process was managed by the author of this thesis, who was also responsible for validating all data, calculating Z-scores and extrapolating anatomical features from the descriptions provided from all imaging modalities.

Clinical data collection included:

- Major comorbidity
- Sex
- Age at diagnosis
- Date of diagnosis
- Date of discharge
- Date of symptom onset
- Date of defervescence
- Date of first IVIG treatment
- Response to first IVIG
- Symptoms at diagnosis
- Acute laboratory data (Pre IVIG)

- Type of KD
- Date of subsequent IVIGs
- Number of IVIG doses
- Date of IVMP/ prednisone
- Date of thrombosis *
- Date of stenosis *
- Date of intervention
- Type of intervention
- Description of intervention
- Aspirin, Clopidogrel, Warfarin and LMWH start and end dates

* Date when first identified on any imaging modality.

Specific data from the extraction and interpretation of various imaging reports:

- Date of first echo
- Date when CA aneurysm was identified
- Date of echo with highest Z-score
- Date of last abnormal echo
- Date of last echo

- Date of echo
- Maximum Z-score
- Maximum diameter
- Maximum length
- Coronary artery branch classification
- Coronary artery aneurysm location
- Coronary artery aneurysm shape

2.2.6 Calculating maximum Z-score

As previously described, there are a number of formulas available for the calculation of BSA-adjusted Z-scores for coronary artery aneurysms after Kawasaki disease. One would ideally choose to use either the Kobayashi[167] or Dallaire[94] equations, both of which are derived from rigorous studies. However neither of the two formulas

were widely used or evaluated. Furthermore, the Z-score stratification system outlined by Manlhiot *et al.* used the McCrindle formulas, which were also used by many North American hospitals under the Pediatric Heart Network at the time; although the network has since developed its own set of formulas for calculating CA aneurysm Z-scores[91, 92]. Manlhiot *et al.* also validated the use of the McCrindle LAD formulas for the LCX.

Subsequently, this body of work makes use of the McCrindle formulas for Z-score calculation using the recommended Haycock formula for BSA calculation (Table 4); thereby standardizing the BSA-adjusted Z-scores across the multiple IKDR hospitals. While evidence suggests that using different Z-score systems and BSA formulas results in differences in score[47, 168], this thesis does not aim to elucidate said differences, but must keep them in mind when extrapolating results and drawing conclusions.

Table 4. **BSA and CA branch specific Z-score formulas used**

BSA Formula	
Haycock: $0.024265 \times$ Height $(cm)^{0.3964} \times$ Weight $(kg)^{0.5378}$	
Z-score calculations	**Coronary Branch**
$0.31747 \times (BSA \times 0.36008) - 0.02887 / SD = 0.03040 + (0.01514 \times BSA)$	Left main
$0.26108 \times (BSA \times 0.37893) - 0.02852 / SD = 0.01465 + (0.01996 \times BSA)$	Left anterior descending
$0.26108 \times (BSA \times 0.37893) - 0.02852 / SD = 0.01465 + (0.01996 \times BSA)$	Circumflex
$0.26117 \times (BSA \times 0.39992) - 0.02756 / SD = 0.02407 + (0.01597 \times BSA)$	Right main

2.2.7 Longitudinal Data Validation

Serial measures obtained from assessment during follow-up were prone to abnormal variations resulting from the subjectivity involved with each assessment. Furthermore, since the data were being manually transcribed onto an Excel file, there was a chance of typographical errors occurring due to the quantity of data, multiple data entry persons and lack of constraints on data entry. It should be noted that typographical errors were also found on the actual echocardiogram reports submitted by IKDR hospitals. These errors and variations were adjudicated and validated since small changes in measures of height, weight and luminal dimension can lead to significant changes in Z-score. The serial echo measures were longitudinally evaluated for every individual patient

while accounting for additional information from MRIs, CTs and angiograms. A validation protocol was developed and consistently followed.

Typographical data entry errors were fairly obvious as they result in massive changes in Z-score, dates that don't make sense or an abrupt change in the pattern of aneurysm progression. These errors were easily corrected and verified from the original reports. Typographical errors on the reports themselves were handled in the same manner as variation in serial measures. Measures of height and weight were corrected by plotting the preceding and succeeding measures on a growth chart that was appropriate for the patient's age and sex.

Correcting measures of luminal dimension was a lot trickier. Firstly all the echocardiogram reports for a patient were adjudicated to make sure that only the dimensions of the largest aneurysm per branch was being reported. Aneurysms at the bifurcation of the left main coronary artery were noted by a separate variable and individual measures for the LCA, LAD and LCX were used, if provided. When echocardiogram reports only provided dimensions for the aneurysm at the bifurcation, with normal measures of the LCA and proximal LAD and LCX, the aneurysm dimensions were transcribed as part of the proximal LAD. This was done after consulting with Kawasaki disease experts (Dr. Brian McCrindle and Dr. Cedric Manlhiot).

The individual aneurysm measures were also adjudicated with respect to the understood pattern of KD CA aneurysm progression, while considering outcomes (thrombosis or stenosis) and interventions (Coronary artery bypass grafts (CABG), Percutaneous coronary interventions (PCI) or thrombolytics) that could justify observed abnormalities. Abnormal measures that did not conform to an observable longitudinal pattern were corrected using the preceding and succeeding reports within 1 month, or the advanced imaging (MRI, CT, angiogram) reports within 3 months of the echocardiogram in question. In the very rare instances where neither of these solutions were possible, the IKDR site was contacted and asked to re-measure the aneurysm dimensions on the reported echocardiogram.

The above describe how errors and unexplained abnormal variations were handled. However, missing measures of luminal dimension were a more widespread

issue. This occurred in one of 4 situations: CA branches with no abnormalities; CA branches whose aneurysm diameters had returned to normal; CA branches where there was no significant change in aneurysm diameter from the previous report; and CA branches with distal CA aneurysms that became hard to visualize as the child aged. The first and second situations did not need to be adjudicated since there were no CA aneurysms to characterize, or dimensional normalization has already occurred. For missing measures on echocardiograms that reported no significant change from the previous study, the luminal dimensions of the previous study were used. Luminal measures for distal CA aneurysms that became hard to visualize were replaced with measures from advanced imaging (Angio/MRI/CT) reports, if available. If neither of these solutions was an option, values remained missing.

Validating the data from echocardiogram reports was an important step for part one of this study as it qualified the investigations to follow. The validation process went hand-in-hand with the characterization of coronary artery aneurysm and branch anatomy which are described below.

2.2.8 Determining CA aneurysm Shape

Aneurysm shape is traditionally defined as either saccular or fusiform. However, there is some subjectivity involved with this qualitative definition and the same aneurysm may be classified differently by different physicians. Consequently, there have been multiple attempts to quantify aneurysm shape on a continuum, some using measures of sphericity[140] or multiple aspect ratios[169]. Unfortunately, neither of these methods were feasible in the setting of this study as they required measures of either volume or a third dimension in addition to diameter and length. Such measures were not provided on echocardiogram reports. Consequently, we used a novel two-dimensional aspect ratio of width to height to quantitatively define CA aneurysm shape on a spectrum where values approaching 1 indicated a more saccular shape.

Shape was also defined categorically based on the reporting physician's qualitative assessment and explicit mention of either saccular or fusiform shape. This was done for every CA branch with an aneurysm. The most consistent definition, closest to the date of

maximum Z-score was used. In cases where a single branch had multiple CA aneurysms, the shape reported for the largest aneurysm was used. It was understood that this may be an over simplification of the issue, but it was the most feasible way to standardize the classification of coronary artery aneurysm shape.

2.2.9 Determining CA aneurysm cross-sectional area

As previously mentioned, it was not possible to obtain measures of aneurysm volume from an echocardiology report. However, it was possible to estimate cross-sectional area using the formula for the area of an oval, defined as *0.8 x Vertical CA aneurysm diameter (width) x Horizontal CA aneurysm diameter (length)*. Cross-sectional area could serve as a surrogate, simplified measure of CA aneurysm volume and may also be useful in quantifying the affected endothelium to a limited degree. Cross-sectional area was calculated for the few patients where aneurysm length was provided, and only lengths within a year of maximum diameter were used. Furthermore, the measure is not wholly accurate since aneurysms are not always in the shape of a perfect oval.

2.2.10 Determining CA aneurysm location

Unlike aneurysm shape, aneurysm location had a definite classification based on the distance from the aortic ostia with segmental definitions based on important bifurcations. Since the LMCA only has 1 short segment, it was not assigned a location. The circumflex CA branch has 2 segments separated by the obtuse marginal branch and is easy to classify. The RCA and LAD have 3 main segments each, also defined by obvious branching. However, this branching was not very clear on echocardiograms and some physicians preferred to report aneurysms of the medial segments as being either proximal or distal. This is further complicated due to the difficulty of visualizing the distal segments of the coronary arteries. Such reports could not be adjudicated due to the lack of imaging files and the data in the report was taken as is. Furthermore, CA branches with multiple aneurysms across multiple segments made it difficult to define an aneurysm's location, as did giant aneurysms spanning the length of the vessel. Consequently, CA aneurysm location was addressed in the same manner as CA aneurysm shape where the

physician's report was taken *ad verbatim*. For instances of CA aneurysms that involved multiple sections of a branch we defined the location as being "both", proximal and distal. Coronary artery aneurysms of the medial segments were defined as being proximal.

2.2.11 Determining Branch Anatomy

In the context of this thesis, "branch anatomy" was the term used to describe the specific characteristics of a coronary artery branch with regards to the number of aneurysms and areas of dilation present. This was done under the assumption that the risk for negative outcomes in patients with KD related CA aneurysms increases with the number and complexity of aneurysms in each branch. The branch was said to have no involvement if the diameters had a Z-score less than 2.5 throughout the branch. CA aneurysms with some sectional diameters of Z-score between 2.5 and 5 were said to be dilated. Branches with focal aneurysms were classified with respect to other abnormalities within the branch. If no other abnormalities were present the branch was said to have an isolated aneurysm in a normal vessel. If regions of dilation were present in addition to the focal CA aneurysm, the branch was said to have an isolated aneurysm in a dilated vessel. Branches with more than one CA aneurysm were classified as complex regardless of the additional number of aneurysms in the branch.

2.2.12 Determining Branch Complexity

Coronary artery branch complexity was defined by the number of aneurysms present in a coronary artery branch, as well as the amount of dilation within non-aneurysmal segments of the branch. Branches were categorically defined to have only dilation, an isolated aneurysm with no dilation, an isolated aneurysm and dilation, or more than one aneurysm in the branch. Echocardiography reports as well as any available advanced cardiac imaging was used to define the extent of branch complexity as per the four categories defined above.

2.2.13 Determining Outcomes

Diagnoses of coronary artery thrombosis and stenosis were identified from clinical information provided by IKDR collaborators who reviewed patient charts. These diagnoses have been confirmed via different cardiac imaging modalities, and some thrombi have required further treatment. A CA branch was said to have achieved dimensional normalization if it ever had a maximum diameter of Z-score $\geq$ 2.5 that subsequently decreased below 2.5. For the most part, this determination was fairly easy where measures of luminal diameter were available. However, as mentioned in the longitudinal data validation section, some patients with distal CA aneurysms were missing measures for luminal dimensions on later echocardiogram reports. Dimensional normalization for these branches was adjudicated using clinical data on antiplatelet and anticoagulation treatments in adjunction with data on the progression of CA aneurysms in the other CA branches. The individual coronary artery branches of a patient were classified as having either no CA aneurysm involvement, dimensional normalization, or persisting CA aneurysms. The date of dimensional normalization was deemed to be the same as the first echocardiogram that showed a Z-score < 2.5 following the development of a CA aneurysm. CA branches that had luminal dimensions of Z-score $\geq$ 2.5 on the last available echo were said to have persisting coronary artery aneurysms.

2.2.14 Statistical Analyses Part One

All analyses for part one were conducted at the branch or aneurysm level without adjusting for repeated measures, since the primary risk factors of interest were features of the branch/aneurysm itself, and not of the patients. Analyses only included patients with CA aneurysms of Z-score $\geq$ 10 since adverse outcomes were only present for 2 patients with smaller aneurysms. This was in keeping with previous reports on the IKDR cohort. The Kaplan-Meier method was used to analyse associations between each CA aneurysm structural feature (7) and each time-related outcome (3) up to 10 years post diagnosis. Results were presented as failure rates rather than freedom from outcomes, with means and standard error as well as cohort size at the given time point. Since very few patients in this cohort died (4/440), there is little survivor bias for any related time-

to-event analyses for study part one. A multivariable Cox proportional hazard model was used to determine relevant associations while accounting for age at KD diagnosis, sex, type of KD (complete/incomplete), arthritis, duration of fever before IVIG, total acute fever duration, number of IVIG treatments, IV steroid use, oral steroid use, Infliximab use, NSAID use, and the acute laboratory measures of serum albumin, C-reactive protein, erythrocyte sedimentation rate and white blood-cell count. Independent variables tested included measures of CA aneurysm shape (Saccular vs Fusiform or Aspect ratio), artery location (RCA, LCA, LAD, LCX), branch location (proximal, distal, both), cross-sectional area, and branch anatomy as previously defined. Outcome variables included the time-related incidence of thrombosis, stenosis and dimensional normalization. Relevant associations were evaluated between each independent and outcome variable. Bootstrap resampling was used to refine variable selection (500 random samples, $p<0.05$ to enter, $p<0.10$ to remain). The final Cox proportional hazard model used backward selection of variables and only included those with high reliability, selected in more than 50% of the random samples. Univariate linear and logistic regression analyses were conducted for structural features not selected in the multivariable model. These complex statistical analyses were performed in conjunction with the Cardiovascular Data Management Center at SickKids using SAS version 9.4.

2.3   Part 2: CA aneurysm hemodynamics investigation[170]

2.3.1 Objective 2:

Evaluating associations between CA aneurysm and branch hemodynamics versus thrombotic risk.

Aim 6: Determine the relationship between hemodynamic measures and thrombotic risk.

Aim 7: Evaluate the adjunct use of hemodynamic measures for risk stratification in patients with persisting large CA aneurysms following Kawasaki Disease

2.3.2 Collaboration

Study part 2 involved analyses of an established cohort through collaboration with a CFD focused biomedical engineering team. Dr. Alison Marsden's team at Stanford University were the ideal partners for such an undertaking since they had previously developed a CFD protocol for use in patients with KD related CA aneurysms. The partnership was setup such that the author of this thesis would be responsible for establishing the study cohort and obtaining all required data to be used for this investigation. Noelia Grande Gutierrez, a PhD. student from the Marsden lab, was responsible for running the CFD simulations and generating the appropriate variables.

2.3.3 Cohort

The Hospital for Sick Children in Toronto, Canada, maintains a database of all patients admitted with a diagnosis of Kawasaki disease. This historical database was reviewed to identify all KD patients who had developed CA aneurysms and undergone cardiac magnetic resonance imaging (CMRI) investigations. Patients who did not have a CA aneurysm or CMRI were excluded from this study. All other inclusion and exclusion criteria were defined at the coronary artery branch level.

It is important to note that all CMRI investigations that were evaluated were done after a thrombotic event. Consequently, CA branches with unresolved occlusive thrombi, or those involving CABG were excluded from the analyses, since there would be little merit in hemodynamic evaluations of such branches in terms of associations. CMRI reports and files were reviewed for all remaining patients in the group and image quality for branches with thrombotic events was assessed. The image quality had to be sufficient enough to allow for manual segmentation of the coronary artery as well as the CA aneurysm. The feasibility of segmentation distal to this aneurysm was not considered. Branches were excluded if the image quality was deemed insufficient. If these exclusions were the only CA branches with aneurysms in a specific patient, the patient was excluded. After these exclusions, there were 5 patients with CA branches that had a thrombotic event. Five other patients with large CA aneurysms were also included for comparison, bringing the cohort size to 10 patients.

2.3.4 CMRI Protocol and Parameters

At SickKids, CMRIs for KD patients were only ordered on physician request. Dr. Brian McCrindle, a Kawasaki disease expert, requested CMRIs for patients with significant CA involvement or adverse outcomes. Consequently, KD CA aneurysm patients with thrombotic events had CMRI investigations either years before the event, or shortly after. There were significant changes in CA anatomy from early CMRI investigations to the time of thrombosis, with some patients lacking early CMRIs entirely. As such, it was decided that post outcome CMRIs would be used after a review of validity. This review involved an evaluation of pre- and post-event luminal dimensions and CA anatomy based on echocardiography and conventional angiography reports. If there were no significant changes in Z-score and absolute dimension, the patient's thrombosed CA aneurysm's were included in the analysis. No such evaluation was necessary to include Non-thrombosed CA aneurysms. This decision may have some implications regarding the time at risk, but it was necessary given the limited availability of eligible patients.

CMRIs were conducted with the objectives of assessing ventricular function, wall motion abnormalities, myocardial perfusion defects at rest and at stress, CA anatomy and thrombotic or stenotic events. A 1.5T Siemens MRI scanner was used for all CMRI investigations. Coronary arteries were best visualized using 3D TrueFISP sequences with the variables outlined in Table 5. TrueFISP is the Siemens trade name for a steady-state coherence sequence where balanced gradients were used along all three axes[171]. The sequence was available for GE and Phillips machines as well, under the names FIESTA (GE) and Balanced-FFE (Phillips). These sequences highlight fluids such as blood with a high signal intensity, making them ideal for cardiovascular imaging.

Table 5. Sequence parameters for MRA imaging

Characteristics	Measures
Sequence Type	TrueFISP
Bandwidth	599 Hz/Px
Echo spacing	3.8 ms
TR	285.54 ms
TE	1.62 ms
Flip angle	90°
Slices	80
slice thickness	1.2 mm
Phase resolution	90%

Table 5: TR = Repetition time; TE = Echo time

Images were acquired after injection of a gadolinium based contrast, but before administration of any pharmacological agents that may have affected heart rate. Low spatial resolution, Cine-mode, phase contrast imaging was performed in the ascending aorta, just distal to the aortic valve. Phase contrast imaging assessed planes orthogonal to the aorta, over 60 phases using an encoding velocity of 150 cm/s. Phase contrast MRIs allow for quantification of flow measurements while velocity encoding is based on an estimate of physiological arterial flow. Myocardial perfusion was not assessed as per the scope of this project.

2.3.5 Three Dimensional Model Creation

Three dimensional, patient specific anatomic models were created for all 10 patients using the 3D TrueFISP sequences and the SimVascular[172] open-source software package. The first step in the process involved the definition of centerline paths for the aorta and all involved branches. The aortic centerline path (Fig.5A) began just inferior to the cardiac apex and followed the vessel before ending just inferior to the ostia of the coronary arteries. Paths were also defined for the brachiocephalic, left subclavian and left common carotid arteries from their ostia until the level of the brachiocephalic bifurcation. The centerline paths for the coronary arteries followed the respective vessels for as long as they could be accurately visualized. The second step in the modeling process involved manual 2D segmentation of the arterial lumen at discrete locations along the all the centerline paths (Fig.5B). The ostia of other coronary artery branches stemming off the main coronary arteries were occluded in the segmentations. The 2D segmentations were then lofted together to create the desired 3D model (Fig.5C). Lofting is the computational process by which discrete segmentations are connected together along the centerline path by way of smooth curves.
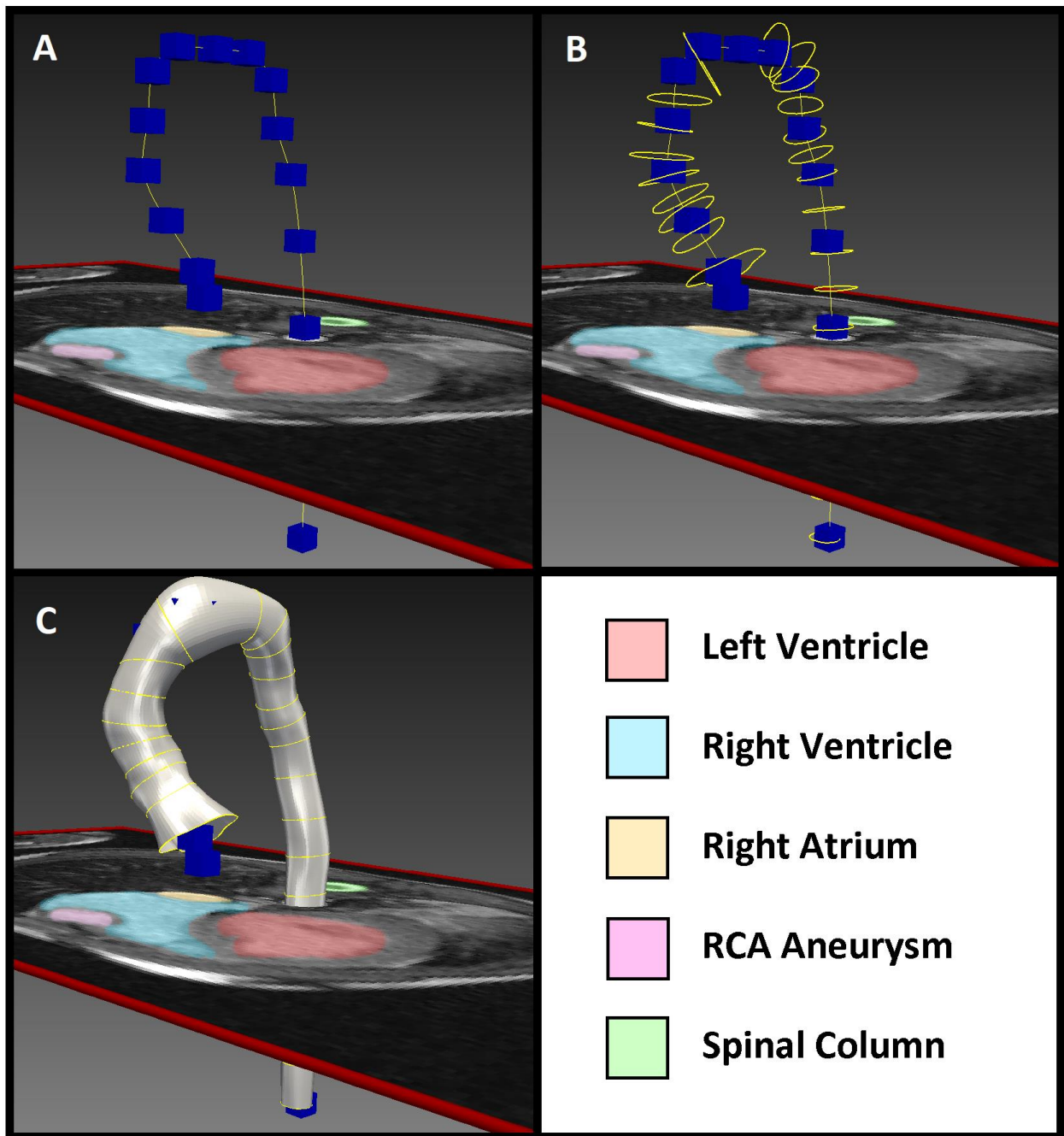
Figure 5. Creating CA models from MRAs: (A) Centerline pathing; (B) 2D segmentations; and (C) lofting segmentations to create 3D patient specific model of the aorta. (Patient 3 from Fig.30)
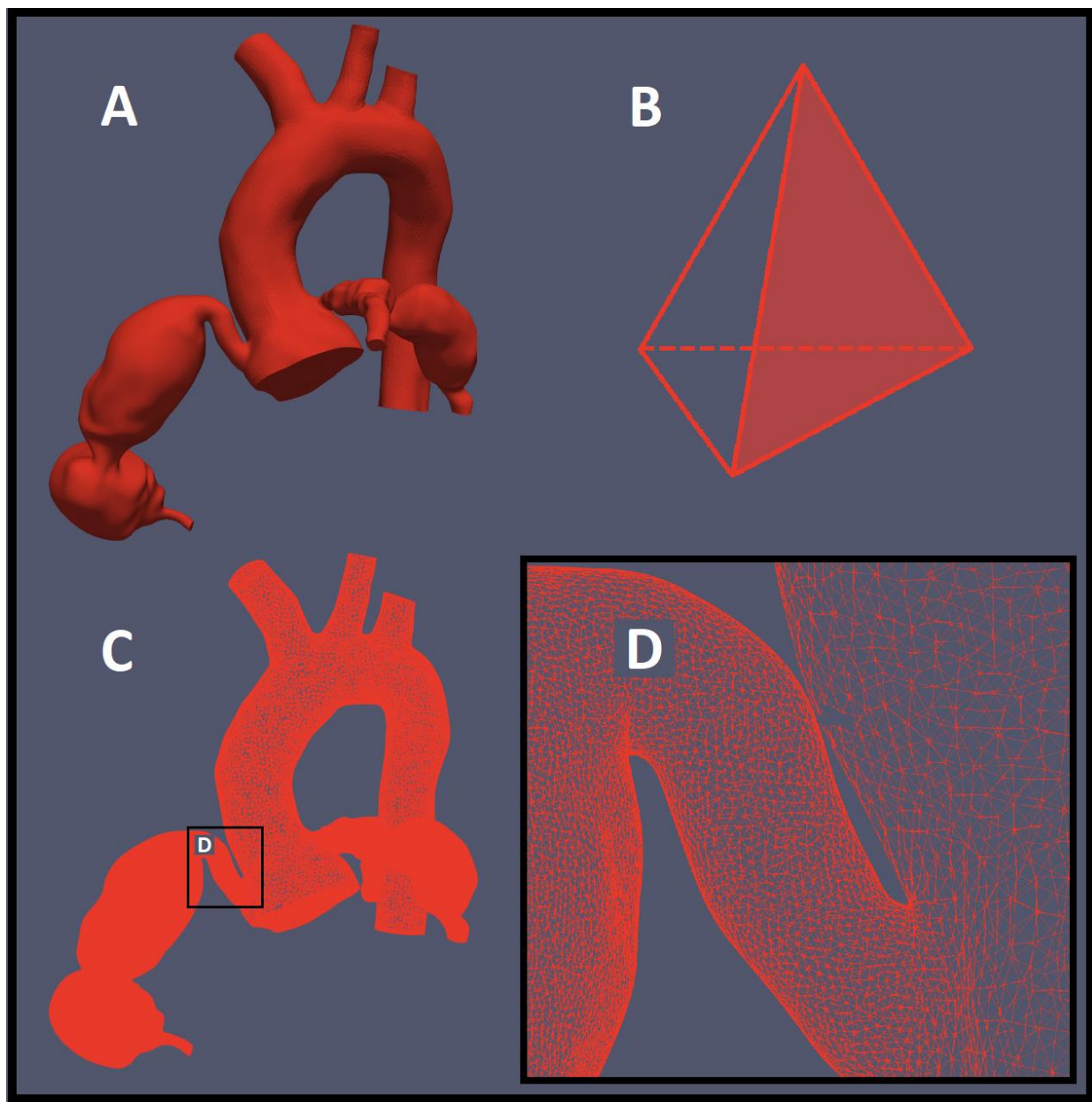
Figure 6. Refined tetrahedral mesh of a patient specific CA model used in CFD simulations (A; Patient 3 from Fig.30). B) Sample tetrahedral with inner wire frame and surface shade (red side). C) CA model for Patient 3, without surface shade (wire frame only). D) Close up of proximal RCA emphasizing tetrahedral elements of different sizes (smaller size and greater number in more refined areas)

The final step in the modeling process was the discretization of the model into a finite element tetrahedral mesh (Fig.6) using the TetGen[173] open-source software package included with SimVascular. A boundary layer mesh with a larger number of finite elements was created to increase the accuracy of simulations near the vessel wall. The meshed model was further refined at the locations of CA aneurysms and bifurcations. Refining the meshed model was an iterative process that involved further tests to determine the convergence of hemodynamic variables while validating the modified model against the original imaging data. Such refinement was necessary to ensure convergence of the solutions. At the end of the process, the meshes for all models contained between 0.6 and 5.6 million elements depending on the size of the patient, length of the modeled vessel and the number of aneurysms per patient. The figure below (Fig.7) allows for a limited comparison of pre-thrombosis conventional angiograms versus models created from MRA segmentation.
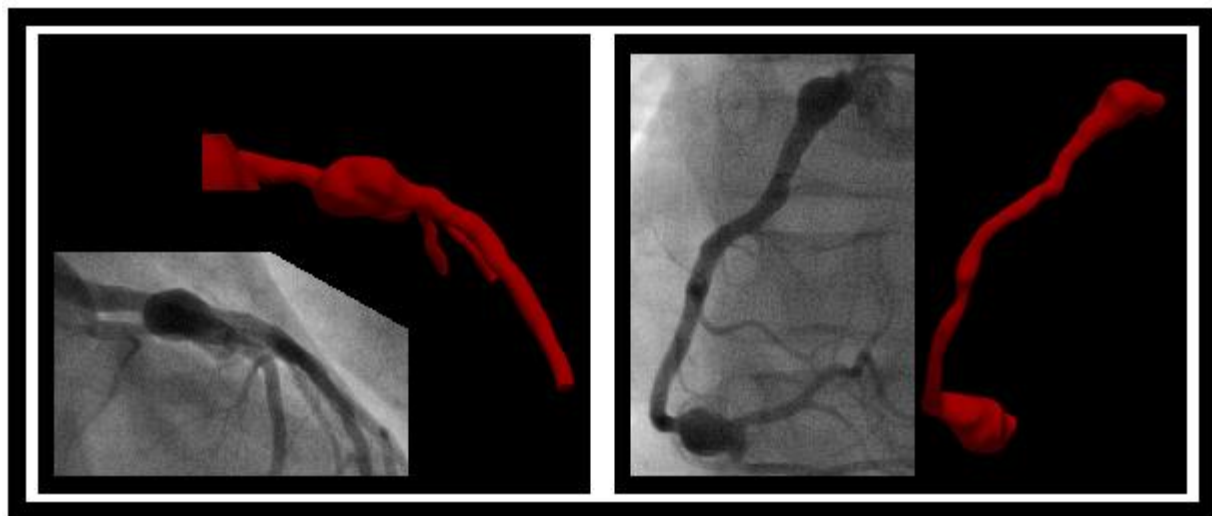
Figure 7. **Comparison of pre-thrombosis conventional angiogram (Greyscale) versus model created from MRA imaging following thrombotic resolution (Red); 2 years between angiogram and MRA; Left coronary system (LCA, LAD, LCX) on left, Right coronary system (RCA) on right. (Patient 1 from Fig.30)**

2.3.6 Coronary artery blood-flow simulations

Blood-flow simulations in coronary arteries are particularly challenging because segmentation models truncate several smaller coronary artery vessels; the vessel wall is compliant and wave propagation and reflection needs to be accounted for; and coronary artery flow is out of phase with aortic flow due to increased flow resistance in distal coronaries during ventricular contraction. As such, sophisticated simulation models and boundary conditions were required to effectively determine patient-specific blood-flow characteristics in coronary arteries.

"Boundary conditions" can be thought of as constraints applied to the equations of a simulated model. They are used to account for the influence of factors external to the model system, and are very important in all types of simulations including CFD. Choosing the correct boundary conditions pose the greatest challenge for simulation methodologies and can determine how meaningful the results are. For each simulation, these conditions may be iteratively refined until simulated behaviour mirrors that expected of real world physiology. Consequently, real world measures (systolic/diastolic blood pressure and cardiac output) were necessary for establishing and validating boundary conditions.

2.3.7 Modelling Blood-flow

Blood was modelled as an incompressible Newtonian fluid, the simplest mathematical model of a fluid that accounts for its viscosity. Blood density and dynamic viscosity were set to 1.06 g/cc and 0.04 dynes/cm^2 respectively, representing physiological measures at 37^{0}C[174]. The finite element solver included with SimVascular was used to perform a finite element analysis on the discretized elements of the 3D models. Specifically, the program was used to solve the time-dependent Navier-Stokes equations that describe the motion of viscous fluids such as blood.

2.3.8 Modelling Vessel Wall Deformability

Arterial walls are deformable in the sense that their structure can be influenced by external or internal forces such as those of blood-flow. This deformability can greatly affect blood pressure and velocity fields and needs to be accounted for. Consequently, the coupled momentum method described by Figueroa *et al.* was used to establish a new boundary condition for the fluid[175]. The method simulates wall deformation using membrane approximations and the small deformation theory. The small deformation theory assumes that the deformations of a material do not affect its constitutive properties such as density or stiffness. Vessel wall properties and wall thickness for the aorta and coronary arteries were assigned based on prior work from the Marsden lab[176, 177]. Phase contrast CMRI data was used to estimate the patient-specific elastic modulus (Young's modulus; measure of the ability of a material to withstand changes in length) for the aorta. The elastic modulus for the coronary artery and aortic branches were assigned based on values reported in the literature[178, 179]. Wall thickness for the coronary arteries was also assigned based on pre-existing literature[180], but was calculated for the other arterial branches using reported radius to wall thickness ratios[181].

2.3.9 Closed-Loop Lumped Parameter Models

"Lumped parameter models" are reduced order mathematical models (less computational complexity) that succinctly account for the influence of multiple factors (Eg. Resistance from other minor coronary artery branches that were occluded from the model) outside the simulated system (the 3D CA model). These models are based on the application of electrical circuit schematics to pressure-driven flow systems. Electrical voltage, current, capacitance, resistance and inductance are used to model pressure, flow rate, dissipative forces, vessel wall compliance and inertial effects respectively. Multiple lumped parameter models can work together to form a lumped parameter network (LPN). The flow output from an LPN can feed back into the inlets to create a closed-loop model if appropriate. In the case of the arterial models used in this study, the distal ends of the CAs, the descending aorta and the 3 branches of the aortic arch acted as flow outlets. The ostia of the aortic root was the only inlet.

An investigation on the validity of LP networks was beyond the scope of this thesis, but closed-loop LPNs have been widely used in simulation based cardiac studies, including those involving the coronary arteries[182-185]. A similar framework was applied to the discretized, patient specific anatomical models in this study (Fig.8), where pressure and flow information for the LPN was solved numerically to establish a "0D" domain. This 0D domain was coupled with the 3D finite element flow solver using the complex semi-implicit scheme described by Moghadam *et al*[186]. Backflow at the coupled faces of the model (Eg. Flow from 3D aorta model to 0D heart model during systole), leads to rapid divergence (failure) of the simulation solution. To prevent such divergence, additional stabilization elements were added to the outlet nodes, active only during periods of flow reversal (backflow)[186].
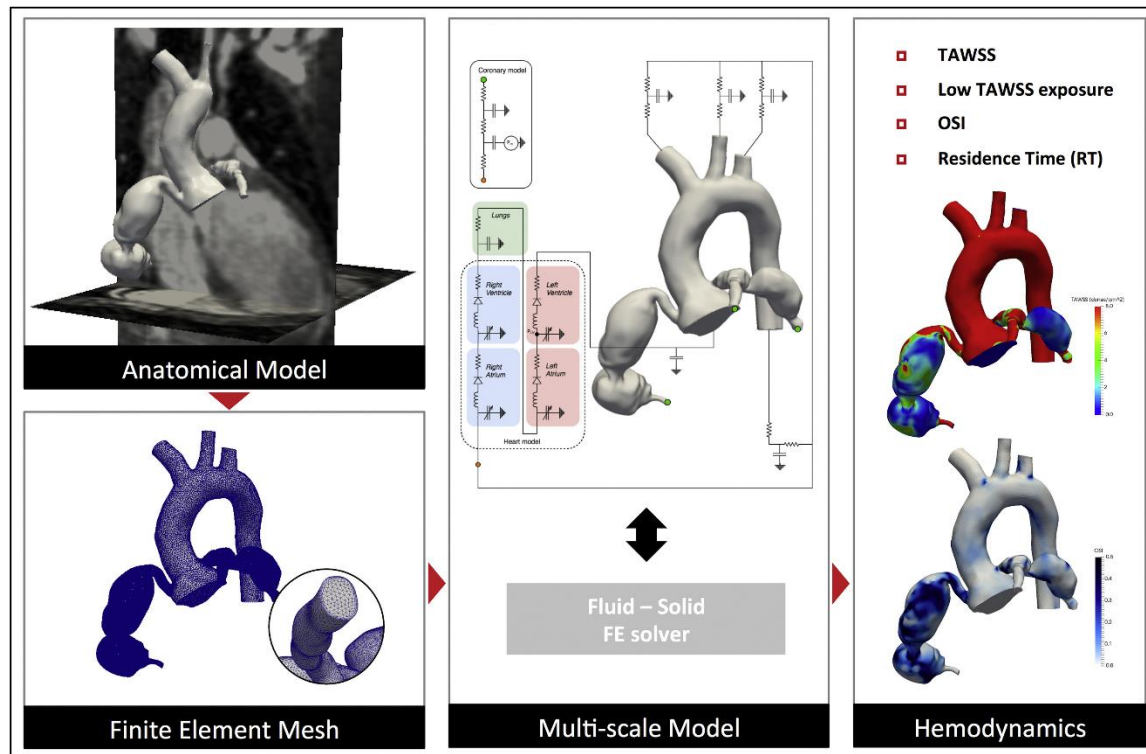
Figure 8. Schematic of the methodology used to obtain the hemodynamic variables. 1) Creating a patients specific 3D model, 2) Applying a finite element tetrahedral mesh, 3) Closed-loop lumped parameter network coupled with a finite element solver, 4) Post processing to obtain hemodynamic variables of interest[170]

An automated tuning method[187] was used to estimate patient specific LPN variables, which were validated using clinical measurements of systolic/diastolic blood pressure and cardiac output for each patient. These variables were normalized to patient specific stroke volume and body surface area to facilitate the automatic tuning process. Estimates matched patient specific clinical measures systematically, with an average error (5.4±4.1%) within clinically accepted ranges.

2.3.10 Hemodynamic and Anatomic Variables

Pressure and velocity fields were obtained for every patient-specific model via CFD simulations. These fields were used to derive measures for hemodynamic variables presumed to be related to thrombus formation. Time averaged wall shear stress (TAWSS) and oscillatory shear indices (OSI) were calculated using Paraview, an open-source visualization and post-processing software package[188]. The quantities were temporarily averaged over one cardiac cycle and spatially averaged over the area of each aneurysm. The proximal ends of aneurysms were defined from the first instance of a Z-score ≥5 and the distal ends were defined at the first instance of Z-score ≤5. Diameters and Z-scores were based on the 3D patient-specific models, not the true image data. Residence time (RT_{branch}) was calculated for each branch (as opposed to each CA aneurysm) using a non-discrete, Eulerian approach that required solving an advection-diffusing equation as described by Moghadam *et al*[189]. This simply means that residence time was calculated by examining how long blood particles stayed in a specified spatial location in the model rather than by following the blood particles through the entire model. Time was advected as a scalar measure in a pre-computed velocity field, and the average time that a parcel of fluid spent in each branch was calculated. The solutions were solved using a finite element method under the assumption of negligible diffusion (diffusion coefficient was set as zero).

2.3.11 Hemodynamics and Risk Stratification

To identify possible hemodynamic thresholds that may help refine current risk stratification criteria for patients with persisting CA aneurysms following KD, receiver operating curves were analyzed for hemodynamic measures found to be associated with thrombosis. Thresholds that maximized the distance from the identity line were considered optimal, and indicative of increased thrombotic risk.

2.3.12 Clinical Measures and Patient Reports

Patient-specific measures of blood pressure, elastic moduli and cardiac output were required to establish and validate the boundary conditions for the CFD simulations. Blood pressure recordings were obtained directly from the MRI and echocardiogram (within a month of MRI) reports and corresponded to measurements from an arm cuff. The patient specific aortic elastic moduli were calculated from changes in cross-sectional area over the cardiac cycle as measured via phase contrast MRI. The elastic moduli for the coronary arteries and the aortic branches were set as per values defined in other literature[178, 179, 181]. Cardiac output was calculated by multiplying the heart rate with the difference between left ventricular end diastolic and systolic volumes. Ventricular volumes were measured from the MRIs. Heart rate was calculated from R-wave to R-wave intervals (electrocardiographic measure of heart rate) averaged with apical measures of heart rate within a month of the MRI. The earliest date recorded for thrombotic or stenotic events corresponded to the date of the first echocardiogram they were visualized on, if confirmed on succeeding angiograms, MRIs or CTs. Patient reports described additional findings from clinical chart review and included details on patient presentation, aneurysm progression, cardiac interventions and original imaging findings as well as acute and long-term medical management.

2.3.13 Statistical Analysis Part Two

Hemodynamic and anatomic measures (TAWSS, OSI, Maximum Diameter and Maximum Z-score) were compared between thrombosed and non-thrombosed CA aneurysms and branches using a Wilcoxon rank test with p-values <0.05 considered

significant. The same test was used to compare residence times between CA branches with thrombotic occlusions and those with only CA aneurysms. Repeated measures were not accounted for and flow features were considered coronary artery branch specific although the CFD simulations treated the entire model as a whole. A Pearson's linear correlation test then evaluated correlations between hemodynamics features and CA aneurysm diameter or Z-score. Finally, receiver-operating characteristic curves were plotted for both hemodynamic and dimensional measures and the area under the curves were compared.

Chapter 3: Results

3.1 Part 1: Coronary artery anatomy based investigations

3.1.1 Cohort characteristics

Table 6 provides descriptive statistics for the cohort used in study part one. Clinical variables considered for the Cox proportional hazard models are included as well as incidents of thrombosis or stenosis. Results are presented as either numbers and proportions, means and IQR or means and standard error, as deemed appropriate. Patients with large CA aneurysms represent more than 25% of the total cohort, and are noticeably different with regards to adverse outcomes and medical management. It is especially important to note that only 2 patients with CA aneurysms of Z-score <10 had any adverse outcomes. This formed the basis for exclusion of branches with only small or medium CA aneurysms in all subsequent analyses. Results from the subsequent analyses are presented with Cox proportional hazard survival plots using failure rates rather than freedom from outcomes, with means and standard error as well as number at risk at the given time point. All figures define the upper and lower limits of the 95% confidence interval with appropriate shading and provide p-values for univariate analyses. The number of patients remaining at risk are presented below the trend lines, at significant time points.

Table 6. Patient characteristics of the cohort used in study part one

Characteristics	(N)	All patients	(N)	Large CAAs
Cohort	1,651		440	
Sex (male)	-	1,184 (72%)	-	316 (72%)
Echocardiogram reports	-	5 (3 − 8) / patient	-	9 (5 − 14) / patient
Duration of follow-up (years)	-	2.05 (0.89 − 6.38)	-	5.16 (1.93 − 8.94)
Duration of fever pre-IVIG (days)	1,578	7 (5 − 10)	406	9 (6 − 14)
Total Fever Duration (days)	1,553	9 (7 − 13)	407	13 (9 − 17)
Age at diagnosis	1,651		440	
<6 months	-	282 (17%)	-	128 (29%)
0.5 to <1 year	-	240 (15%)	-	66 (15%)
1 to <5 years	-	744 (45%)	-	142 (32%)
5 to <10 years	-	306 (18%)	-	79 (18%)
≥10 years	-	79 (5%)	-	25 (6%)
Type of KD reported	1,633		433	
Complete	-	973 (60%)	-	225 (52%)
Incomplete	-	660 (40%)	-	208 (48%)
Laboratory values pre-IVIG	-		-	
Hemoglobin (g/L)	1,350	105.74 ± 14.19	323	101.21 ± 15.65
Hematocrit (%)	1,300	0.31 ± 0.04	302	0.30 ± 0.04
ESR (mm/hr)	1,166	62.00 (46.00 − 88.00)	262	70.00 (50.00 − 100.00)
White blood cells (WBC) (x109/L)	1,358	16.08 ± 6.82	326	18.21 ± 8.41
Platelets (x109/L)	1,339	441.86 ± 219.71	325	522.84 ± 265.41
Albumin (g/L)	1,003	31.61 ± 6.44	228	28.81 ± 6.18
C-reactive protein (CRP) (mg/L)	1,140	59.16 ± 77.94	265	65.08 ± 75.11
Acute treatment	-		-	
IVIG	1,646	1,592 (97%)	437	414 (95%)
Steroids IV	1,525	288 (19%)	428	141 (33%)
Convalescent treatment	-		-	
Aspirin	1,648	1,637 (99%)	440	439 (100%)
Clopidogrel/Plavix	1,555	283 (18%)	435	171 (39%)
Low molecular weight heparin (LMWH)	1,556	223 (14%)	434	187 (43%)
Warfarin/Coumadin	1,551	204 (13%)	438	190 (43%)
Beta blockers	1,535	134 (9%)	433	113 (26%)
Statins	1,632	55 (3%)	439	43 (10%)
Outcomes	1,651		440	
Thrombosis	-	68 (4%)	-	67 (15%)
Stenosis	-	61 (4%)	-	60 (14%)
Branches	-	3,535	-	865

3.1.2 Evaluating the effects of CA anatomy on thrombotic risk in patients with large CA aneurysms following KD

Table 7 outlines the clinical and structural features selected by the multivariable Cox proportional hazard model for thrombotic risk. The upper (UCL) and lower (LCL) limits are presented for the 95% confidence interval. Selected clinical features included treatment with IVIG or IV steroids as well as laboratory measures of pre-IVIG C-reactive protein (CRP). Early treatment with IVIG and higher levels of pre-IVIG CRP were associated with decreased thrombotic risk; treatment with IV steroids was associated with increased thrombotic risk.

Maximum CA aneurysm Z-score was consistently selected, and larger CA aneurysms were associated with increased thrombotic risk. The only other structural feature selected by the model was branch anatomy where branches with multiple aneurysms were more like to thrombose than those with isolated aneurysms. Vessel dilation around an isolated aneurysms did not seem to have much of an effect on thrombotic risk (Fig.9). It is also evident that most thrombotic events occur within a year of illness, after which there is a lower but constant risk phase.

The model did not select coronary artery branch, involvement of the left bifurcation, aneurysm location within a branch, aneurysm shape, aspect ratio or cross-sectional area. However, univariate analyses weakly suggested that aneurysms of the RCA and LAD (Fig.10), or those that involve the left bifurcation (Fig.11), are more likely to thrombose. Aneurysm location (Fig.12) and shape (Fig.13) were not univariately associated with thrombotic risk. Larger (Fig.14) and more saccular (Fig.15) CA aneurysms, as determined by cross-sectional area and aspect ratio, were associated with increased thrombotic risk.

Table 7. Cox proportional hazard model for thrombosis with percent reliability, estimates (EST) and standard errors (SE), hazard ratios, lower (LCL) and upper (UCL) confidence limits and p-values.

Multivariable risk factors	Reliability	EST (SE)	Hazard	LCL	UCL	p
Structural features						
Maximum CAA z-score (/z unit)	100	0.0674 (0.0051)	1.07	1.058	1.082	<0.001
Branch Anatomy	89					
Isolated aneurysm in normal vessel		Referent category	-	-	-	-
Isolated aneurysm in a dilated vessel		0.3063 (0.4329)	1.358	0.581	3.173	0.48
Complex aneurysms		0.9121 (0.4173)	2.489	1.099	5.641	0.03
Clinical features						
Treatment with IVIG	95	-1.3300 (0.3826)	0.264	0.125	0.56	0.001
IV steroids	64	0.4432 (0.2375)	1.558	0.978	2.481	0.06
C-reactive protein (/mg/L)	71	-0.0053 (0.0024)	0.995	0.99	0.999	0.03
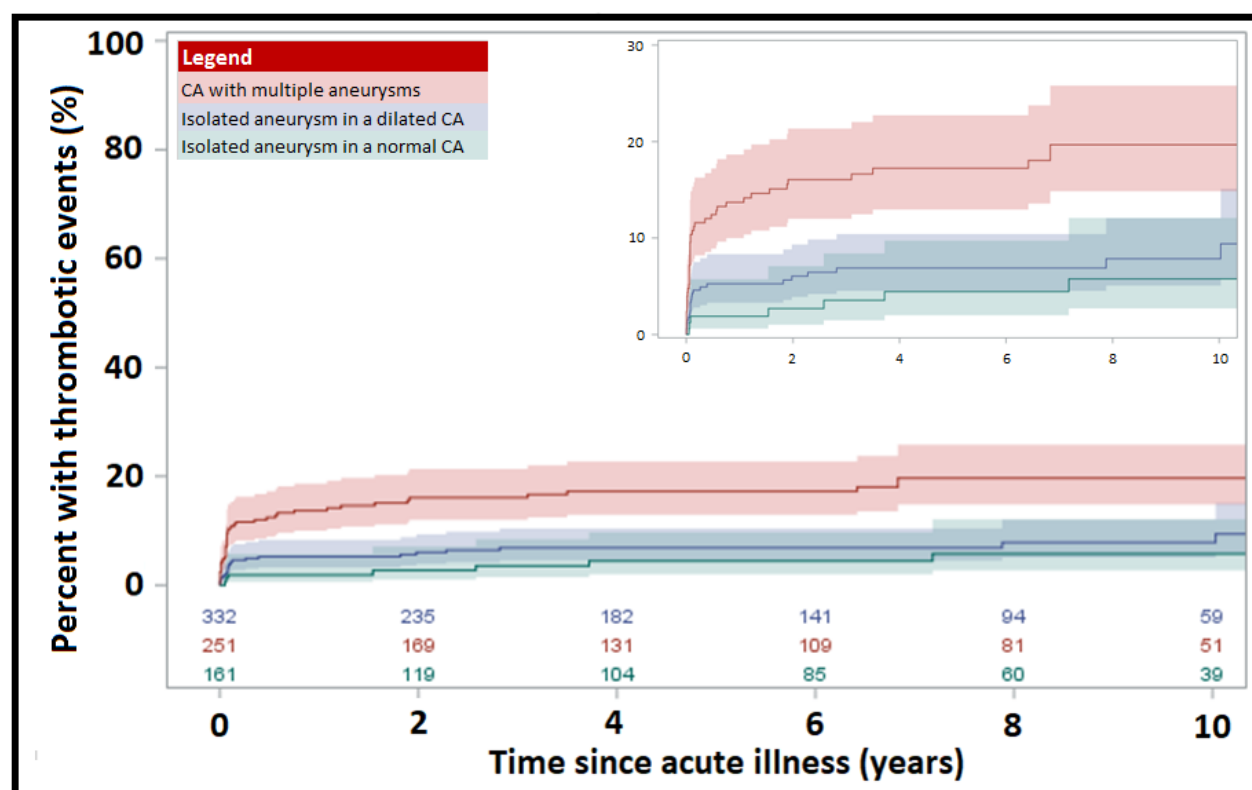
Figure 9. Percentage of CA branches with aneurysms with Z-score >10 and thrombotic events within 10 years following KD diagnosis, classified by the branch complexity with regards to aneurysms and dilations. Classifier selected by multivariable model with p<0.05. Inset (top-right corner)
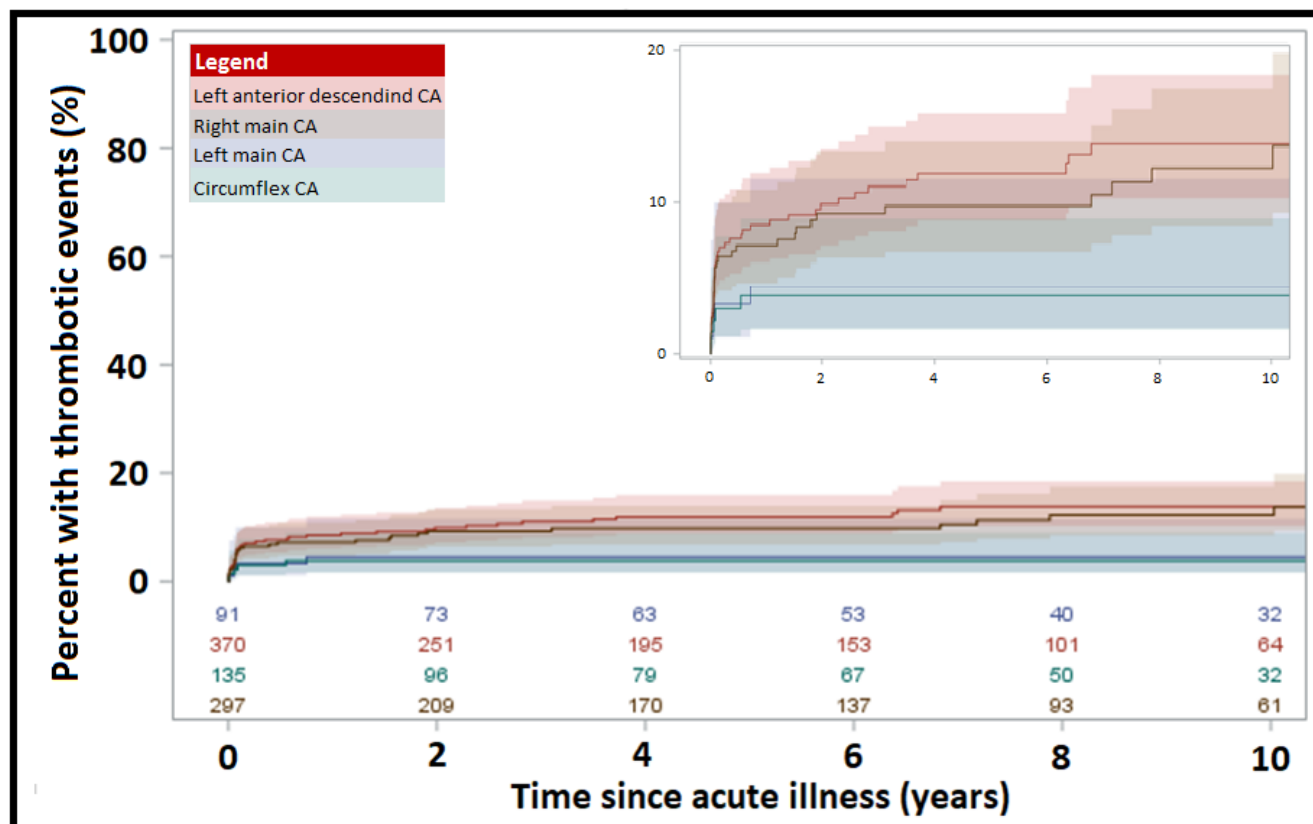
Figure 10. Percentage of CA branches with aneurysms of Z-score >10 and thrombotic events within 10 years following KD diagnosis classified by CA branch. Univariately significant with p=0.01. Inset (top-right corner)
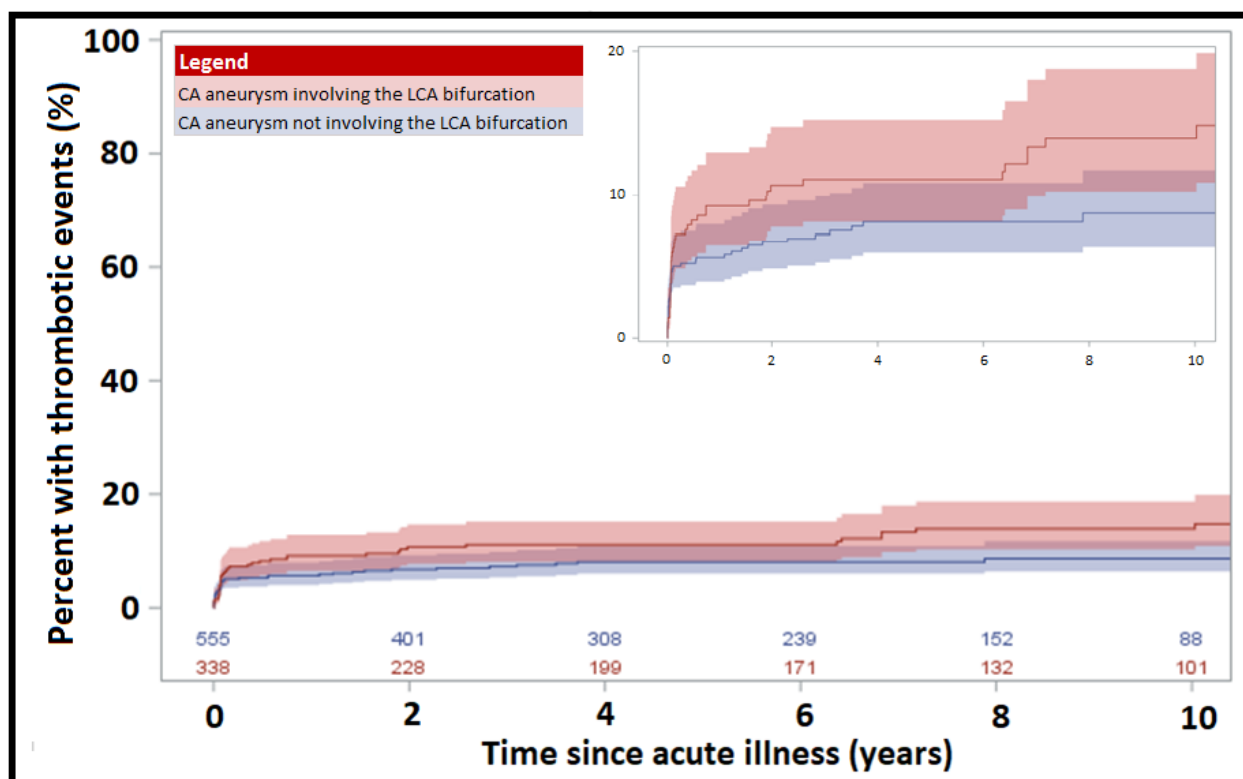
Figure 11. Percentage of CA branches with aneurysms of Z-score >10 and thrombotic events within 10 years following KD diagnosis classified by aneurysmal involvement of the left main CA bifurcation. Univariately significant with p=0.05. Inset (top-right corner)

Figure 12. Percentage of CA branches with aneurysms of Z-score >10 and thrombotic events within 10 years following KD diagnosis, classified by aneurysm location within a CA branch. Not univariately significant with p=0.08. Inset (top-right corner)

Figure 13. Percentage of CA branches with aneurysms of Z-score >10 and thrombotic events within 10 years following KD diagnosis, classified by aneurysm shape. Not univariately significant with p=0.21.

Inset (top-right corner)

Figure 14. Percentage of CA branches with aneurysms of Z-score >10 and thrombotic events within 10 years following KD diagnosis, classified by aneurysm cross-sectional area. Univariately significant with p<0.001

Figure 15. Percentage of CA branches with aneurysms of Z-score >10 and thrombotic events within 10 years following KD diagnosis, classified by aneurysm aspect ratio. Univariately significant with p<0.003.

Inset (top-right corner)

3.1.3 Evaluating the effects of CA anatomy on risk for stenosis in patients with large CA aneurysms following KD

Table 8 outlines the clinical and structural features selected by the Cox proportional hazard model for risk of CA stenosis. The upper (UCL) and lower (LCL) limits are presented for the 95% confidence interval. Younger patients who present with a longer duration of fever and are treated with a lower number of IVIG doses have an increased long-term risk of CA stenosis. Acutely, arthritic symptoms, higher WBCs and lower serum albumin levels are associated with increased stenotic risk.

Maximum CA aneurysm Z-score was consistently selected, and larger aneurysms were associated with increased incidence of stenosis. The model also selected the CA branch, branch anatomy and the involvement of the left bifurcation. The RCA and LAD (Fig.16) as well as branches with multiple CA aneurysms (Fig.17), or those with coronary artery aneurysms involving the left bifurcation (Fig.18) are at a higher risk for stenosis. However, vessel dilation around an isolated CA aneurysm did not seem to have any influence on outcomes. The risk for CA stenosis was constant regardless of time at risk.

The model did not select aneurysm location within a CA branch, aneurysm shape, aspect ratio or cross-sectional area. Aneurysm shape does not affect stenotic risk regardless of the means of reporting (Fig.19; Fig.20). While there does not appear to be a difference in the risk for stenosis in proximal versus distal CA aneurysms, those that involve both segments of the coronary artery do have an increased risk of stenosis (Fig.21). The cross-sectional area of an aneurysm was also univariately associated with an increased risk for stenosis (Fig.22).

Table 8. Cox proportional hazard model for stenosis with percent reliability, estimates (EST) and standard errors (SE), hazard ratios, lower (LCL) and upper (UCL) confidence limits and p-values

| Multivariable risk factors	Reliability	EST (SE)	Hazard	LCL	UCL	p
Structural features						
Maximum CAA z-score (/z unit)	100	0.0363 (0.0065)	1.037	1.024	1.050	<0.001
Branch Anatomy	99					
Isolated aneurysm in normal vessel		Referent category				0.95
Isolated aneurysm in a dilated vessel		0.0261 (0.4570)	1.026	0.419	2.514	0.03
Complex aneurysms		0.9153 (0.4280)	2.497	1.079	5.779	<0.001
Branch	87					
Right main CA		Referent category				
Left main CA		-3.1471 (1.1036)	0.043	0.005	0.374	0.004
Left anterior descending CA		-0.4560 (0.2409)	0.634	0.395	1.016	0.06
Circumflex CA		-1.5056 (0.6175)	0.222	0.066	0.744	0.02
Left Main bifurcation involvement	51	0.5720 (0.2505)	1.772	1.084	2.895	0.03
Clinical features						
Number of IVIG doses (/dose)	96	-0.6628 (0.1686)	0.515	0.370	0.717	<0.001
Age at acute KD (/year)	54	0.0637 (0.0311)	1.066	1.003	1.133	0.04
Total fever duration (/day)	71	0.0341 (0.0129)	1.035	1.009	1.061	0.008
Acute phase arthritis	62	-0.8723 (0.4528)	0.418	0.172	1.015	0.054
Albumin level (/g/L)	78	-0.0656 (0.0310)	0.937	0.881	0.995	0.03
White blood cell count (/x10^9/L)	75	0.0460 (0.0156)	1.047	1.015	1.080	0.003
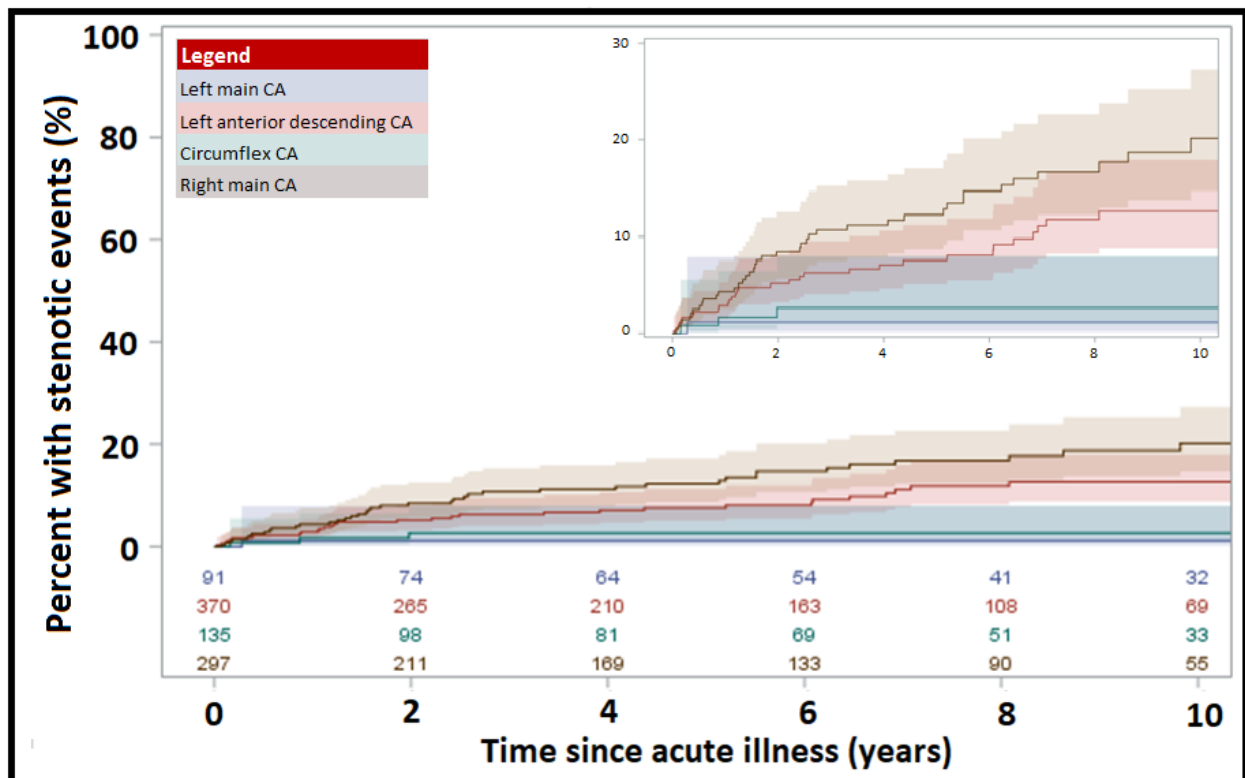
Figure 16. Percentage of CA branches with aneurysms of Z-score >10 and stenotic events within 10 years following KD diagnosis classified by CA branch. Classifier selected by multivariable model with p<0.005. Inset (top-right corner)

Figure 17. Percentage of CA branches with aneurysms of Z-score >10 and stenotic events within 10 years following KD diagnosis, classified by the branch complexity with regards to aneurysms and dilations. Classifier selected by multivariable model with p<0.001. Inset (top-right corner)
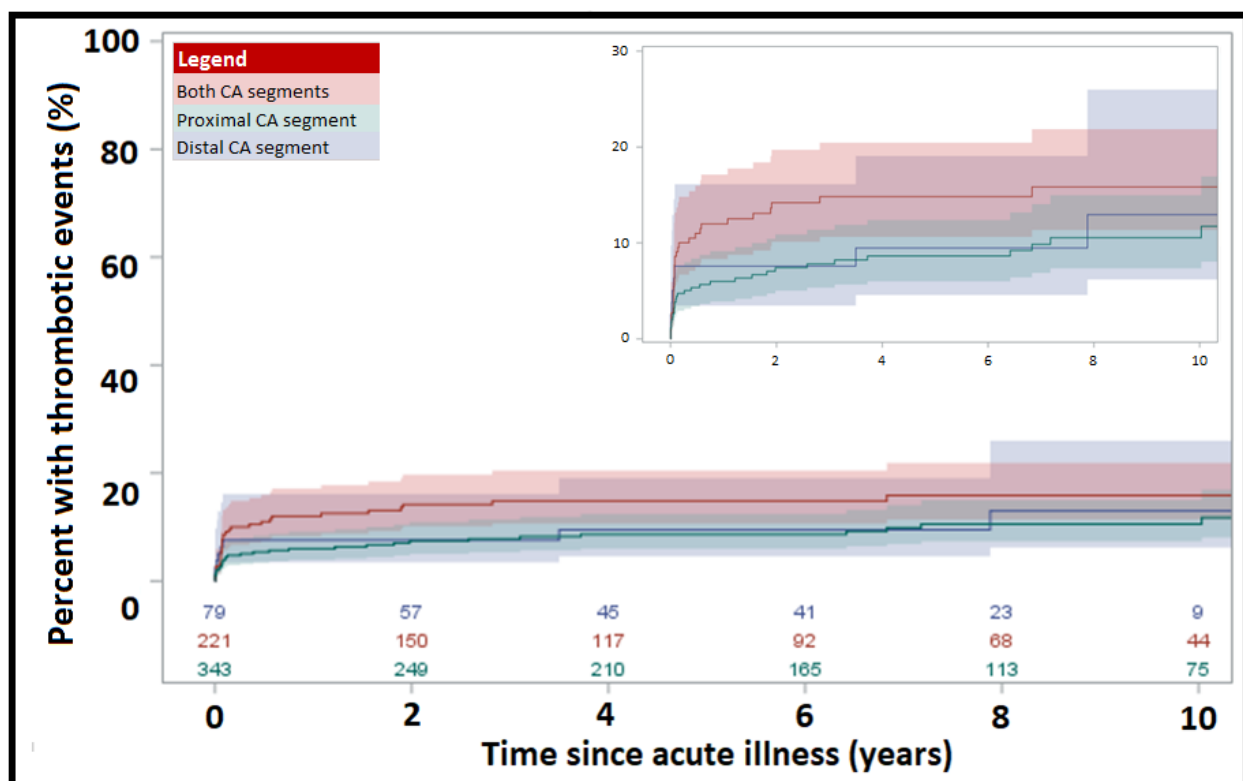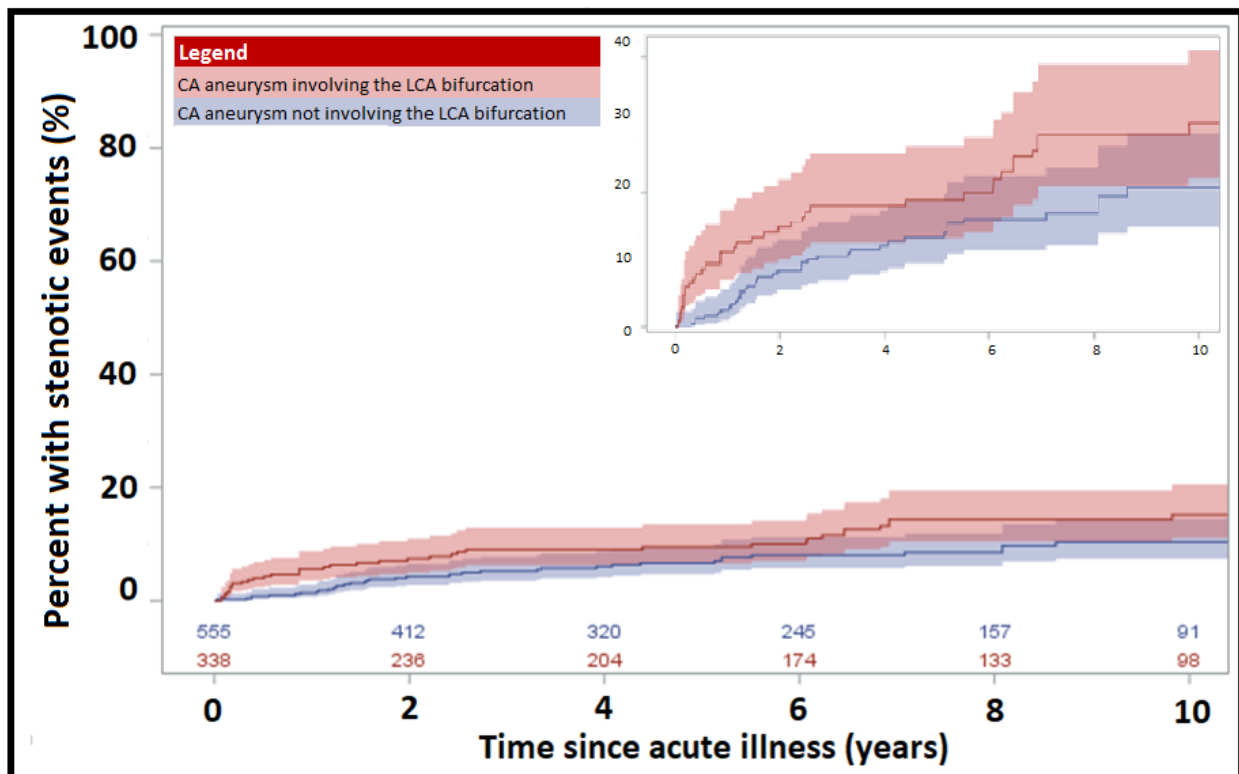
Figure 18. Percentage of CA branches with aneurysms of Z-score >10 and stenotic events within 10 years following KD diagnosis, classified by aneurysmal involvement of the left main CA bifurcation. Classifier selected by multivariable model with p<0.05. Inset (top-right corner)
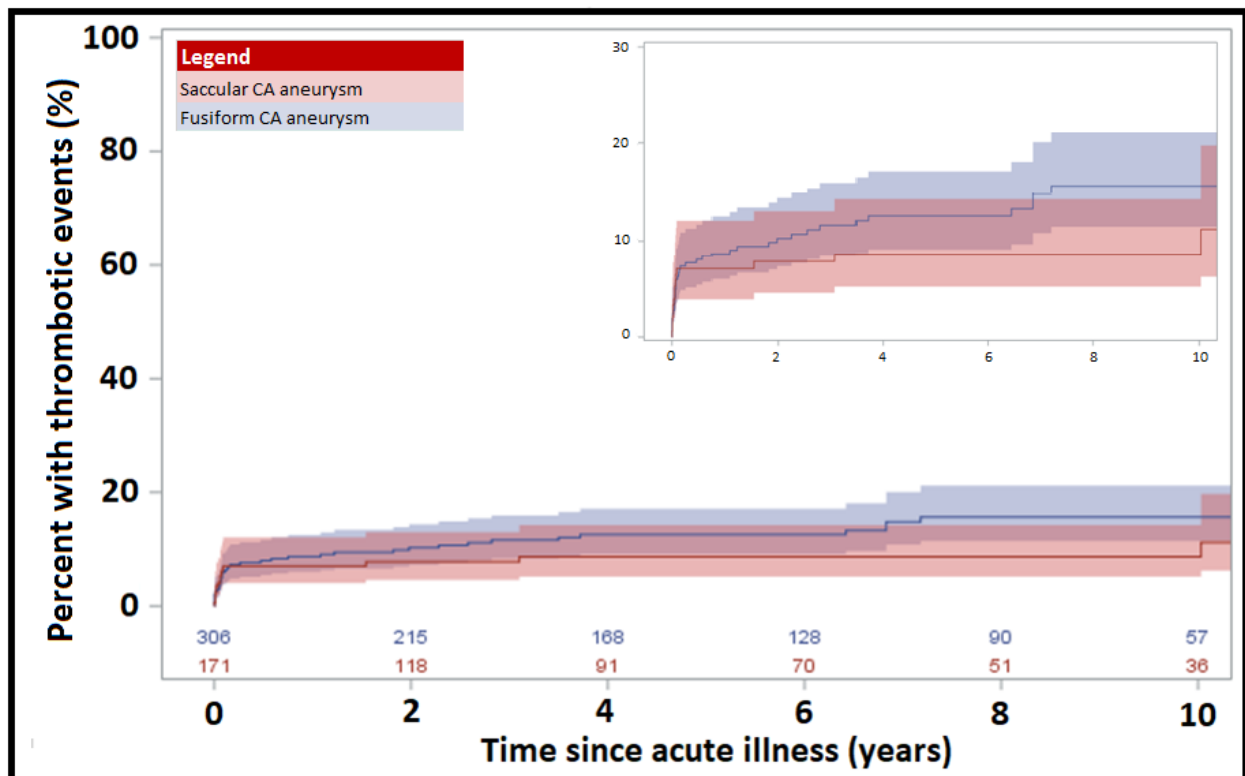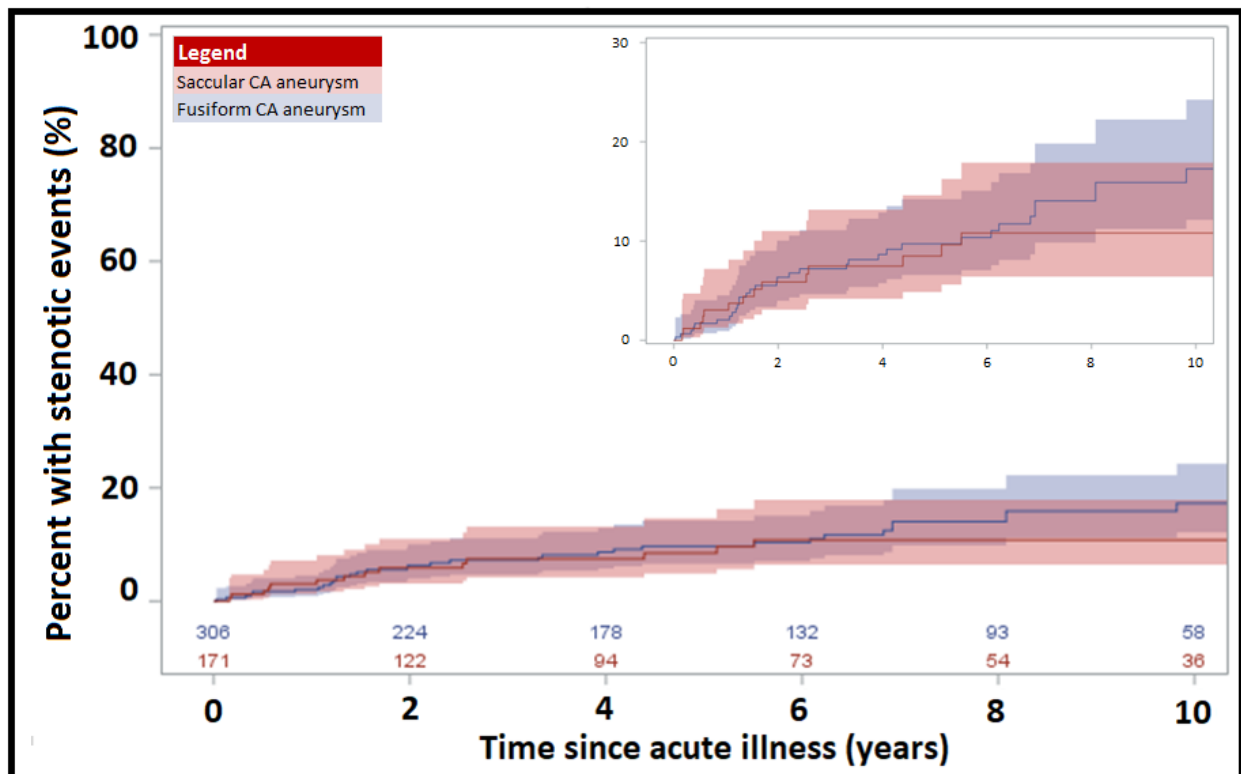
Figure 19. Percentage of CA branches with aneurysms of Z-score >10 and stenotic events within 10 years following KD diagnosis, classified by aneurysm shape. Univariately not significant with p=0.49.
Inset (top-right corner)
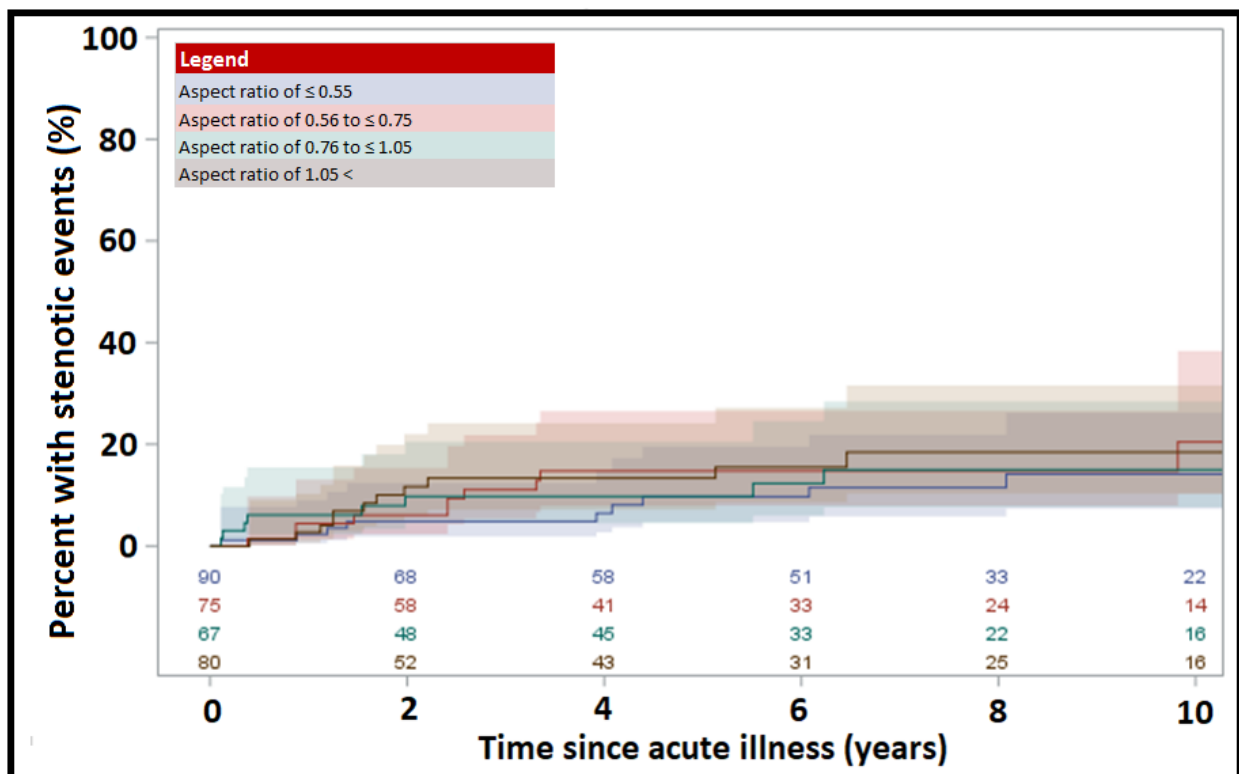
Figure 20. Percentage of CA branches with aneurysms of Z-score >10 and stenotic events within 10 years following KD diagnosis, classified by aneurysm aspect ratio. Univariately not significant with p=0.87
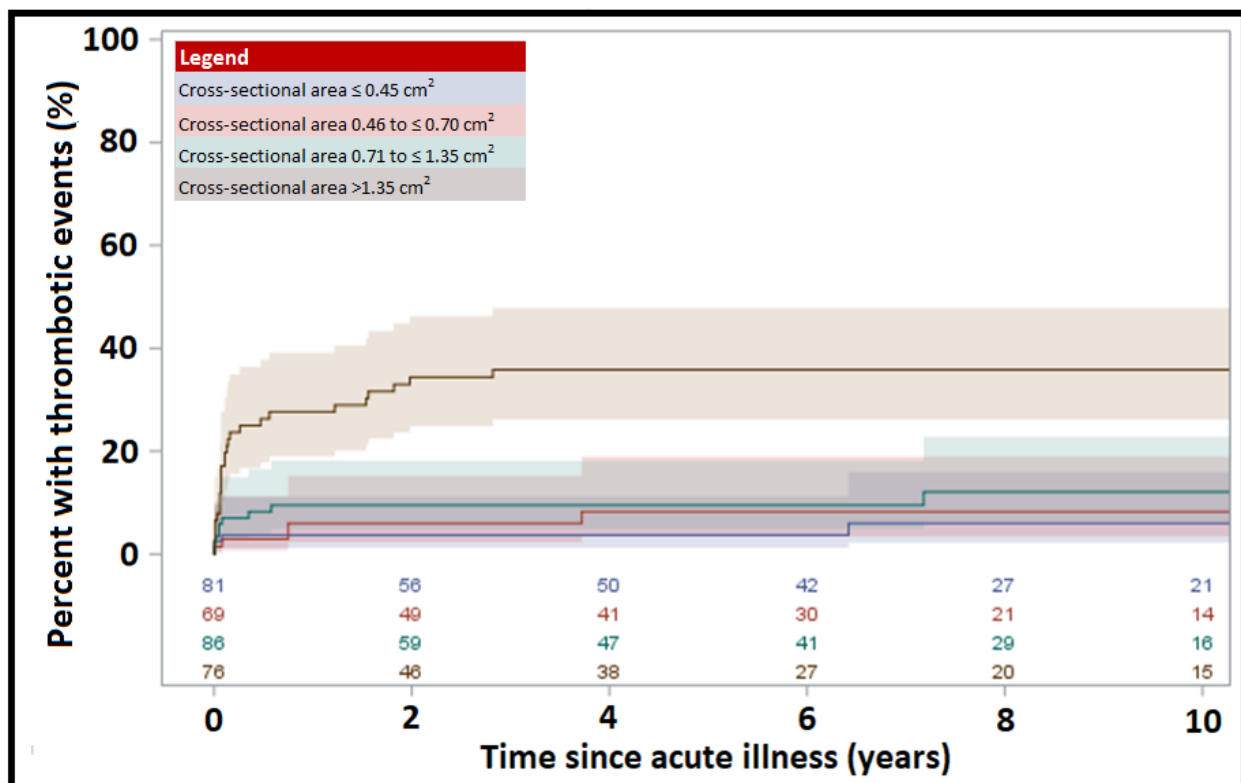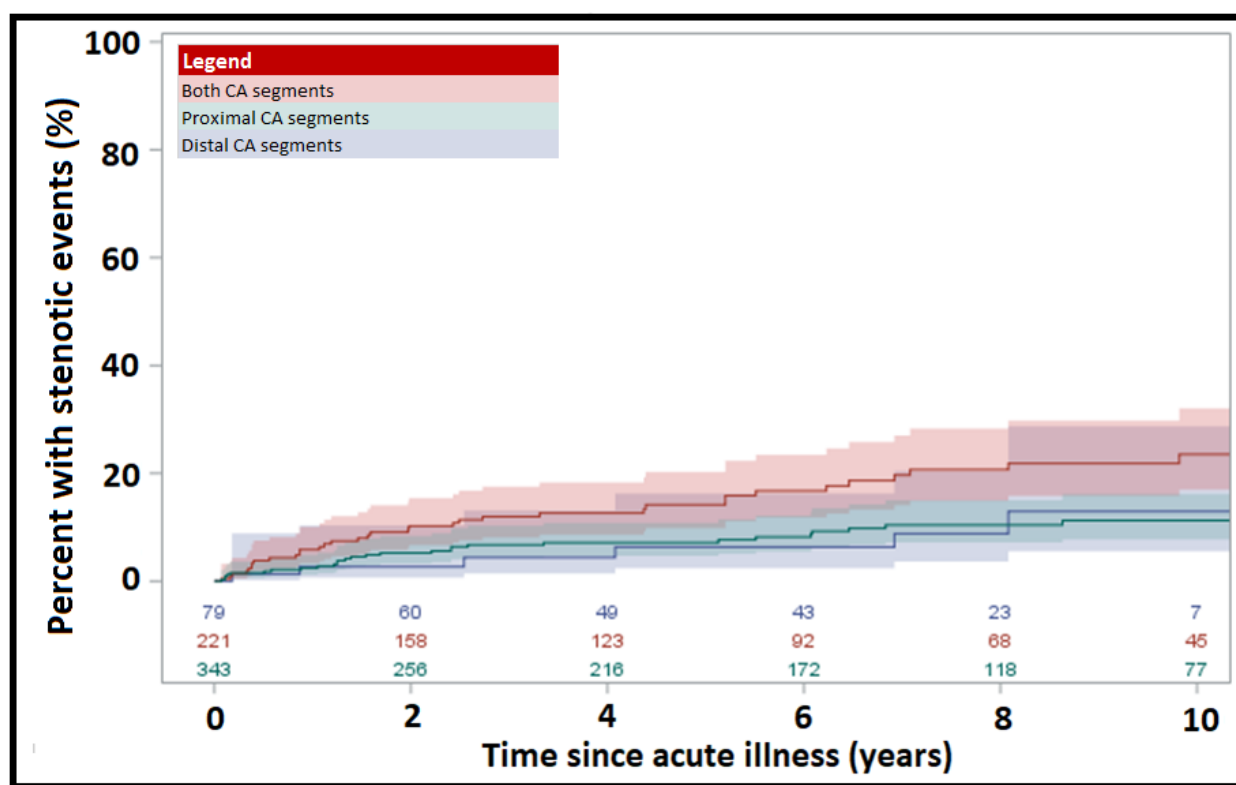
Figure 21. Percentage of CA branches with aneurysms of Z-score >10 and stenotic events within 10 years following KD diagnosis classified by aneurysm location within a CA branch. Univariately significant with p=0.006
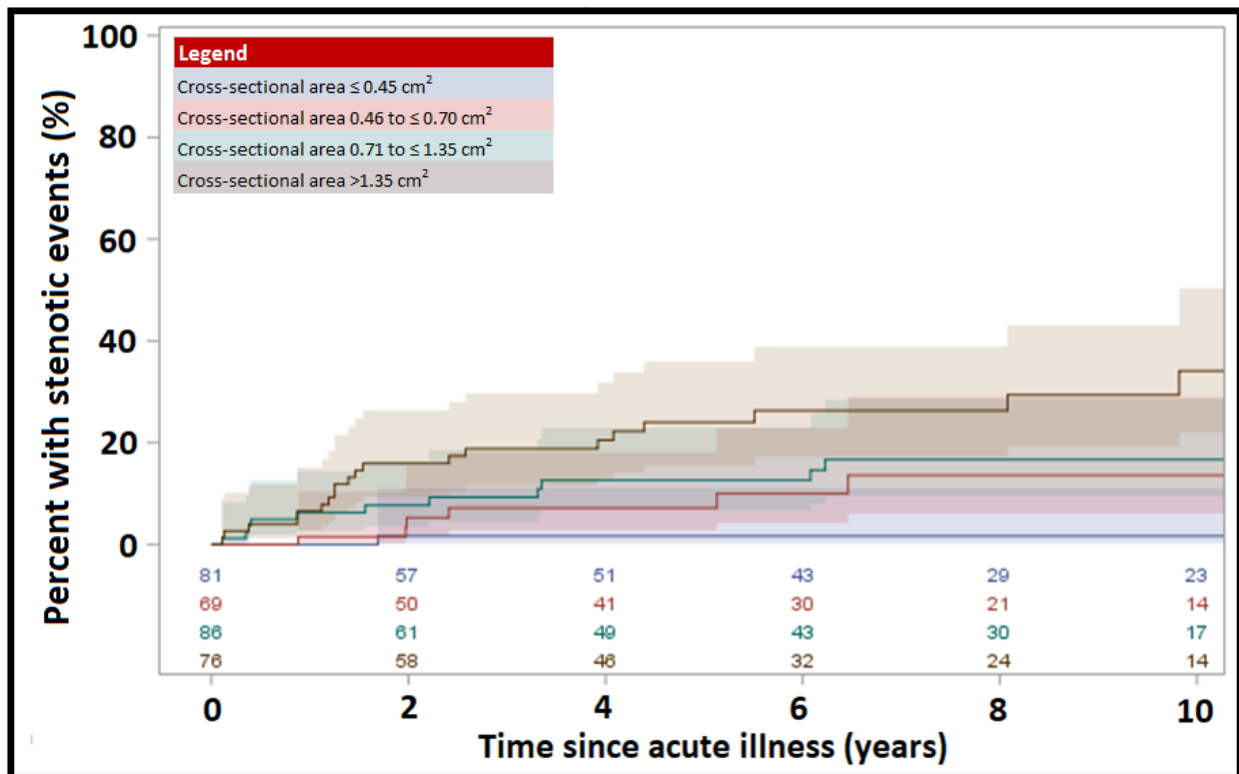
Figure 22. Percentage of CA branches with aneurysms of Z-score >10 and stenotic events within 10 years following KD diagnosis classified by aneurysm cross-sectional area. Univariately significant with p<0.001

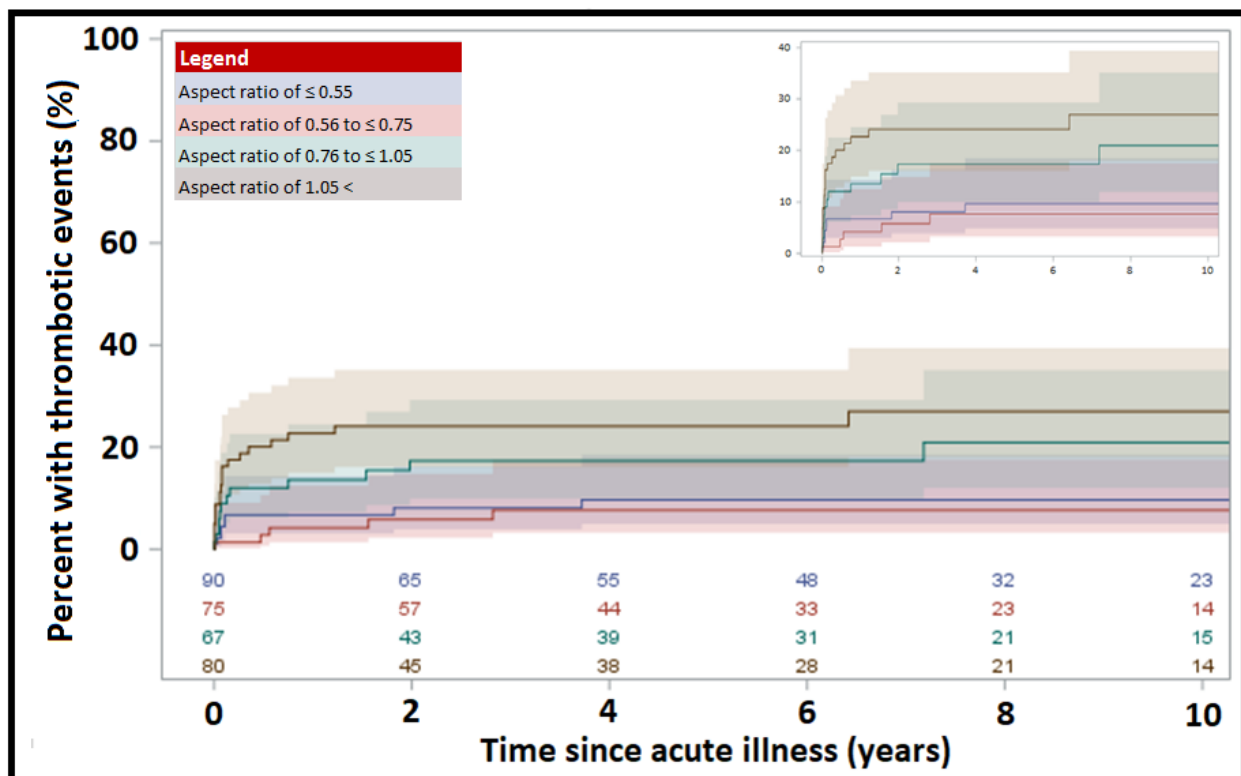### 3.1.4 Evaluating how CA anatomy effects dimensional normalization in patients with large CA aneurysms following KD

Table 9 outlines the clinical and structural features selected by the Cox proportional hazard model for dimensional normalization. The upper (UCL) and lower (LCL) limits are presented for the 95% confidence interval. Younger, female patients diagnosed with complete KD and treated with IVIG are more likely to achieve DN. CA aneurysms in patients with lower pre-IVIG erythrocyte sedimentation rates (ESR) are also more likely to dimensionally normalize over time.

Maximum CA aneurysm Z-score and cross-sectional area were selected by the model, where larger aneurysms using either measure were associated with decreased incidence of dimensional normalization (Fig.23). CA branch was the only other structural feature selected. The LCX and LAD (Fig.24) are more likely to achieve dimensional normalization as compared to the RCA and LCA.

The model did not select branch anatomy, CA aneurysm location, shape, aspect ratio, or involvement of the left bifurcation. Univariate analyses suggest that dilation around an isolated aneurysm was not associated with dimensional normalization, but CA branches with complex aneurysm formation were less likely to normalize than those with isolated aneurysms (Fig.25). Dimensional normalization was more likely for aneurysms further away from the aortic ostia, and CA branches with both proximal and distal portions were least likely to normalize (Fig.26). CA aneurysms that involve the bifurcation of the LCA were also less like to normalize (Fig.27). Aneurysm shape did not affect dimensional normalization regardless of the means of reporting (Fig.28; Fig.29).

Table 9. Cox proportional hazard model for dimensional normalization with percent reliability, estimates (EST) and standard errors (SE), hazard ratios, lower (LCL) and upper (UCL) confidence limits and p-value

Multivariable risk factors	Reliability	EST (SE)	Hazard	LCL	UCL	p
Structural features						
Maximum CAA z-score (/z unit)	100	-0.0651	0.937	0.917	0.957	<0.001
Aneurysm area (cm^2)	100					
>1.35		Referent category	-	-	-	-
0.70 to ≤1.35		0.3379 (0.6048)	1.402	0.428	4.587	0.58
0.45 to ≤0.70		1.3422 (0.5522)	3.827	1.297	11.297	0.02
≤0.45		1.7786 (0.5405)	5.921	2.053	17.083	0.001
Branch	98					
Right main CA		Referent category	-	-	-	-
Left main CA		-0.5733 (0.2278)	0.564	0.361	0.881	0.01
Left anterior descending CA		0.6954 (0.1410)	2.004	1.52	2.643	<0.001
Circumflex CA		0.7464 (0.1645)	2.109	1.528	2.912	<0.001
Clinical features						
Treatment with IVIG	97	1.1540 (0.3480)	3.171	1.603	6.272	0.001
Age at acute KD (/year)	93	-0.0749 (0.0231)	0.928	0.887	0.971	0.001
Incomplete KD	76	0.2460 (0.1147)	1.279	1.021	1.601	0.03
ESR (mm/hr)	71	-0.0051 (0.0021)	0.995	0.991	0.999	0.02
Sex = Female	68	0.2919 (0.1241)	1.339	1.05	1.708	0.02
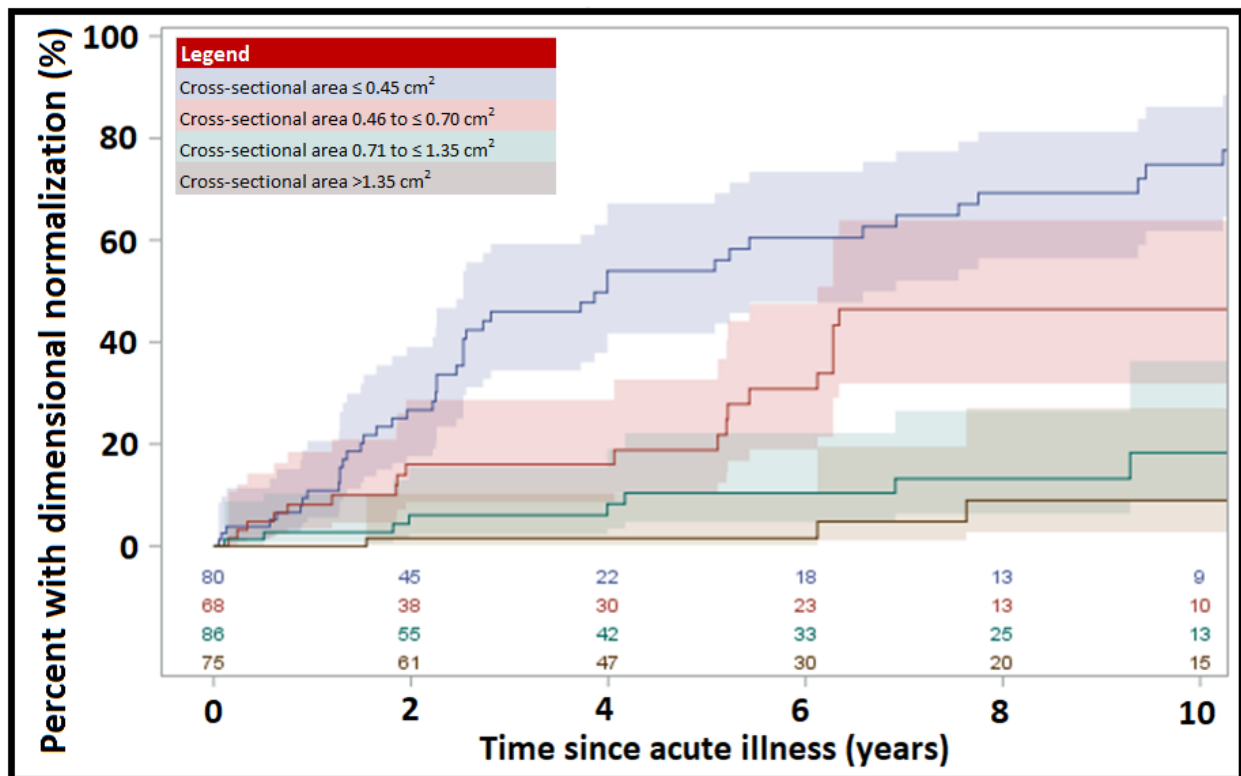
Figure 23. Percentage of CA branches with aneurysms of Z-score >10 that achieve dimensional normalization within 10 years following KD diagnosis classified by aneurysm cross-sectional area. Classifier selected by multivariable model with p<0.005
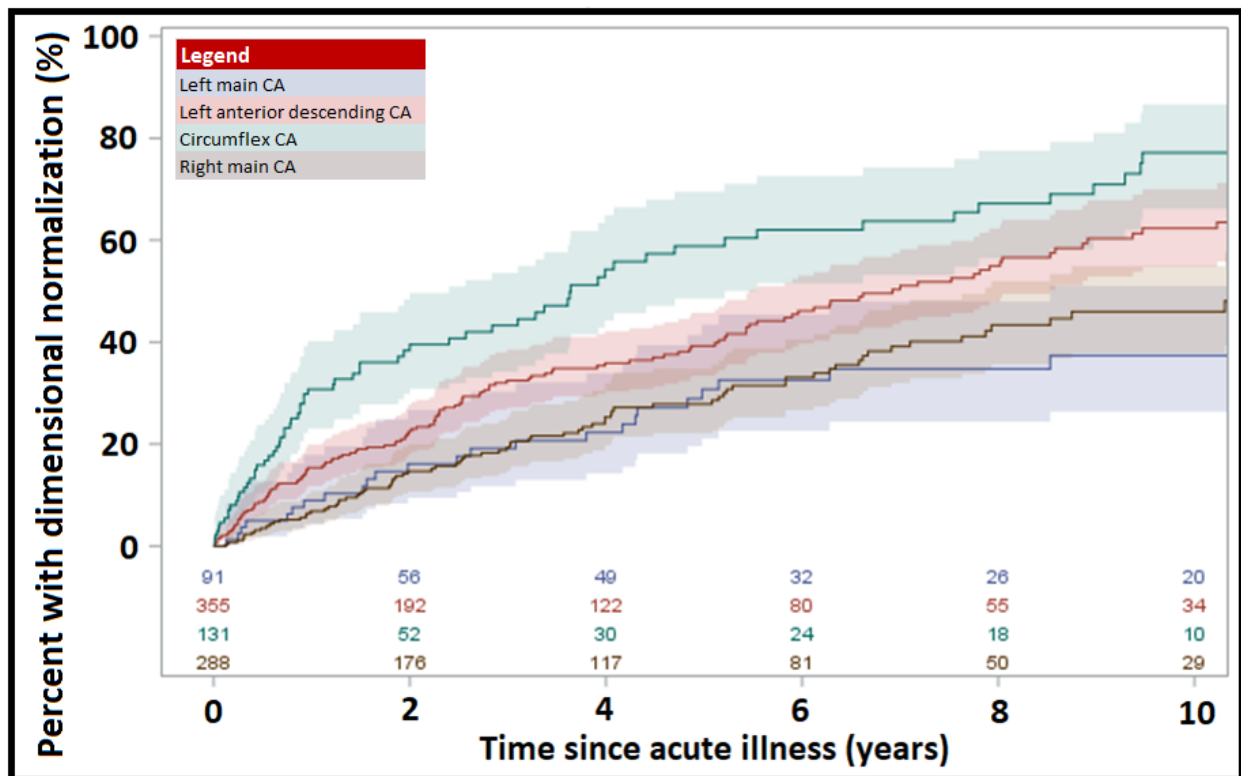
Figure 24. Percentage of CA branches with aneurysms of Z-score >10 that achieve dimensional normalization within 10 years following KD diagnosis classified by CA branch. Classifier selected by multivariable model with p<0.001
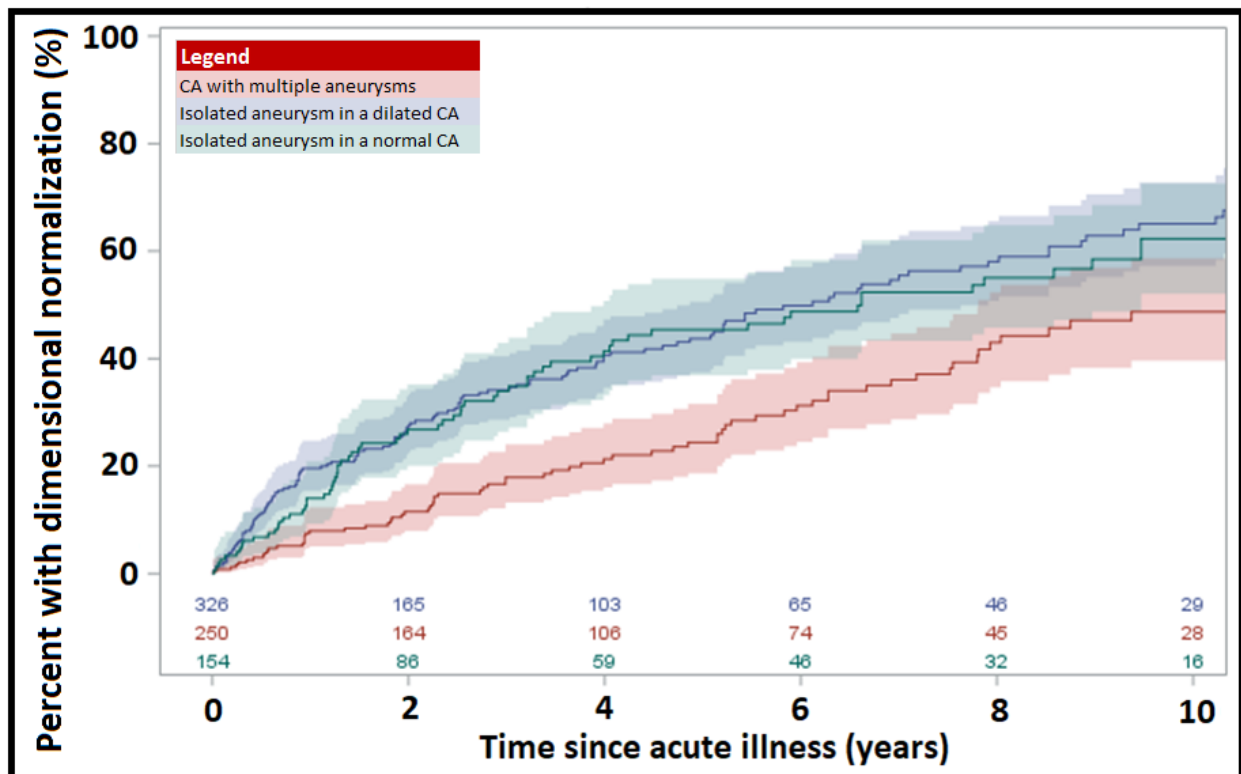
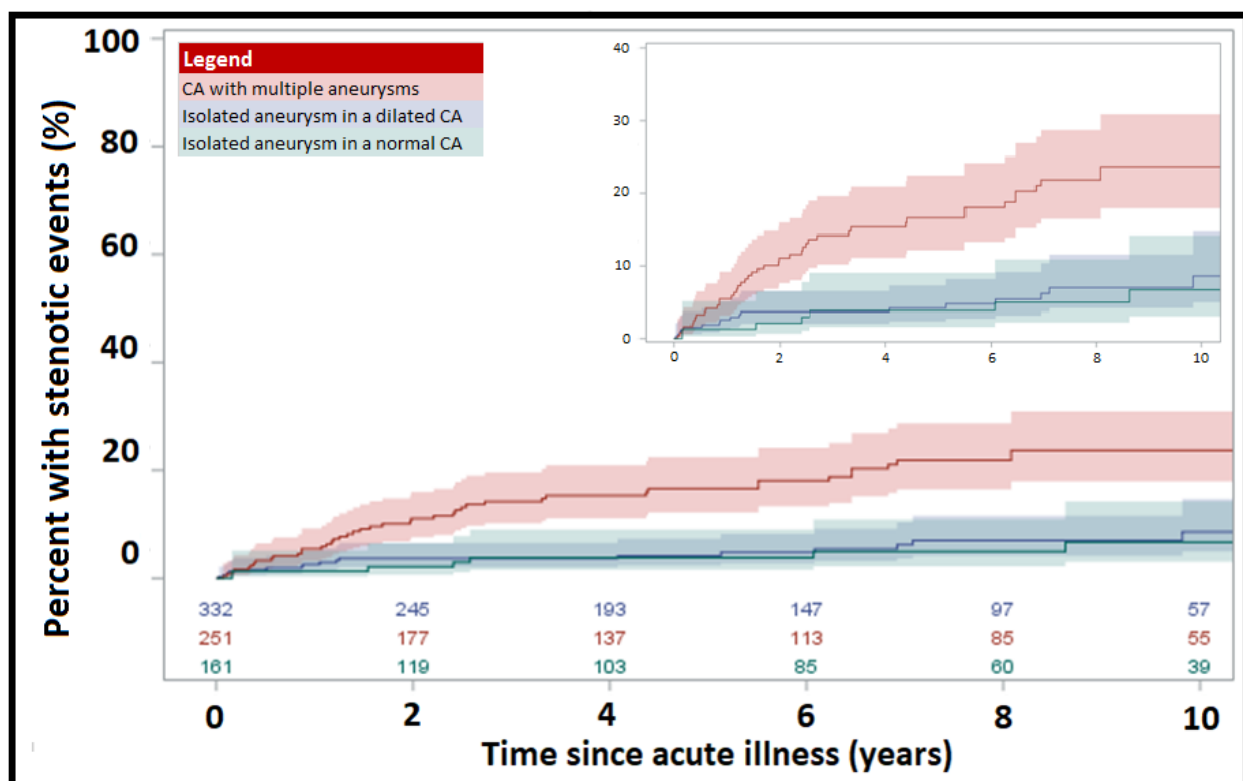**Figure 25.** Percentage of CA branches with aneurysms of Z-score >10 that achieve dimensional normalization within 10 years following KD diagnosis, classified by the branch complexity with regards to aneurysms and dilations. Univariable significant with p<0.001
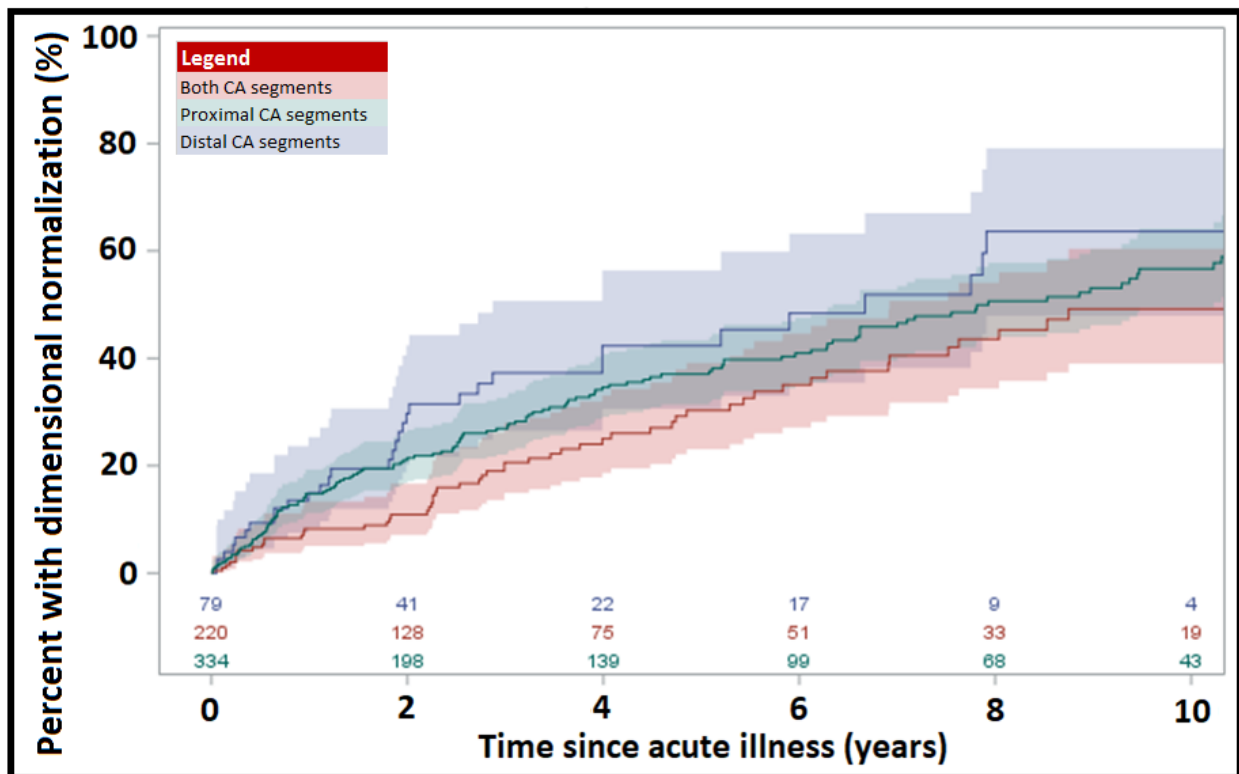
Figure 26. Percentage of CA branches with aneurysms of Z-score >10 that achieve dimensional normalization within 10 years following KD diagnosis classified by aneurysm location within a CA branch. Univariately significant with p=0.03
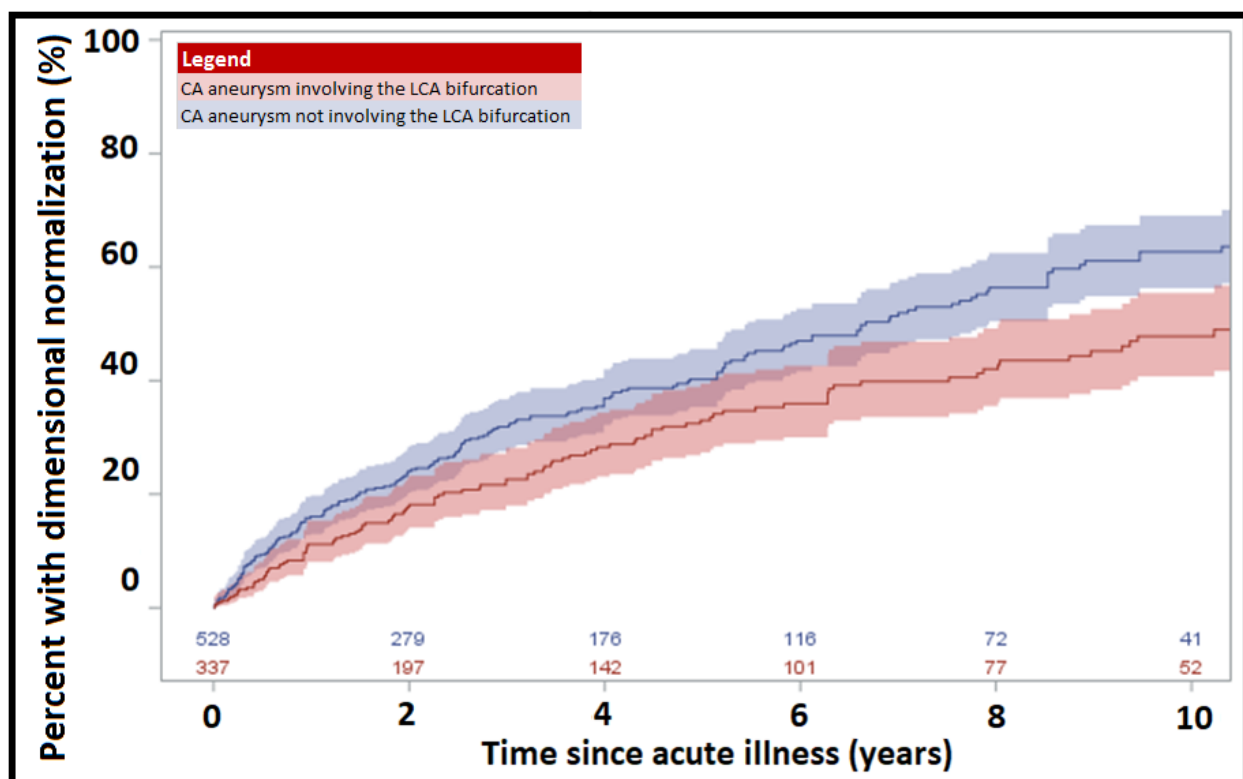
Figure 27 Percentage of CA branches with aneurysms of Z-score >10 that achieve dimensional normalization within 10 years following KD diagnosis, classified by aneurysmal involvement of the left main CA bifurcation. Univariately significant with p=0.005
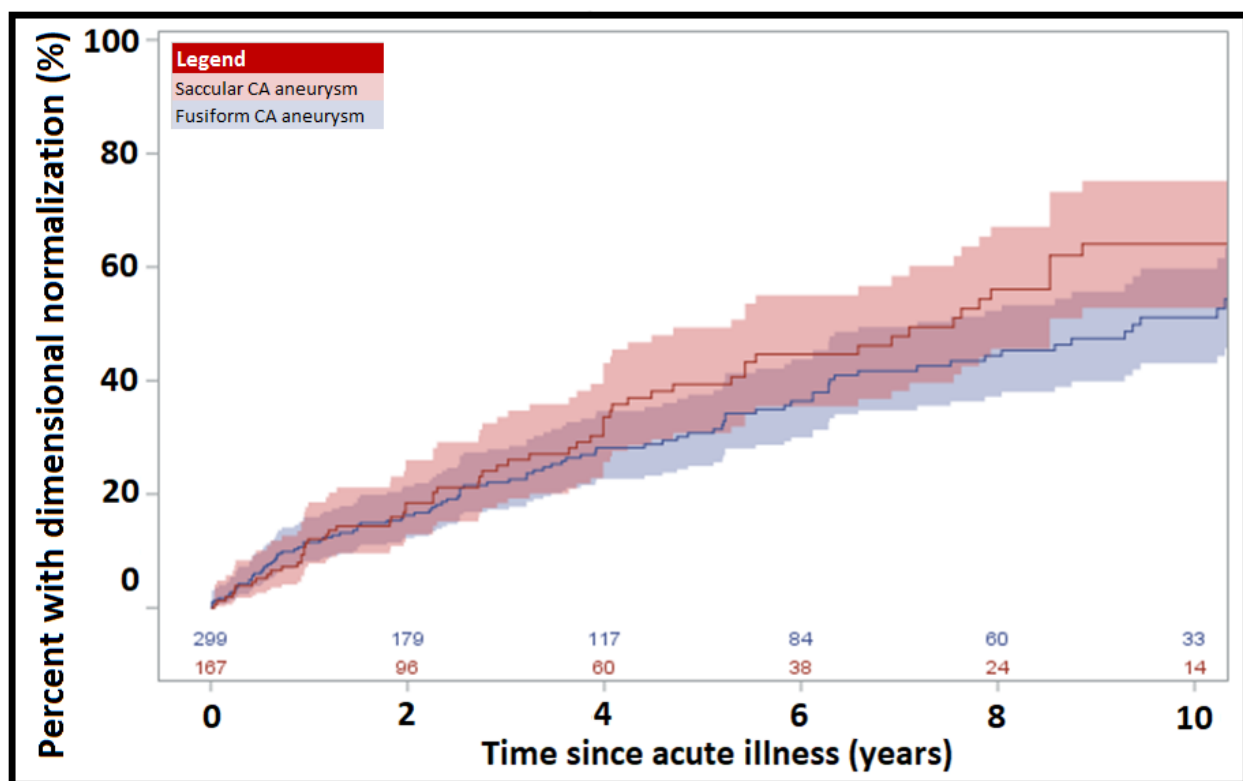
Figure 28. Percentage of CA branches with aneurysms of Z-score >10 that achieve dimensional normalization within 10 years following KD diagnosis, classified by aneurysm shape. Not univariately significant with p=0.11
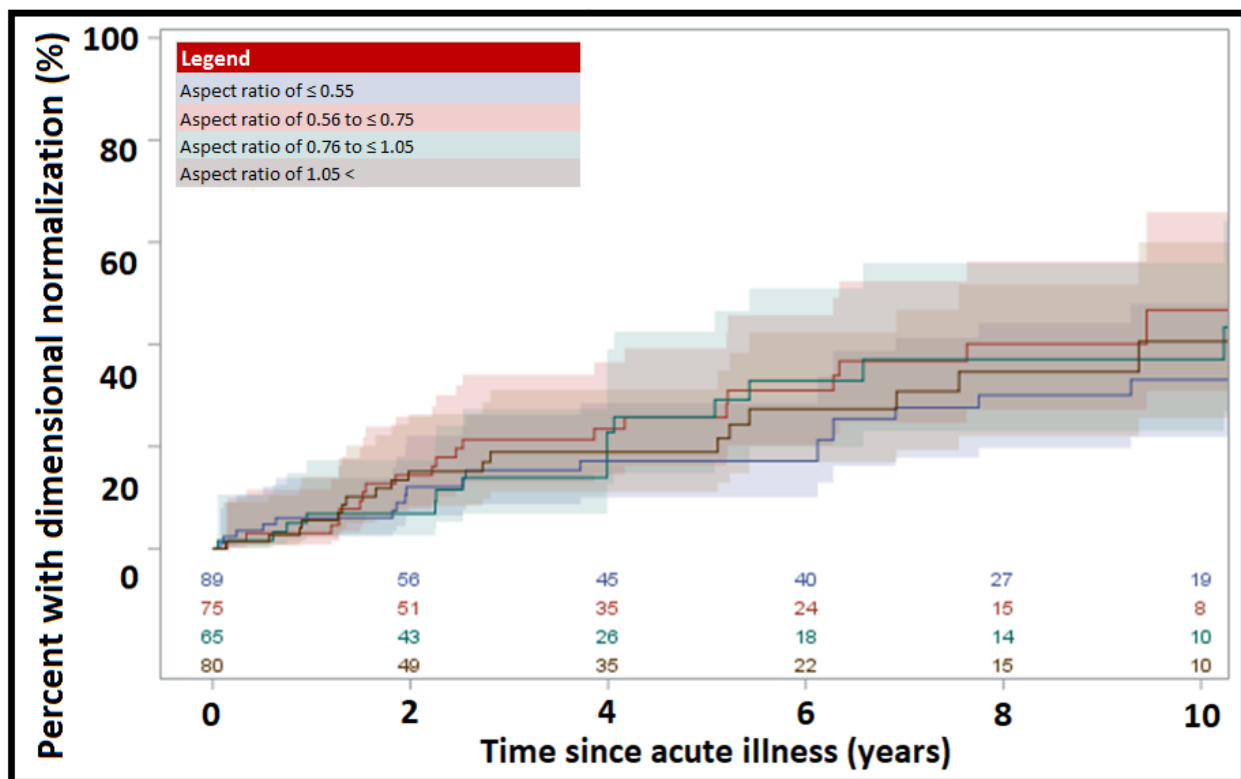
Figure 29. Percentage of CA branches with aneurysms of Z-score >10 that achieve dimensional normalization within 10 years following KD diagnosis, classified by aneurysm aspect ratio. Not univariately significant with p=0.79

## 3.2   Part 2: Coronary artery hemodynamics based investigation

3.2.1 Cohort characteristics

Demographic and clinical data for the 10 patients selected for study part 2 are summarized in Table 10. Significant heterogeneity was noted especially regarding medical management, time to thrombosis and maximum Z-scores of the CA aneurysms. Patient-specific models of the coronary arteries are presented in Figure 30 where 32 CA aneurysms (19 RCA, 10 LMCA/LAD and 3 LCX) are identified, 5 of which are thrombosed.

3.2.2 Hemodynamics and thrombotic risk

Thrombosed and non-thrombosed CA aneurysms did not significantly vary by Z-score (23.58±8.78 vs. 15.58±8.99, p=0.077) or absolute measures of maximum diameter (12.09±4.32 vs 9.4±3.78 mm, p=0.213). Regarding CA aneurysm hemodynamics, the OSI did not significantly differ between thrombosed and non-thrombosed CA aneurysms (0.14±0.05 vs. 0.15±0.06, p=0.880). However, time averaged wall shear stress (TAWSS) was found to be significantly lower in aneurysms that developed thrombi when compared to those that remained incident free (1.2±0.94 vs. 7.28±9.77 dynes/cm^2; p=0.006). This finding is illustrated in Figure 30 that depicts patient specific models for all patients mapped with TAWSS, while highlighting the confirmed locations of thrombi. Thrombosed CA aneurysms also had a significantly larger proportional area exposed to a TAWSS <1 dyne/cm^2 (A_{WSS1}) than their non-thrombosed counterparts (0.69±0.17 vs. 0.25±0.26 dynes/cm^2; p=0.005). At the CA branch level, branches with thrombosed aneurysms had greater residence times (9.07±6.26 vs. 2.05±2.91 cardiac cycles; p=0.004) than branches in which no thrombosis occurred (Fig.31).

Table 10. Patient characteristics for the cohort used in study part two

Patient ID	1	2	3	4	5	6	7	8	9	10
Sex	Male	Male	Male	Male	Female	Male	Female	Male	Male	Male
Age at diagnosis (years)	0.4	8.4	3.0	5.4	0.5	7.9	12.1	8.7	11.0	0.1
Age at CMRI (years)	6.8	16.7	3.5	6.9	0.6	14.9	16.7	9.1	17.6	11.1
Thrombosis	Yes	Yes	Yes	Yes	Yes	-	-	-	-	-
Thrombus location	RCA	LAD	RCA	RCA	LAD	-	-	-	-	-
Age at thrombosis (years)	9.1	16.7	4.4	7.4	2.6	-	-	-	-	-
Time from diagnosis to thrombosis (years)	8.7	8.3	1.4	2.0	2.1	-	-	-	-	-
Time from thrombosis to CMRI (years)	2.2	<0.1	0.9	0.5	0.6	-	-	-	-	-
Medications at thrombosis or CMRI										
Aspirin	+	+	+	+	+	+	+	+	+	+
Clopidogrel	-	-	+	-	-	-	-	-	-	-
Enoxaparin	-	+	-	-	-	-	-	+	-	-
Warfarin	+	-	-	+	-	+	+	-	+	+
Max ever Z-score (Z-score at CMRI)										
RCA	29.1 (8.9)	9.0 (4.1)	44.6 (40.9)	37.3 (35.8)	26.8 (10.8)	15.5 (13.9)	40.3 (40.3)	9.5 (1.2)	22.1 (11.2)	15.7 (10.6)
LCA	2.4 (0.6)	6.1 (2.7)	11.9 (5.9)	1.5 (1.2)	9.7 (4.2)	2.1 (0.65)	4.7 (0.4)	9.9 (5.9)	9.1 (8.1)	1.6 (-0.3)
LAD	18.6 (8.3)	39.4 (25.1)	34.6 (22.4)	45.2 (45.2)	62.1 (29.6)	12.7 (4.6)	52.6 (36.5)	13.2 (6.3)	24.5 (20.9)	10.8 (0.3)
CCX	17.3 (0.6)	13.2 (4.8)	20.3 (18.7)	14.8 (5.1)	15.2 (6.6)	1.2 (-1.8)	3.6 (1.4)	8.3 (2.5)	3.1 (3.1)	7.6 (-1.8)
BSA (m^2) at thrombosis or max Z-score	1.0	1.8	0.7	0.9	0.6	1.4	1.6	1.3	1.4	1.2
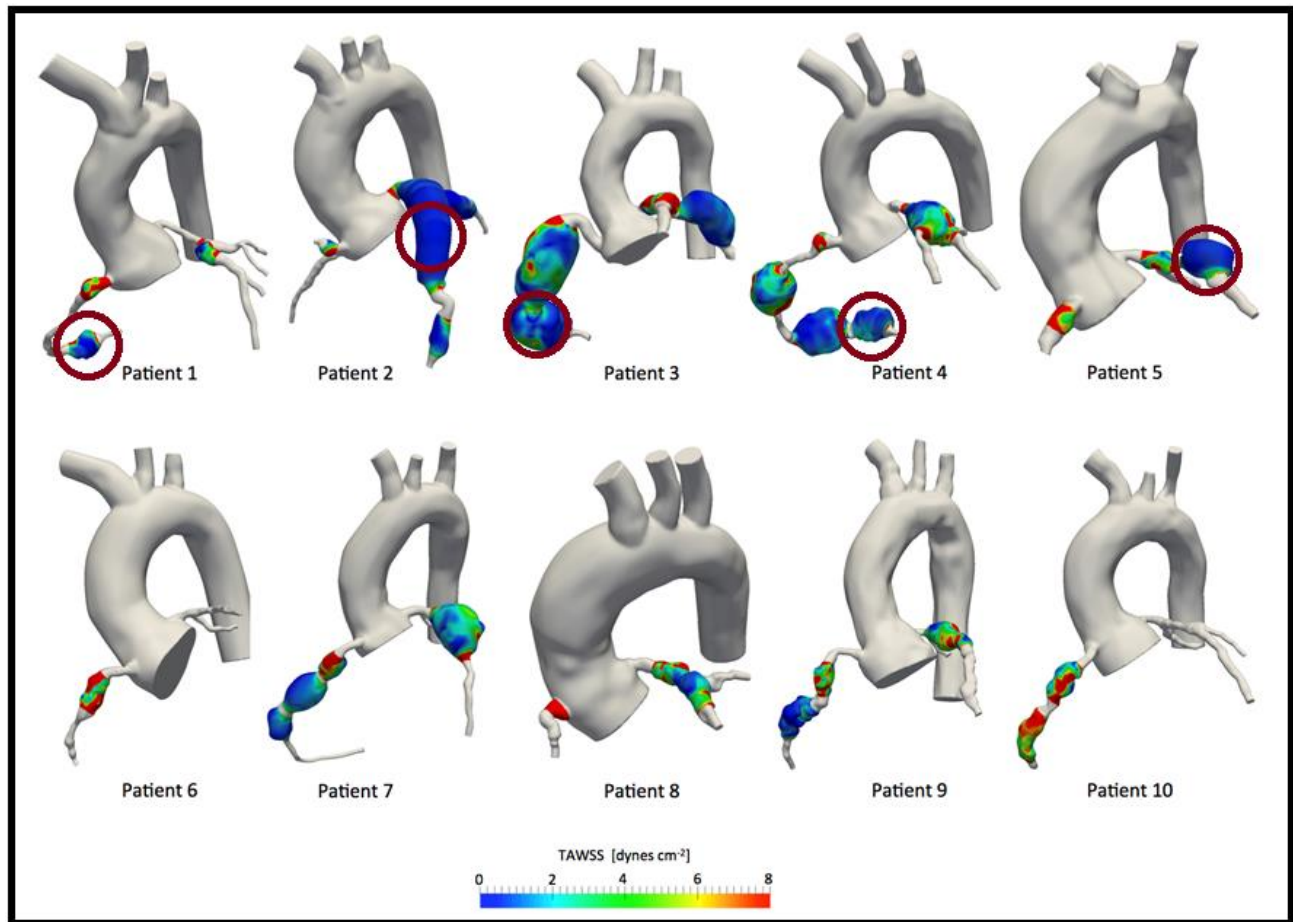
Figure 30. Patient-specific models of the aorta and the coronary artery branches with location of thrombi (red circles) and spatial distribution of TAWSS (gradient)

3.2.3 Hemodynamics and risk stratification

Following the previous analyses, ROC curves for TAWSS, A_{WSS_l} and residence times were evaluated to determine appropriate thresholds for thrombotic risk assessment (Fig.32). These thresholds had similar sensitivity and greater specificity when compared to clinical standards of Z-scores and absolute dimensional diameter. Furthermore, there was a large spread of values for TAWSS over the range of Z-scores and luminal diameters measured (Fig.33) and little correlation was noted between either measure and TAWSS

(Z-score: r^2= -0.35, p=0.047; luminal diameter: r^2= -0.36, p=0.044) or A_{WSS1} (Z-score: r^2= 0.39, p=0.028; luminal diameter: r^2= 0.45, p=0.011). Table 11 succinctly summarizes the cohort for study part 2 with regards to established and proposed structural or hemodynamic thresholds.
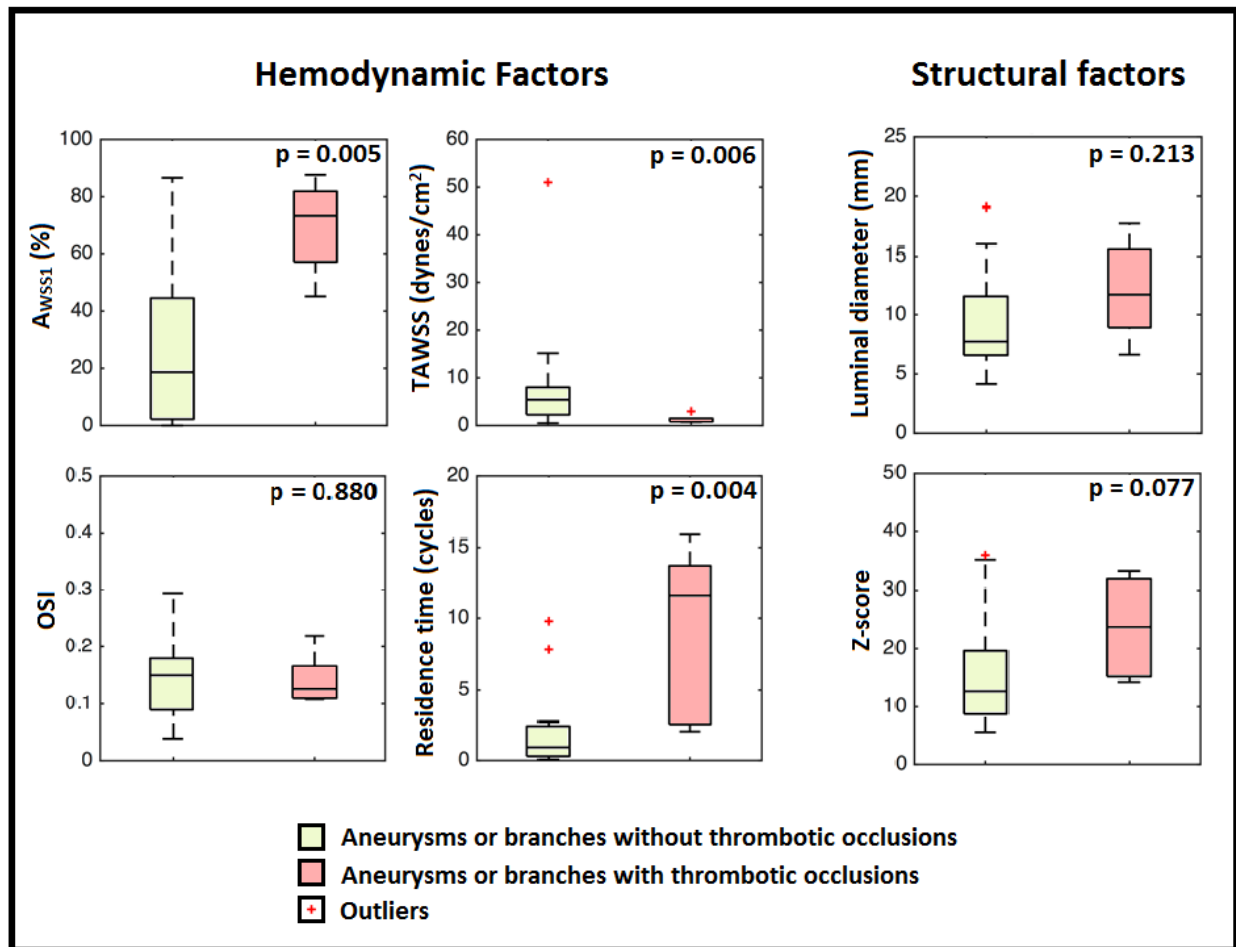
Figure 31. A comparison of hemodynamic and structural variables between thrombosed (Red) and non-thrombosed (Green) coronary artery aneurysms or branches
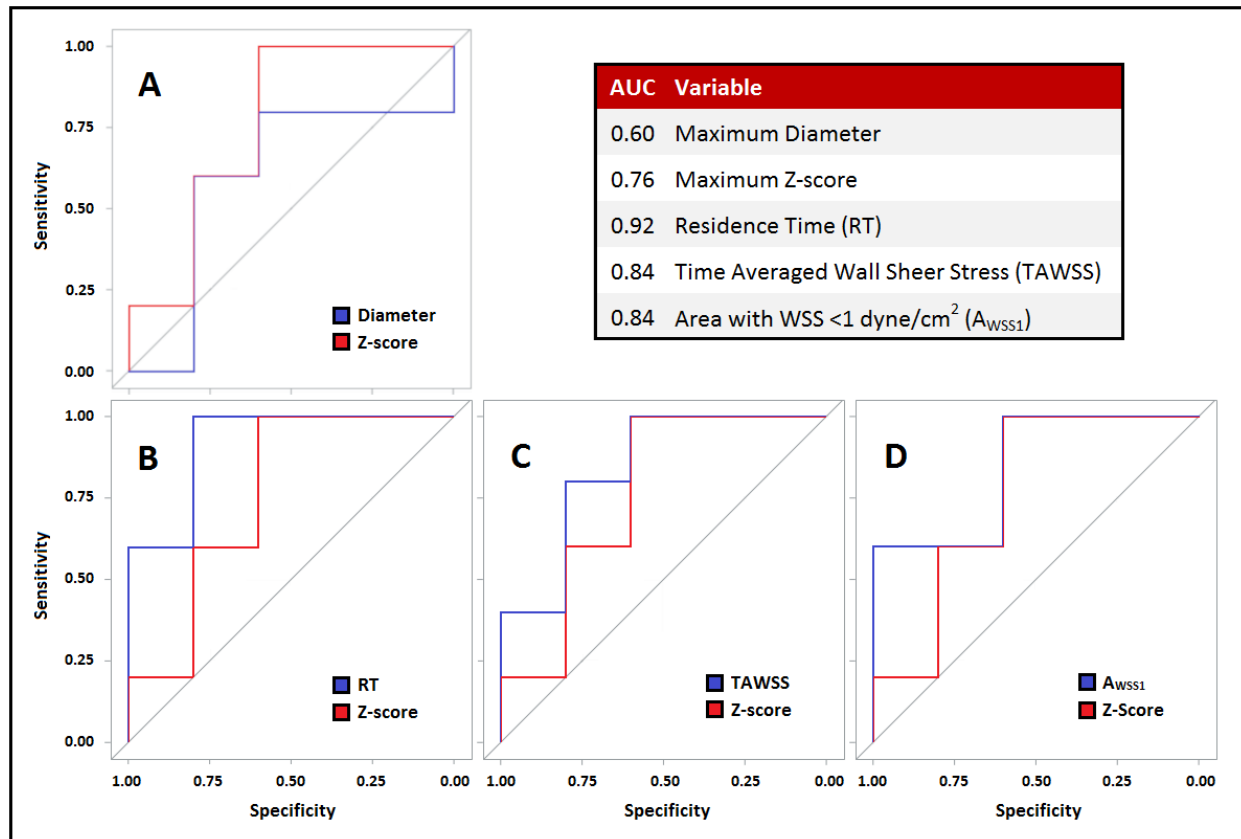
Figure 32. Receiver Operating Characteristic (ROC) curves and Area Under the Curve (AUC) for structural and hemodynamic variables. A) Z-score vs Diameter; B) Z-score vs recirculation time (RT); C) Z-score vs time-averaged wall shear stress (TAWSS); D) Z-score vs area with wall shear stress <1 dyne/cm^2 (A$_{WSS1}$)
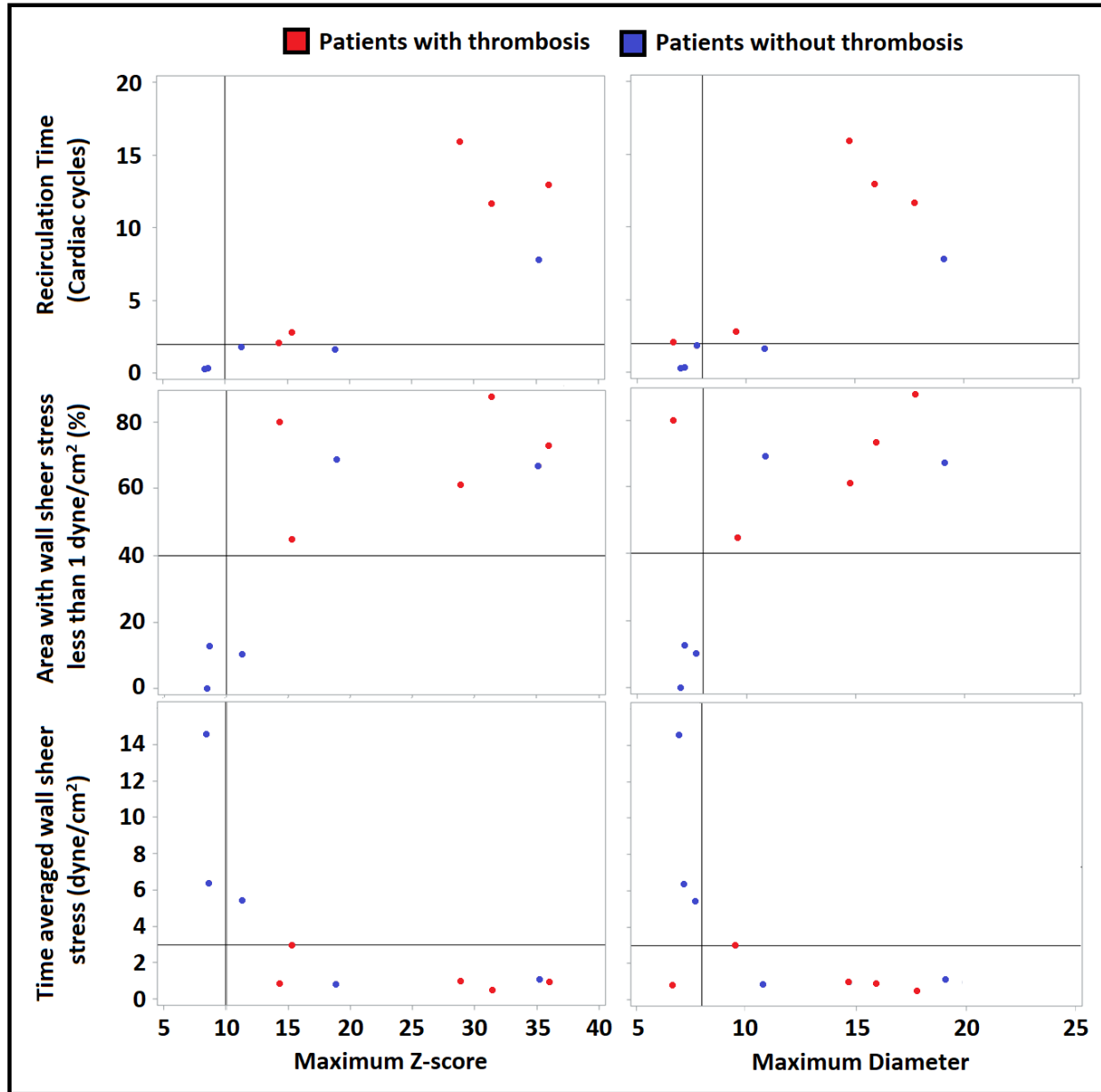
Figure 33. Comparing proposed hemodynamic thresholds (horizontal lines on vertical axes; RT >2 cycles, A_{WSS1} > 40%, TAWSS <3 dynes/cm^2) with established structural thresholds (vertical lines on horizontal axes; Z-score >10, diameter >8mm) on thrombosis prediction for all patients in the cohort (red = patients with thrombosis, blue = patients without thrombosis)

Table 11. Summary of current and proposed risk stratification thresholds (O's predict thrombosis and X's predict no thrombosis) and patient specific CA models for patients who had CA aneurysm thrombosis (Left 5, green) and patients who did not (Right 5, red)

Coronary artery models (Right) Structural and hemodynamic thresholds (Bottom)										
Luminal diameter ≥ 8mm	O	O	O	O	X	X	O	O	O	O
Z-score ≥ 10	O	O	O	O	O	O	O	O	O	O
TAWSS < 3dynes/cm^2	O	O	O	O	O	X	O	X	O	X
A_{WSS1} > 40%	O	O	O	O	O	X	O	X	O	X
RT > 2 cardiac cycles	O	O	O	O	O	X	O	X	X	X

Chapter 4: Conclusions

4.1 Overview

The notion that larger CA aneurysms are associated with a greater risk for adverse outcomes has been widely acknowledged in the world of Kawasaki disease research from as early as the 1990's[20, 47, 73, 144]. Investigative efforts have repeatedly confirmed this association while attempting to identify other factors that could potentially modulate CA aneurysm related risks. This study confirmed that larger CA aneurysms are associated with increased risk of thrombosis, stenosis and failure to achieve dimensional normalization. The investigation also evaluated the associations between various other structural and hemodynamic features of CA aneurysms and negative outcomes. From 1,651 KD patients with CA aneurysms, only 2 children developed thrombosis or stenosis in medium aneurysms of Z-score <10. These results support previous findings from the IKDR cohort[190], and allowed for the exclusion of patients with CA aneurysms of Z-score <10 from subsequent analyses. Regardless of this exclusion, the multivariable Cox proportional hazard models for thrombosis, stenosis and dimensional normalization consistently and reliably selected maximum CA aneurysm Z-score as the most important CA aneurysm feature for defining risk. Results suggested that an aneurysm with a Z-score of 20 is about half as likely to achieve dimensional normalization, has almost double the risk of thrombosis and almost 50% increased risk of stenosis, when compared to a CA aneurysm with a Z-score of 10. Nonetheless, a number of other variables were selected in the hazard model, and univariate structural and hemodynamic analyses also revealed significant associations. When taken together, they reflect and validate many of this thesis' hypotheses while offering novel avenues for future studies. These can be further elucidated by examining their unique associations with the individual outcomes and their interplaying effects.

4.2　Discussion

4.2.1 Coronary artery aneurysm cross-sectional area

Larger aneurysms imply greater damage to the arterial wall and lead to more aberrant luminal flow through the affected areas. These factors result in an increased risk for adverse outcomes through a variety of means, as explored in Chapter 1. Measures of absolute diameter or derived BSA-adjusted Z-scores are incomplete, one-dimensional measures of aneurysm size. Complete quantification of CA aneurysm size is only possible with metrics such as aneurysm volume or surface area. Currently, neither of these metrics are possible with the non-invasive imaging modalities commonly used for diagnosis and management of KD related CA aneurysms. Cross-sectional area is a two-dimensional estimated measure of aneurysm size that can easily be obtained from routine echocardiography. This surrogate measure is often used to characterize the risk for adverse outcomes of larger aneurysms in cerebral[191, 192] and aortic[193, 194] vessels. Consideration of CA aneurysm cross-sectional area may also help refine risk stratification criteria in children with KD related aneurysms, as supported by results from this thesis. CA aneurysms with larger cross-sectional areas have an increased risk for adverse outcomes. However, cross-sectional area was only selected by the hazard model for dimensional normalization, while being univariately significant with regards to thrombotic and stenotic risk. This could be due to the confounding of Z-scores and cross-sectional area (CA aneurysm width vs width:length respectively). Given these results, under the assumption that CA aneurysm length represents breadth of endothelial damage (a greater portion of the endothelium may be affected in longer aneurysms) and width represents intensity (deeper endothelial layers may be affected in wider aneurysms), one could speculate that the LMP process may be more strongly related to dimensional normalization than to stenotic events. Appreciating this postulate requires one to consider that more intense vessel wall damage may result in the loss of the medial layer associated with the LMP process; while broader damage may expose a larger portion of the layer to luminal flow, thereby facilitating the process[57]. The postulate would also be supported when considering that a stenosing lesion would be associated with higher

levels of WSS which could inhibit the LMP process[119, 120]; although this too is a speculation at this time. Nonetheless, these speculations allow for study results to support hypotheses that the later stages of stenosis in KD patients with CA aneurysms may be driven by other pathological processes, besides the LMP process[47, 195, 196]. With regards to thrombosis, the results support the possibility that more saccular CA aneurysms pose a greater risk for events; a recurring concept that will be explored in the following sections.

4.2.2 Coronary artery aneurysm shape and aspect ratio

The following discussion on CA aneurysm shape and aspect ratio directly stems from the preceding discussion on CA aneurysm cross-sectional area, with greater emphasis on hemodynamics and the 3 vasculopathic processes involved in CA aneurysm formation and progression. Orenstein *et al.* suggest that the acute necrotizing arteritis process causes progressive destruction of the luminal wall into the adventitia, weakening the wall and resulting in saccular aneurysms that can thrombose or rupture[57]. This supports the prior assumption that greater aneurysm width (diameter) represents a higher intensity of damage to the vessel wall. Orenstein *et al.* hypothesize that the sub-acute/chronic inflammatory (SA/C) process that follows can also result in saccular or fusiform CA aneurysms depending on the degree of inflammation and accompanying tissue damage, but is less prone to destroying the medial layer as compared to NA[57]. Consequently, this thesis postulates that saccular CA aneurysms would have a lower incidence of dimensional normalization and stenosis as compared to fusiform aneurysms, following results from similar investigations[197, 198]. However, results show no significant differences between aneurysm shape for any of the 3 adverse outcomes evaluated. It is possible that these results are affected by the qualitative nature and infrequent reporting involved with classification of CA aneurysm shape rather than a true effect. This is especially true when considering results regarding aspect ratio, a quantitative measure for aneurysm shape. Univariate analysis revealed that CA aspect ratio was not significantly associated with dimensional normalization and stenosis, although more saccular

aneurysms were significantly associated with increased thrombotic risk. These results also suggest that hemodynamics may have an influence on thrombotic risk. To elaborate, consider that vessel wall derived tissue factor (TF) would mostly be responsible for initiating the slow intrinsic pathway of the clotting cascade, whereas blood-borne TF carried by platelets would be involved in propagating the thrombus[199]. Turbulent or stagnant blood-flow would increase this rate of propagation, and one may infer that fusiform CA aneurysms would have more laminar blood flow as compared to saccular CA aneurysms of a similar Z-score. Saccular CA aneurysms may also have recirculation zones that lower WSS and increase blood particle time within the aneurysm, both of which contribute to thrombotic risk[47, 113]. Nevertheless, coronary artery aneurysm size can be considered a surrogate measure for both endothelial damage and irregular blood flow in the corresponding regions. As such aspect ratios would only contribute to thrombotic risk stratification of aneurysms secondarily to measures of aneurysm size. The Cox proportional hazard model for thrombosis supports this claim as neither measures of aneurysm shape were selected in the model, despite aspect ratio being univariately significant.

4.2.3 Coronary artery aneurysm location within a branch

The location of an aneurysm within a coronary artery may also have an effect of the risk for negative outcomes. The distal portions of the 4 main coronary artery branches are known to taper, and have a reduced WSS[80]. Lower WSS could increase the risk of thrombosis by facilitating cell-cell and cell-wall interactions and reducing shear related diffusion[111, 112]. Distal CA aneurysms are also thought to resolve faster than proximal aneurysms of a similar maximum diameter[198]. However, contrarily to hypotheses made in this thesis, CA aneurysms location within a branch was not selected in any multivariable models nor was it univariately associated with any negative outcome. This would suggest that the physiological differences between the proximal and distal portions of the coronary arteries, such as WSS, peak velocity ratios[200] and fractional flow reserves[201], are not large enough to affect the risk of negative outcomes. The results

could also reflect the qualitative nature of the definitions used, as they did with aneurysm shape. Particularly, CA branches with aneurysms in both the proximal and distal portions, or large aneurysms that extended from the proximal through to the distal segments, were labelled accordingly. This definition slightly confounds the CA branch location variable and the CA branch anatomy variable, creating a common subgroup of CA branches with aneurysms that are located in both segments (location) of a complex (anatomy) CA branch. Furthermore, it is difficult to accurately evaluate distal aneurysms, especially in older patients who are more likely to be evaluated for the long-term outcomes in question[47, 202]. As such, there may be an underestimation of the negative outcomes associated with aneurysms in the distal regions of the coronary arteries.

4.2.4 Coronary artery branch anatomy

Prior sections of this thesis examined associations between the risk of negative outcomes (thrombosis, stenosis and failure to achieve dimensional normalization) and features of CA anatomy at the aneurysm level (shape, area and location within branch). The following sections examine similar associations at the branch level (branch anatomy, CA branch and involvement of the left bifurcation). CA branch anatomy refers to the characterization of the CA structure with regards to regions with aneurysms and/or dilations, as outlined in the methods chapter of this thesis. It was hypothesized that more complex branch anatomy with a greater number of aneurysms would compound the effects of the individual aneurysms and their associations with negative outcomes. As described in the introduction chapter of this thesis, CA aneurysms can result in increased blood viscosity, blood-particle collisions, blood-particle residence times, smooth muscle cell proliferation, endothelial damage, circulating coagulation factors, platelet activation and platelet adhesion; while lowering wall shear stress and shear induced diffusion[47, 57, 111-114, 164]. The increased blood-particle residence time and collisions along with lower WSS and shear induced diffusion would result in compounded effects, especially for cell-cell and cell-wall interactions. Altogether, these effects are thought to increase the risk of thrombosis and stenosis in affected patients, as reflected in the results where branch

anatomy was selected by the multivariable Cox proportional hazard models for both outcomes, with high reliability. More complex branch anatomy may result from greater inflammation during the acute phase of KD which could be associated with greater vessel wall damage and alterations in coagulation profiles; 2 factors that are beyond the scope of this thesis. CA branch anatomy was not selected by the Cox proportional hazard model for dimensional normalization, but reduced incidence of dimensional normalization was univariately associated with increased complexity in CA branch anatomy.

These results suggest that aneurysm level characteristics carry greater weight than branch level characteristics with respect to achieving dimensional normalization as compared to risk for thrombosis and stenosis. This finding supports previous results from the investigations on aneurysm shape and cross-sectional area. This is understandable, given that dimensional normalization is mostly a product of the vessel wall related LMP process and laminar thrombosis. Consequently, branch anatomy may not have been selected in the multivariable model for DN since its effects may be outweighed by those of aneurysm cross-sectional area and the CA branch itself. This also supports previous results suggesting differences between the progression of DN and stenosis. Nonetheless, the effects of dilation around an isolated aneurysm are considered negligible with respect to the risk for all 3 negative outcomes, and need not be considered in future assessments of coronary artery branch complexity.

4.2.5 Coronary artery aneurysms and branches

CA branch anatomy does not account for differences between the features of the individual branches themselves (RCA vs LCA vs LAD vs LCX). This is important when considering that flow velocity, flow patterns and wall shear stresses can vary between the main CA branches[80, 83, 84]. Particularly, RCA measures of blood-flow velocity are lower than those of the LAD or LCX, with the LCA having the highest measures. Predictions regarding the influence of CA branches on risk for negative outcomes of CA aneurysms stem from the hemodynamic implications of the different flow velocities. Multivariable models for stenosis and dimensional normalization as well as univariate analysis of

thrombotic risk suggest that the LCA has the lowest risk for negative outcomes of CA aneurysms. Hypotheses regarding the RCA were also supported by results that suggest it to be the branch with the highest risk for thrombosis or stenosis. However, the results for dimensional normalization differ from original predictions. Aneurysms of the RCA had a very low rate of dimensional normalization, with the LCX being far more likely to achieve a positive outcome. This once again suggests that flow characteristics play a greater role in the processes of thrombosis and stenosis, while dimensional normalization is more significantly influenced by the extent of vessel wall damage for CA aneurysms of similar luminal diameter. Further review of vessel wall differences between the different coronary arteries revealed that the medial layers of the LAD and LCX are almost 10% and 40% thicker than that of the RCA, respectively[203]. As such, LCX and LAD aneurysms are more likely to have preserved a greater portion of their medial layer following the NA or SA/C processes. Since the LMP process, assumed to be largely responsible for dimensional normalization, originates from SMCs in the medial layer of the vessel wall, the increased incidence of dimensional normalization in aneurysms of the LCX and LAD is understandable.

4.2.6 Coronary artery aneurysms at the bifurcation of the LCA

The background section of this thesis describes the increase in wall shear stress and oscillatory shear index associated with bifurcations in the coronary arteries. Unfortunately, neither coronary artery branch nor branch anatomy account for these effects, as doing so would overly complicate both classification and analysis. Furthermore, the extent to which these bifurcations effect the risk of CA aneurysm related negative outcomes is unknown. Consequently, this thesis investigated how aneurysms at the bifurcation of the left main coronary artery differed from other CA aneurysms with regards to their risks of thrombosis, stenosis and failure to achieve dimensional normalization. This bifurcation is one of the most prominent coronary artery divisions, and analysis may allow for insights regarding other bifurcations in the coronary arteries. Results suggest that aneurysms involving the bifurcation of the LCA are more likely to

thrombose, stenose or fail to achieve dimensional normalization. It was hypothesized that these aneurysms would have some regions with decreased WSS and increased OSI (most aneurysms), and other regions with increased WSS and increased OSI (most bifurcations). This regional co-occurrence of high and low wall shear stresses as well as high OSI could significantly increase thrombotic risk[111-113]. Interpretation of results from the stenosis and dimensional normalization investigations are a little more complicated. The following discussion proceeds under the assumption that rheological factors known to increase vascular smooth muscle cell (VSMC) proliferation and survival also increase myofibroblastic proliferation. Higher WSS decreases VSMC proliferation and increases SMC apoptosis, while higher OSI increases SMC proliferation and survival[119-121]. The results for stenosis suggest that the effect of OSI is larger since CA aneurysms with bifurcation involvement are more likely to stenose. Contrarily, results for dimensional normalization suggest that the effect of higher WSS is greater since CA aneurysms with bifurcation involvement are less likely to achieve dimensional normalization. Given that involvement of the left bifurcation was a factor selected in the multivariable model for stenotic risk, one might presume that the effect of increased OSI is truly greater than that of increased WSS. However such a presumption may not be accurate given the limitations of this investigation, as will be discussed later. Regardless, this investigation highlights the impracticalities of considering bifurcation involvement for risk stratification of KD related CA aneurysms.

4.2.7 Coronary artery aneurysm hemodynamics and thrombotic risk

The rationale for the analyses above is rooted in the idea that structural characteristics influence hemodynamic and vessel wall features which, are associated with the risk for negative outcomes of KD related CA aneurysms. Although investigations on vessel wall features are difficult in this patient population, modern advances in the field of computational fluid dynamics allow for explorative studies on associated hemodynamics and rheology. Part Two of this thesis involved collaboration with biomedical experts in the field of CFD, who used novel methodologies to investigate the

effects of wall shear stress, oscillatory shear index and recirculation time on thrombotic risk in patients with persisting CA aneurysms following KD. Results from these analyses are statistically underpowered due to the limited cohort size, but provide important insights that broaden the current understanding of KD related CA aneurysms and qualify prior results regarding coronary artery anatomy and thrombotic risk.

Dr. Alison Marsden and her team have prior experience with CFD simulations in patients with KD related CA aneurysms, and have previously reported abnormal hemodynamics in these patients[139, 140]. The current investigation supports their prior findings, but uses a novel methodology that incorporates deformable wall capabilities and a closed loop lumped parameter network that better simulate physiological flow conditions in patient specific coronary artery models. Furthermore, the study is the first to use MRI based segmentations for CA model construction and may be considered a proof of concept. Although CT based segmentations may provide more detailed CA models, MRI imaging is more acceptable in pediatric populations due to the lack of radiation exposure. This is a marked distinction when considering the routine imaging studies that would be needed to effectively analyse time-to-event outcomes such as thrombosis, stenosis and dimensional normalization.

Nonetheless, this study used post-outcome MRI images to create the patient specific coronary artery models on which the CFD simulations were run. Wall shear stress values in an aneurysm were computed over time to provide a more representative time-averaged measure (TAWSS). Thrombosed CA aneurysms were found to have much lower measures of TAWSS as compared to their non-thrombosed counterparts, as well as a larger proportional area exposed to a TAWSS of <1 dyne/cm². Blood recirculation times were also significantly lower in CA branches with thrombosed aneurysms. Both these results support their related hypotheses which were generated under the assumption that lower WSS and increased flow stagnation facilitate cell-cell and cell-wall pro-thrombotic interactions via different mechanisms. Consequently, the co-occurrence of these hemodynamic features in CA aneurysms exacerbates their pro-thrombotic effects. No significant difference was appreciated between the averaged measures of OSI for

thrombosed and non-thrombosed aneurysms. However, all CA aneurysms had an elevated OSI and thrombosed aneurysms had regions where a TAWSS <1 dyne/cm² was co-located with an OSI measure > 0.25.

Non-thrombosed CA aneurysms in close proximity to thrombosed aneurysms also had lower measures of TAWSS; and blood recirculation times substantially increased for CA branches with multiple aneurysms. These results support conjectures about the compounding hemodynamic effects in CA branches with multiple aneurysms as well as hypotheses regarding structural features thought to influence the respective rheological measures as previously described. This is especially true of pro-thrombotic cell-cell interactions that accumulate with each succeeding aneurysm that the cells pass through.

4.2.8 Exploring hemodynamic thresholds for thrombotic risk stratification.

Thrombotic risk stratification criteria for patients with persisting CA aneurysms following KD may be refined through adjunct consideration of hemodynamic thresholds secondary to aneurysm Z-scores. Thresholds for the OSI of an aneurysm may not be very useful in this regard since no significant difference was noted between the aneurysmal measures regardless of thrombotic occurrence. However TAWSS measures <3 dynes/cm² were appreciated for all thrombosed CA aneurysms. Considering the proportional aneurysmal area with TAWSS <1 dyne/cm² allows for a composite measure (A_{WSS_1}) that attempts to account for both hemodynamics, and its effects on the vessel wall. An A_{WSS_1} threshold of 40% accounts for all thrombosed CA aneurysms in this patient cohort, with a higher specificity as compared to standard structural criteria such as absolute dimensions or Z-scores (Fig.33). Moreover, all thrombosed CA aneurysms were located in branches where blood-particles took longer than 2 cardiac cycles to recirculate. Proposed hemodynamic thresholds were proposed and evaluated from these data (TAWSS <3 dynes /cm², A_{WSS_1} >40% and RT_{branch} >2 cardiac cycles), but must be considered in light of the fact that they were derived from a very narrow and specific cohort (n=10) and may only hold true for said cohort. Nonetheless, in this cohort, these thresholds have a high

sensitivity and specificity for estimating thrombotic risk, where significant differences are noted between thrombosed and non-thrombosed CA aneurysms despite there being no significant difference in either luminal diameter or Z-score. Table 11 compares current and proposed thresholds for stratification of thrombotic risk. The table also highlights specific patients who do not have any thrombosis despite meeting all 5 (patient 7) or 4/5 (patient 9) structural and hemodynamic thresholds. This once again reinforces the idea that other factors such as vessel wall characteristics or coagulation profiles also play a significant role in coronary artery thrombosis or management.

4.2.9 Other clinical variables

To increase robustness, the multivariable proportional hazard models accounted for clinical features associated with the acute phase of KD, which are believed to be associated with long-term outcomes[47]. Patients who received IVIG were at a lower risk for negative outcomes, and the variable was consistently selected with high reliability. This finding adheres to the well-established understanding of the benefits of IVIG treatment during the acute phase of KD, associated with decreased incidence and severity of coronary artery abnormalities[47, 71, 72, 134, 135]. A longer duration of fever is also known to be associated with a greater risk for negative outcomes in Kawasaki disease patients. Incomplete KD may delay diagnosis and treatment of the disease whereas patients who do not respond to IVIG may be treated with IV steroids; both of which lead to a longer duration for the acute phase pathological processes involved in KD, especially those that increase the risk of coronary artery abnormalities[47]. Therefore, it is understandable that these features (fever duration, incomplete KD diagnosis and treatment with IVMP) were selected by the multivariable models. In fact, laboratory markers for increased inflammation (↑WBC, ↑ESR, ↓Serum albumin) were associated with increased risk for negative outcomes, as would be expected. However, thrombotic risk was associated with lower levels of CRP, while inflammation is associated with increased CRP levels. This would suggest that greater acute phase inflammation is associated with decreased risk for coronary artery thrombosis, which is contrary to well established findings in the field.

Given the lack of stratified plots, the low estimate and a hazard ratio of almost 1.0 for CRP associations with thrombotic risk, the finding is more likely to be a statistical effect rather than a true association. The finding thereby highlights the importance of determining how much of the risk for outcomes is attributable to each of the various factors selected in the multivariable proportional hazard models.

The hazard models also suggest that CA aneurysms in younger KD patients are more likely to achieve dimensional normalization, and less likely to stenose. In general, younger age at diagnosis has been associated with better outcomes in patients with KD[47]. Furthermore, the increased incidence of dimensional normalization could be due to pseudo-normalization being more common in younger children; specifically normalization via growth of the surrounding vessel to match luminal diameters of the aneurysm. The decreased incidence of stenosis suggests that patient age is a greater consideration for stenotic risk as compared to time at risk; a recurrent suggestion from studies on atherosclerosis[204, 205]. These findings also support prior postulates regarding the differences in the mechanism of stenosis vs dimensional normalization. Age at diagnosis was not selected in the model for thrombotic risk, suggesting that structural features of the CA aneurysms have a bigger effect on thrombosis as opposed to age.

Female patients were more likely to achieve structural normalization and patients with acute phase arthritis were more likely to develop stenosis, which makes sense from a clinical perspective. Kawasaki disease has a predilection for male children, who are more likely to acquire the disease, develop coronary artery aneurysms and were noted to have a higher mortality rate than similar females in a Japanese cohort study[45, 47]. Kawasaki disease related arthritis is a short-lived symptom in children, associated with increased systemic inflammation which in turn is associated with worse outcomes regarding CA aneurysms; the long-term significance is unknown[206]. In fact, the significance of many clinical factors selected in the multivariable models are not clearly defined in the medical literature (with regards to KD) and their influence on associated outcomes has been postulated based on current knowledge. It is important to note that many structural features selected by the hazard models had a much higher reliability than the clinical

variables. This is likely due to the fact that the clinical variables were measured during the acute phase of the disease before IVIG administration, while all outcomes investigated are time-dependent to a certain extent. Additional investigation of the clinical and laboratory features associated with the negative outcomes being evaluated was beyond the scope of this thesis. Furthermore, the hazard models do not express the weight of the selected variables in relation to each other. The consideration of a few select variables may account for the risk associated with the remaining majority. It is reasonable to assume that structural and hemodynamic features would be a part of the select few, but a clustering analysis would be required to truly determine this significance.

4.2.10 Medication considerations

Patient age was not selected in the multivariable model for thrombotic risk, suggesting that current Z-score based thromboprophylactic strategies for KD related CA aneurysm management are very efficient. But strategies can still be improved, particularly for patients with medium and large CA aneurysms. From least aggressive to most aggressive, the 2017 American Heart Association guidelines for KD suggest that patients with current or persistent medium CA aneurysms be treated with either a single antiplatelet or dual antiplatelet therapy. Patients with current or persistent large CA aneurysms may be treated with an anticoagulant + antiplatelet, or anticoagulant + dual antiplatelet strategy[47]. Consideration of hemodynamic and structural features of the related aneurysms may advise attending physicians regarding appropriately aggressive thromboprophylactic strategies. This would require more refined classification of structural features and hemodynamic thresholds. Furthermore, follow-up of patients who achieved dimensional normalization after large or medium CA aneurysms, should include a detailed examination of the vessel wall to determine whether the endothelium has truly recovered; or normalization occurred via LMP or organized thrombosis. Patients with organized thrombi should consider continued use of anticoagulants to prevent thrombotic occlusion, whereas those with LMP related normalization should at least have one annual echocardiogram follow-up to determine progression towards stenosis.

The 2017 American Heart Association guidelines also recommend empirical statin therapy for all KD patients with CA aneurysms due to their host of pleiotropic effects. This thesis supports the empirical use of statins in KD patients with CA aneurysms, but also speculates a benefit of statin therapy during the acute stages of KD as well. Firstly, there is evidence suggesting that low-dose statin therapy is safe to use in young children, with appropriate monitoring[159]. Statins are known to have a lipid-independent anti-inflammatory pleiotropic effect[145, 207] that may reduce the vasculitis associated with acute KD; thereby decreasing the incidence and severity of coronary artery aneurysms. Statins are also known to ameliorate endothelial dysfunction, largely via their lipid lowering effects, but also through increasing production of nitric oxide (promoting good endothelial function) and inhibiting NADPH oxidase (reducing oxidative damage)[208, 209]. These effects may reduce acute KD related endothelial damage while promoting recovery and regression of transient dilation. In fact, a lot of these pleiotropic effects may have beneficial effects long after the initial KD episode[210, 211], supporting continued use in patients with persisting coronary artery abnormalities. There is also some evidence to suggest that low-dose statin therapy may be angiogenic[212, 213]. This effect could encourage collateral formation in the coronary arteries, which could be cardioprotective in patients at risk for thrombotic occlusions. Finally, statin use has been shown to reduce VSMC proliferation, migration and invasion; and multiple studies on large cohorts of patients have shown that pre- and post-operative statin therapies reduce the rate of ensuing re-stenosis or neointimal thickening[155, 214, 215]. As such, KD patients whose aneurysms have normalized via the LMP process may benefit from statin therapy which could reduce the risk of LMP related stenosis. However, this final suggestion is speculative and based on a number of assumptions about the relationships between stenosis, the LMP process and VSMCs.

4.3   Critique

4.3.1 Limitations

It is important to highlight the limitations associated with this study and its ensuing discussion of results to qualify derived conclusions. Firstly, this thesis assumes that reducing the proliferation of vascular smooth muscle cells, would also decrease the proliferation of derived myofibroblasts that are associated with the LMP process. A lot of the discussion related to stenosis and dimensional normalization also assumes that hemodynamic and drug related effects on the VSMCs would have a similar impact on myofibroblasts. Further research is required to determine the extent to which these assumptions are true or false.

Secondly, the study analyses and discussion for stenosis treats all KD related stenosis as being at the location of the largest CA aneurysm in the branch. This assumption allows for easier analyses of structural and hemodynamic features associated with stenosis, but is generally untrue since KD related stenosis can occur anywhere in the CA branch. Consequently, related findings should be considered at the coronary artery branch level rather than at that of the individual aneurysm. Similarly, no distinction is made between early and late onset thrombosis. Early thrombi are more likely to be a result of patient-specific coagulation and endothelial factors as well as acute inflammation, where late onset thrombi are more likely due to hemodynamic abnormalities. It is impressive that structural and hemodynamic associations were discovered with high significance and reliability, despite this confounding.

Structural analyses involving aspect ratios and cross-sectional areas may also have inherent biases. This bias stems from measures of aneurysm length. All coronary artery measures used in study part 1 were obtained from echocardiography reports, where aneurysm length was rarely reported; usually in the case of very large aneurysms. Larger coronary artery aneurysms are known to pose a greater risk for negative outcomes which may result in exaggerated risk associated with fusiform aneurysms, or CA aneurysms with smaller cross-sectional areas. This issue is more significant in the analyses for aspect ratios, which did not account for CA aneurysm size in any way. Consequently, it is likely

that coronary artery aneurysms with a more saccular shape, or those with a larger cross-sectional area are at greater risk for negative outcomes than expressed in the results of their respective studies.

The small sample size was the greatest limitation of the hemodynamic investigations. Furthermore, there was significant heterogeneity within the cohort where patients differed on important characteristics such as time-at-risk/event, age and antithrombotic medications. These limitations result in very low statistical power, and findings should only be considered at the cohort level despite allowing for population level inferences. Subsequently, the recommended hemodynamic thresholds (derived from thrombotic events in 5 patients) should be considered more of a proof of concept that highlights important hemodynamic variables, their potential benefit to thrombotic risk stratification criteria and the means by which they can be incorporated into said criteria.

4.3.2 Future directions

The limitations addressed in this thesis should advise future investigations on the risk of thrombosis, stenosis or failure to achieve dimensional normalization in patients with persisting CA aneurysms following Kawasaki disease. Studies involving the structural features of CA aneurysms should include detailed review of echocardiograms rather that rely on extrapolation from reports. Such detailed review would allow for more accurate and consistent measures of aneurysm length, thereby improving accuracy and consistency of aspect ratio and cross-sectional area data. Ideally, such studies should involve controls matched by CA aneurysm Z-score or diameter. Further stratification of Z-scores above 10 may also reveal interesting findings with implications for long-term management of KD patients with CA aneurysms. However, the BSA-adjusted z-score formula used in such studies should be scrutinized, since differences are noted between the different formulas at the higher end of the scoring spectrum.

Studies investigating thrombotic risk in KD patients with persisting CA aneurysms should distinguish between early and late onset thrombosis; although this may not be possible in the near future due to the small number of patient events, especially during

the acute phase of KD. A more likely and important investigation would consider the difference in thrombotic risk for patients with medium CA aneurysms depending on antithrombotic treatments suggested in the 2017 American Heart Association guidelines; especially for patients receiving single antiplatelet therapy versus dual antiplatelet therapy. Similarly future investigations should evaluate the potential benefit of statin treatment in patients with Kawasaki disease. Although, long-term benefits of statin treatment may not be evaluated in the near future, such studies would be able to consider the incidence, severity and time to dimensional normalization for KD patients acutely treated with the drug. Such investigations would also set the groundwork for long-term follow-up studies. These long-term studies could re-evaluate associations between stenosis and the structural features of a CA branch, with greater focus on the location of the lesion. In fact, complex branch anatomy may also be further stratified as the available cohort size increases.

Hemodynamic investigations on KD related CA aneurysms can also be improved, primarily through increases in study cohort size. Besides the natural increase in eligible patients with time, cohort size may also be increased through collaborative efforts with multiple institutions (perhaps through the IKDR), or advances in non-invasive, low risk modalities for detailed coronary artery imaging. Historically, MRIs were the non-invasive modality of choice for KD patients since they do not involve radiation exposure. However, MR imaging studies are very expensive and have low image resolution making evaluation of the distal segments of the coronary arteries difficult. Computed tomography (CT) is a non-invasive modality that is much cheaper and allows for a far more detailed view of the coronary artery anatomy, but is avoided in pediatric populations due to radiation exposure. Novel imaging techniques such as dual-source CT angiography with ECG-triggering allow for high-quality images with a much lower radiation dose[216]. Consequently, physicians treating KD CA aneurysm patients may be more likely to consider using the technique routinely for annual follow-up of high-risk patients. This would increase the cohort size available for imaging based hemodynamic studies as well as allowing for patient-specific models to be constructed from pre-outcome CA imaging.

Hemodynamic studies with a larger cohort size would provide statistically significant results of higher impact. Hemodynamic associations with stenosis and dimensional normalization may also be investigated with a larger cohort. Furthermore, it may be worth evaluating the hemodynamics in KD patients who develop small to medium CA aneurysms as this may shed more light on the significance of the results obtained from patients with large CA aneurysms.

Future studies should also investigate myofibroblast response to hemodynamic factors such as wall shear stress and oscillatory shear index, *in vitro* and *in* vivo. Such investigations would add context and perspective to results and discussion surrounding CA aneurysm stenosis, dimensional normalization, hemodynamics, structural features and the LMP process in KD patients. Prospective studies could also examine the coronary artery vessel wall anatomy of patients with normalized or stenosed coronary arteries using optical coherence tomography. Optical coherence tomography is a relatively new imaging modality that allows for micrometer-resolution and characterization of coronary artery tissue[217, 218]. Such characterization would help answer many questions regarding ongoing risk in dimensionally normalized aneurysms; and the mechanistic differences in progression of KD CA aneurysm related stenosis versus dimensional normalization. Prospective studies may include other novel imaging modalities coupled with advanced algorithms or machine learning based processing to no invasively evaluate myocardial perfusion in KD patients to better predict long-term prognosis. Other studies could investigate coagulation profiles in KD CA aneurysm patients, allowing for a comprehensive understanding of thrombotic risk in accordance with Virchow's triad (consideration of hemodynamics, endothelial damage and coagulation).

4.4   Summary

Kawasaki disease related coronary artery aneurysms are the leading form of acquired heart disease in children of the developed world. The aneurysms significantly increase the risk of coronary artery thrombosis and stenosis in KD patients. Luminal dimensions of some CA aneurysms may return within normal parameters over time, but

this does not imply a physiologically normal vessel wall. Furthermore, some CA aneurysms fail to achieve dimensional normalization, which increases the patient's time-at-risk for thrombosis and stenosis. Consequently, long-term management strategies for patients with persisting CA aneurysms following Kawasaki disease are very important. These strategies should focus on maximizing the rate of dimensional normalization while minimizing the incidence and severity of thrombosis and stenosis. Currently, long-term management strategies center around risk stratification based on a patient's maximum and current CA aneurysm luminal dimensions, with subjective consideration of other structural features of the coronary artery system. This thesis sought to aide refinement of current risk stratification criteria by evaluating how negative outcomes (thrombosis, stenosis and failure to achieve dimensional normalization) were affected by the structural or hemodynamic features of a patient's coronary artery system.

Findings suggest that aneurysms of the RCA and LAD, or branches with multiple aneurysms, were at the highest risk for negative outcomes. Furthermore, there was indication that involvement of the left main bifurcation increased the risk of CA stenosis; while more saccular aneurysms, as defined by aspect ratio, were more likely to thrombose. More significantly, larger aneurysms (defined by z-score or cross-sectional area) were strongly associated with negative outcomes. In fact, CA aneurysm z-scores were consistently selected by multivariable hazard models with a high reliability (100%).

Hemodynamic investigations lacked statistical power, but suggest a number of exciting possibilities. Firstly, coronary artery models created from MRI segmentations provide sufficient anatomical detail for CFD simulations on the proximal segments of the 4 main coronary artery branches. These simulations suggest intuitive associations between key hemodynamic variables and thrombotic risk. Branches with longer blood recirculation times and aneurysms with lower wall shear stress or greater area exposed to very low wall shear stress, were at an increased risk for thrombotic events. It is possible to create hemodynamic thresholds for these variables which seem to outperform standard structural criteria for treatment (z-score ≥10 or absolute diameter ≥8) with regards to specificity (similar sensitivity).

When taken together, findings from the structural and hemodynamic analyses allow for postulates regarding the driving factors behind thrombosis, stenosis and dimensional normalization in KD related CA aneurysms. Abnormal coronary artery blood flow is most important for thrombus formation, but may also influence stenotic progression while having little effect on the rate of dimensional normalization. The extent of damage to the CA vessel wall has the greatest influence on dimensional normalization and stenotic progression, but has a lesser effect on thrombotic risk. These hypotheses rely on a number of assumptions that have not been tested, as previously outlined.

As apparent, further research is required to better understand the pathological processes involved in KD CA aneurysm related thrombosis, stenosis and dimensional normalization. Physicians managing high-risk patients with large CA aneurysms related to KD should consider annual follow-up that includes detailed advanced coronary artery imaging via MRI or CT. This would allow for better assessment of risk, and better medical management, while facilitating research efforts in the field. Nevertheless, current risk stratification for negative outcomes associated with KD related CA aneurysms are reliable and efficient, but may still be improved on. Aneurysms that involve the bifurcation of the LCA or coronary artery branches with multiple aneurysms have a significantly higher risk for negative outcomes, a finding that should be taken into consideration for the medical management of relevant patients. Future criteria should also consider other hemodynamic and structural thresholds secondarily to coronary artery z-scores, especially for patients with medium or large aneurysms.

4.5   References

1.   Kawasaki, T., *[Acute febrile mucocutaneous syndrome with lymphoid involvement with specific desquamation of the fingers and toes in children].* Arerugi, 1967. **16**(3): p. 178-222.
2.   Burns, J.C., et al., *Kawasaki disease: A brief history.* Pediatrics, 2000. **106**(2): p. E27.
3.   Gee, S.J., *Cases of morbid anatomy: aneurysms of coronary arteries in a boy.* St Bartholomews Hosp Rep., 1871. **7**: p. 141-178.
4.   Holman, R.C., et al., *Kawasaki syndrome in Hawaii.* Pediatr Infect Dis J, 2005. **24**(5): p. 429-33.
5.   Kushner, H.I., et al., *The two emergencies of Kawasaki syndrome and the implications for the developing world.* Pediatr Infect Dis J, 2008. **27**(5): p. 377-83.
6.   Arkachaisri, T., *Pediatric rheumatology in Southeast Asia: insights from the Singapore experience.* Curr Rheumatol Rep, 2011. **13**(2): p. 117-22.
7.   Davaalkham, D., et al., *Kawasaki disease in Mongolia: results from 2 nationwide retrospective surveys, 1996-2008.* J Epidemiol, 2011. **21**(4): p. 293-8.
8.   Singh, S., et al., *Is Kawasaki disease incidence rising in Chandigarh, North India?* Arch Dis Child, 2011. **96**(2): p. 137-40.
9.   Al-Ammouri, I., S. Al-Wahsh, and N. Khuri-Bulos, *Kawasaki disease in Jordan: demographics, presentation, and outcome.* Cardiol Young, 2012. **22**(4): p. 390-5.
10. Uehara, R. and E.D. Belay, *Epidemiology of Kawasaki disease in Asia, Europe, and the United States.* J Epidemiol, 2012. **22**(2): p. 79-85.
11. Alexopoulos, A., et al., *Kawasaki disease in Greek children: a retrospective study.* J Eur Acad Dermatol Venereol, 2013. **27**(5): p. 580-8.
12. Holman, R.C., et al., *Hospitalizations for Kawasaki syndrome among children in the United States, 1997-2007.* Pediatr Infect Dis J, 2010. **29**(6): p. 483-8.
13. Makino, N., et al., *Epidemiological observations of Kawasaki disease in Japan, 2013-2014.* Pediatr Int, 2018. **60**(6): p. 581-587.
14. Kim, G.B., et al., *Epidemiologic features of Kawasaki disease in South Korea: data from nationwide survey, 2009-2011.* Pediatr Infect Dis J, 2014. **33**(1): p. 24-7.
15. Lin, M.C., et al., *Epidemiologic features of Kawasaki disease in acute stages in Taiwan, 1997-2010: effect of different case definitions in claims data analysis.* J Chin Med Assoc, 2015. **78**(2): p. 121-6.
16. Holman RC, B.E., Christensen KY, Folkema AM, Steiner CA, Schonberger LB., *Hospitalizations for Kawasaki syndrome among children in the United States, 1997-2007.* Pediatr Infect Dis J, 2010. **29**(6): p. 483-488.
17. Manlhiot, C., et al., *Epidemiology of Kawasaki Disease in Canada 2004 to 2014: Comparison of Surveillance Using Administrative Data vs Periodic Medical Record Review.* Can J Cardiol, 2018. **34**(3): p. 303-309.
18. Holman, R.C., et al., *Racial/ethnic differences in the incidence of Kawasaki syndrome among children in Hawaii.* Hawaii Med J, 2010. **69**(8): p. 194-7.
19. Maddox, R.A., et al., *Recurrent Kawasaki disease: USA and Japan.* Pediatr Int, 2015. **57**(6): p. 1116-20.
20. Yanagawa, H., et al., *Results of the nationwide epidemiologic survey of Kawasaki disease in 1995 and 1996 in Japan.* Pediatrics, 1998. **102**(6): p. E65.
21. Fujita, Y., et al., *Kawasaki disease in families.* Pediatrics, 1989. **84**(4): p. 666-9.
22. Harada, F., et al., *Genetic analysis of Kawasaki syndrome.* Am J Hum Genet, 1986. **39**(4): p. 537-9.

23.	Fukuda, S., et al., *Simultaneous development of Kawasaki disease following acute human adenovirus infection in monozygotic twins: A case report.* Pediatr Rheumatol Online J, 2017. **15**(1): p. 39.

24.	Zhang, X., et al., *Kawasaki disease in two sets of monozygotic twins: Is the etiology genetic or environmental?* Pak J Med Sci, 2013. **29**(1): p. 227-30.

25.	Kottek, A., C. Shimizu, and J.C. Burns, *Kawasaki disease in monozygotic twins.* Pediatr Infect Dis J, 2011. **30**(12): p. 1114-6.

26.	Sano, T., et al., *Temporal and geographical clustering of Kawasaki disease in Japan: 2007-2012.* Pediatr Int, 2016. **58**(11): p. 1140-1145.

27.	Kao, A.S., et al., *Spatial and temporal clustering of Kawasaki syndrome cases.* Pediatr Infect Dis J, 2008. **27**(11): p. 981-5.

28.	Burns, J.C., et al., *Seasonality and temporal clustering of Kawasaki syndrome.* Epidemiology, 2005. **16**(2): p. 220-5.

29.	Turnier, J.L., et al., *Concurrent Respiratory Viruses and Kawasaki Disease.* Pediatrics, 2015. **136**(3): p. e609-14.

30.	Chang, L.Y., et al., *Viral infections associated with Kawasaki disease.* J Formos Med Assoc, 2014. **113**(3): p. 148-54.

31.	Burns, J.C., et al., *Seasonality of Kawasaki disease: a global perspective.* PLoS One, 2013. **8**(9): p. e74529.

32.	Leung, D.Y., et al., *Prevalence of superantigen-secreting bacteria in patients with Kawasaki disease.* J Pediatr, 2002. **140**(6): p. 742-6.

33.	Marchette, N.J., et al., *Epstein-Barr virus and other herpesvirus infections in Kawasaki syndrome.* J Infect Dis, 1990. **161**(4): p. 680-4.

34.	Rodo, X., et al., *Revisiting the role of environmental and climate factors on the epidemiology of Kawasaki disease.* Ann N Y Acad Sci, 2016. **1382**(1): p. 84-98.

35.	Pitzer, V.E., et al., *Modelling seasonal variations in the age and incidence of Kawasaki disease to explore possible infectious aetiologies.* Proc Biol Sci, 2012. **279**(1739): p. 2736-43.

36.	Manlhiot, C., et al., *Environmental epidemiology of Kawasaki disease: Linking disease etiology, pathogenesis and global distribution.* PLoS One, 2018. **13**(2): p. e0191087.

37.	Rigante, D., G. Tarantino, and P. Valentini, *Non-infectious makers of Kawasaki syndrome: tangible or elusive triggers?* Immunol Res, 2016. **64**(1): p. 51-4.

38.	Wills-Karp, M., J. Santeliz, and C.L. Karp, *The germless theory of allergic disease: revisiting the hygiene hypothesis.* Nat Rev Immunol, 2001. **1**(1): p. 69-75.

39.	Tsai, Y.J., et al., *The association between Kawasaki disease and allergic diseases, from infancy to school age.* Allergy Asthma Proc, 2013. **34**(5): p. 467-72.

40.	Wei, C.C., et al., *Increased risk of Kawasaki disease in children with common allergic diseases.* Ann Epidemiol, 2014. **24**(5): p. 340-3.

41.	Rodo, X., et al., *Association of Kawasaki disease with tropospheric wind patterns.* Sci Rep, 2011. **1**: p. 152.

42.	Rodo, X., et al., *Tropospheric winds from northeastern China carry the etiologic agent of Kawasaki disease from its source to Japan.* Proc Natl Acad Sci U S A, 2014. **111**(22): p. 7952-7.

43.	Makino, N., et al., *Descriptive epidemiology of Kawasaki disease in Japan, 2011-2012: from the results of the 22nd nationwide survey.* J Epidemiol, 2015. **25**(3): p. 239-45.

44.	Burns, J.C., et al., *Coagulopathy and platelet activation in Kawasaki syndrome: identification of patients at high risk for development of coronary artery aneurysms.* J Pediatr, 1984. **105**(2): p. 206-11.

45.	Nakamura, Y., et al., *Mortality among Japanese with a history of Kawasaki disease: results at the end of 2009.* J Epidemiol, 2013. **23**(6): p. 429-34.

46. Fujiwara, H. and Y. Hamashima, *Pathology of the heart in Kawasaki disease.* Pediatrics, 1978. **61**(1): p. 100-7.

47. McCrindle, B.W., et al., *Diagnosis, Treatment, and Long-Term Management of Kawasaki Disease: A Scientific Statement for Health Professionals From the American Heart Association.* Circulation, 2017. **135**(17): p. e927-e999.

48. Burns, J.C., et al., *Sequelae of Kawasaki disease in adolescents and young adults.* J Am Coll Cardiol, 1996. **28**(1): p. 253-7.

49. Daniels, L.B., et al., *Prevalence of Kawasaki disease in young adults with suspected myocardial ischemia.* Circulation, 2012. **125**(20): p. 2447-53.

50. Leung, D.Y., et al., *Superantigens in Kawasaki syndrome.* Clin Immunol Immunopathol, 1995. **77**(2): p. 119-26.

51. Leung, D.Y., et al., *Evidence for superantigen involvement in cardiovascular injury due to Kawasaki syndrome.* J Immunol, 1995. **155**(10): p. 5018-21.

52. Rowley, A.H., et al., *Oligoclonal IgA response in the vascular wall in acute Kawasaki disease.* J Immunol, 2001. **166**(2): p. 1334-43.

53. Rowley, A.H., et al., *IgA plasma cells in vascular tissue of patients with Kawasaki syndrome.* J Immunol, 1997. **159**(12): p. 5946-55.

54. Franco, A., et al., *Memory T-cells and characterization of peripheral T-cell clones in acute Kawasaki disease.* Autoimmunity, 2010. **43**(4): p. 317-24.

55. Rowley, A.H., et al., *Ultrastructural, immunofluorescence, and RNA evidence support the hypothesis of a "new" virus associated with Kawasaki disease.* J Infect Dis, 2011. **203**(7): p. 1021-30.

56. Rowley, A.H., et al., *RNA-containing cytoplasmic inclusion bodies in ciliated bronchial epithelium months to years after acute Kawasaki disease.* PLoS One, 2008. **3**(2): p. e1582.

57. Orenstein, J.M., et al., *Three linked vasculopathic processes characterize Kawasaki disease: a light and transmission electron microscopic study.* PLoS One, 2012. **7**(6): p. e38998.

58. Parihar, M., et al., *Mid-term Risk for Subclinical Atherosclerosis and Chronic Myocarditis in Children with Kawasaki Disease and Transient Coronary Abnormalities.* Pediatr Cardiol, 2017. **38**(6): p. 1123-1132.

59. Zhang, H., et al., *Meta-analysis of risk factors associated with atherosclerosis in patients with Kawasaki disease.* World J Pediatr, 2016. **12**(3): p. 308-313.

60. Kato, H., *Cardiovascular complications in Kawasaki disease: coronary artery lumen and long-term consequences.* Prog Pediatr Cardiol, 2004. **19**: p. 137-145.

61. Newburger, J.W., et al., *Diagnosis, treatment, and long-term management of Kawasaki disease: a statement for health professionals from the Committee on Rheumatic Fever, Endocarditis and Kawasaki Disease, Council on Cardiovascular Disease in the Young, American Heart Association.* Circulation, 2004. **110**(17): p. 2747-71.

62. Sumitomo, N., et al., *Association of sinus node dysfunction, atrioventricular node conduction abnormality and ventricular arrhythmia in patients with Kawasaki disease and coronary involvement.* Circ J, 2008. **72**(2): p. 274-80.

63. Haney, I., et al., *Ventricular arrhythmia complicating Kawasaki disease.* Can J Cardiol, 1995. **11**(10): p. 931-3.

64. Yagi, S., et al., *Two adults requiring implantable defibrillators because of ventricular tachycardia and left ventricular dysfunction caused by presumed Kawasaki disease.* Circ J, 2005. **69**(7): p. 870-4.

65. Yutani, C., et al., *Cardiac biopsy of Kawasaki disease.* Arch Pathol Lab Med, 1981. **105**(9): p. 470-3.

66.   Harada, M., et al., *Histopathological characteristics of myocarditis in acute-phase Kawasaki disease.* Histopathology, 2012. **61**(6): p. 1156-67.

67.   Printz, B.F., et al., *Noncoronary cardiac abnormalities are associated with coronary artery dilation and with laboratory inflammatory markers in acute Kawasaki disease.* J Am Coll Cardiol, 2011. **57**(1): p. 86-92.

68.   Dominguez, S.R., et al., *Kawasaki disease in a pediatric intensive care unit: a case-control study.* Pediatrics, 2008. **122**(4): p. e786-90.

69.   Kanegaye, J.T., et al., *Recognition of a Kawasaki disease shock syndrome.* Pediatrics, 2009. **123**(5): p. e783-9.

70.   Muniz, J.C., et al., *Coronary artery dimensions in febrile children without Kawasaki disease.* Circ Cardiovasc Imaging, 2013. **6**(2): p. 239-44.

71.   Newburger, J.W., et al., *The treatment of Kawasaki syndrome with intravenous gamma globulin.* N Engl J Med, 1986. **315**(6): p. 341-7.

72.   Newburger, J.W., et al., *A single intravenous infusion of gamma globulin as compared with four infusions in the treatment of acute Kawasaki syndrome.* N Engl J Med, 1991. **324**(23): p. 1633-9.

73.   Dominguez, S.R., et al., *Preventing coronary artery abnormalities: a need for earlier diagnosis and treatment of Kawasaki disease.* Pediatr Infect Dis J, 2012. **31**(12): p. 1217-20.

74.   Lujinovic, A., F. Ovcina, and A. Tursic, *Third coronary artery.* Bosn J Basic Med Sci, 2008. **8**(3): p. 226-9.

75.   Kosar, P., et al., *Anatomic variations and anomalies of the coronary arteries: 64-slice CT angiographic appearance.* Diagn Interv Radiol, 2009. **15**(4): p. 275-83.

76.   Heusch, G., et al., *The coronary circulation in cardioprotection: more than just one confounder.* Cardiovasc Res, 2012. **94**(2): p. 237-45.

77.   Hurst, J.W., et al., *Hurst's the heart*. 13th ed. 2011, New York: McGraw-Hill Medical.

78.   Waller, B.F., et al., *Anatomy, histology, and pathology of coronary arteries: a review relevant to new interventional and imaging techniques--Part IV.* Clin Cardiol, 1992. **15**(9): p. 675-87.

79.   Seon, H.J., Kim, Y.H., *Atherosclerotic Coronary Artery Disease*, ed. T.H. Lim. 2015, Practical Textbook of Cardiac CT and MRI (pg 64): Springer, Berlin, Heidelberg.

80.   Starikov, A., Xiong, G., Min, J.K., *Normal Distribution of Wall Shear Stress in the Coronary Arteries [Abstract].* Circulation, 2015. **132**(A115816).

81.   Amaya, R., L.M. Cancel, and J.M. Tarbell, *Interaction between the Stress Phase Angle (SPA) and the Oscillatory Shear Index (OSI) Affects Endothelial Cell Gene Expression.* PLoS One, 2016. **11**(11): p. e0166569.

82.   Soulis, J.V., et al., *Wall shear stress in normal left coronary artery tree.* J Biomech, 2006. **39**(4): p. 742-9.

83.   Marcus, J.T., et al., *Flow profiles in the left anterior descending and the right coronary artery assessed by MR velocity quantification: effects of through-plane and in-plane motion of the heart.* J Comput Assist Tomogr, 1999. **23**(4): p. 567-76.

84.   Morton, J.K., Tatineni, S., Gudipati, C., Aguirre, F., Ring, M.E., Serota, H., Deligonul, U. , *Regional coronary blood flow velocity and vasodilator reserve in patients with angiographically normal coronary arteries.* Coron. Artery Dis., 1990. **1**(5).

85.   Dallaire, F., et al., *Marked variations in serial coronary artery diameter measures in Kawasaki disease: a new indicator of coronary involvement.* J Am Soc Echocardiogr, 2012. **25**(8): p. 859-65.

86.   *Guidelines for diagnosis and management of cardiovascular sequelae in Kawasaki disease (JCS 2013). Digest version.* Circ J, 2014. **78**(10): p. 2521-62.

87.   de Zorzi, A., et al., *Coronary artery dimensions may be misclassified as normal in Kawasaki disease.* J Pediatr, 1998. **133**(2): p. 254-8.

88. Newburger, J.W., et al., *Diagnosis, treatment, and long-term management of Kawasaki disease: a statement for health professionals from the Committee on Rheumatic Fever, Endocarditis, and Kawasaki Disease, Council on Cardiovascular Disease in the Young, American Heart Association.* Pediatrics, 2004. **114**(6): p. 1708-33.

89. Kurotobi, S., et al., *Coronary diameter in normal infants, children and patients with Kawasaki disease.* Pediatr Int, 2002. **44**(1): p. 1-4.

90. Tan, T.H., et al., *Coronary normograms and the coronary-aorta index: objective determinants of coronary artery dilatation.* Pediatr Cardiol, 2003. **24**(4): p. 328-35.

91. McCrindle, B.W., et al., *Coronary artery involvement in children with Kawasaki disease: risk factors from analysis of serial normalized measurements.* Circulation, 2007. **116**(2): p. 174-9.

92. Manlhiot, C., et al., *Improved classification of coronary artery abnormalities based only on coronary artery z-scores after Kawasaki disease.* Pediatr Cardiol, 2010. **31**(2): p. 242-9.

93. Ogata, S., et al., *Coronary artery outcomes among children with Kawasaki disease in the United States and Japan.* Int J Cardiol, 2013. **168**(4): p. 3825-8.

94. Dallaire, F. and N. Dahdah, *New equations and a critical appraisal of coronary artery Z scores in healthy children.* J Am Soc Echocardiogr, 2011. **24**(1): p. 60-74.

95. Capannari, T.E., et al., *Sensitivity, specificity and predictive value of two-dimensional echocardiography in detecting coronary artery aneurysms in patients with Kawasaki disease.* J Am Coll Cardiol, 1986. **7**(2): p. 355-60.

96. Kato, H., et al., *Long-term consequences of Kawasaki disease. A 10- to 21-year follow-up study of 594 patients.* Circulation, 1996. **94**(6): p. 1379-85.

97. Paredes, N., et al., *Management of myocardial infarction in children with Kawasaki disease.* Blood Coagul Fibrinolysis, 2010. **21**(7): p. 620-31.

98. Suzuki, A., et al., *Myocardial ischemia in Kawasaki disease: follow-up study by cardiac catheterization and coronary angiography.* Pediatr Cardiol, 1988. **9**(1): p. 1-5.

99. Tsuda, E., Arakaki, Y., Shimizu, T., Sakaguchi, H., Yoshimura, S., Yazaki, S., Echigo, S., *Changes in causes of sudden deaths by decade in patients with coronary arterial lesions due to Kawasaki disease.* Cardiol Young, 2005. **15**(5): p. 481-488.

100. Onouchi, Z., et al., *Transformation of coronary artery aneurysm to obstructive lesion and the role of collateral vessels in myocardial perfusion in patients with Kawasaki disease.* J Am Coll Cardiol, 1993. **21**(1): p. 158-62.

101. Tsuda, E., Hirata, T., Matsuo, O., Abe, T., Sugiyama, H., Yamada, O., *The 30-year outcome for patients after myocardial infarction due to coronary artery lesions caused by Kawasaki disease.* pediatr Cardiol, 2011. **32**(2): p. 176-182.

102. Burns, J.C., Glode, M.P., Clarke, S.H., Wiggins, J.Jr., Hathaway, W.E., *Coagulopathy and platelet activation in Kawasaki syndrome: identification of patients at high risk for development of coronary artery aneurysms.* J Pediatr, 1984. **105**(2): p. 206-11.

103. Chen, X., et al., *Hypercoagulation and elevation of blood triglycerides are characteristics of Kawasaki disease.* Lipids Health Dis, 2015. **14**: p. 166.

104. Simpson, H.C., et al., *Hypertriglyceridaemia and hypercoagulability.* Lancet, 1983. **1**(8328): p. 786-90.

105. Carvalho de Sousa, J., et al., *Coagulation factor VII and plasma triglycerides. Decreased catabolism as a possible mechanism of factor VII hyperactivity.* Haemostasis, 1989. **19**(3): p. 125-30.

106. Yau, J.W., H. Teoh, and S. Verma, *Endothelial cell control of thrombosis.* BMC Cardiovasc Disord, 2015. **15**: p. 130.

107. Dhillon, R., et al., *Endothelial dysfunction late after Kawasaki disease.* Circulation, 1996. **94**(9): p. 2103-6.

108. Dietz, S.M., et al., *Peripheral Endothelial (Dys)Function, Arterial Stiffness and Carotid Intima-Media Thickness in Patients after Kawasaki Disease: A Systematic Review and Meta-Analyses.* PLoS One, 2015. **10**(7): p. e0130913.

109. Chiu, J.J. and S. Chien, *Effects of disturbed flow on vascular endothelium: pathophysiological basis and clinical perspectives.* Physiol Rev, 2011. **91**(1): p. 327-87.

110. Mazzolai, L., et al., *Tissue factor activity is upregulated in human endothelial cells exposed to oscillatory shear stress.* Thromb Haemost, 2002. **87**(6): p. 1062-8.

111. Chien, S., et al., *Effects of hematocrit and plasma proteins on human blood rheology at low shear rates.* J Appl Physiol, 1966. **21**(1): p. 81-7.

112. Lipowsky, H.H., *Microvascular rheology and hemodynamics.* Microcirculation, 2005. **12**(1): p. 5-15.

113. Fogelson, A.L. and K.B. Neeves, *Fluid Mechanics of Blood Clot Formation.* Annu Rev Fluid Mech, 2015. **47**: p. 377-403.

114. Bluestein, D., et al., *Steady flow in an aneurysm model: correlation between fluid dynamics and blood platelet deposition.* J Biomech Eng, 1996. **118**(3): p. 280-6.

115. Iwazu, Y., T. Minami, and K. Kotani, *Pulse Wave Velocity in Kawasaki Disease.* Angiology, 2017. **68**(3): p. 189-195.

116. Newburger, J.W., et al., *Altered lipid profile after Kawasaki syndrome.* Circulation, 1991. **84**(2): p. 625-31.

117. Ou, C.Y., et al., *Significant relationship between serum high-sensitivity C-reactive protein, high-density lipoprotein cholesterol levels and children with Kawasaki disease and coronary artery lesions.* J Formos Med Assoc, 2009. **108**(9): p. 719-24.

118. Gupta-Malhotra, M., et al., *Atherosclerosis in survivors of Kawasaki disease.* J Pediatr, 2009. **155**(4): p. 572-7.

119. Ueba, H., M. Kawakami, and T. Yaginuma, *Shear stress as an inhibitor of vascular smooth muscle cell proliferation. Role of transforming growth factor-beta 1 and tissue-type plasminogen activator.* Arterioscler Thromb Vasc Biol, 1997. **17**(8): p. 1512-6.

120. Fitzgerald, T.N., et al., *Laminar shear stress stimulates vascular smooth muscle cell apoptosis via the Akt pathway.* J Cell Physiol, 2008. **216**(2): p. 389-95.

121. Haga, M., et al., *Oscillatory shear stress increases smooth muscle cell proliferation and Akt phosphorylation.* J Vasc Surg, 2003. **37**(6): p. 1277-84.

122. Forte, A., et al., *Role of myofibroblasts in vascular remodelling: focus on restenosis and aneurysm.* Cardiovasc Res, 2010. **88**(3): p. 395-405.

123. Sheriff, J., et al., *High-shear stress sensitizes platelets to subsequent low-shear conditions.* Ann Biomed Eng, 2010. **38**(4): p. 1442-50.

124. Iemura, M., et al., *Long term consequences of regressed coronary aneurysms after Kawasaki disease: vascular wall morphology and function.* Heart, 2000. **83**(3): p. 307-11.

125. Mitani, Y., et al., *In vivo plaque composition and morphology in coronary artery lesions in adolescents and young adults long after Kawasaki disease: a virtual histology-intravascular ultrasound study.* Circulation, 2009. **119**(21): p. 2829-36.

126. Lemura, M., Ishii, M., Sugimura, T., Akagi, T., Kato, H., *Long term consequences of regressed coronary aneurysms after Kawasaki disease: vascular wall morphology and function.* Heart, 2000. **83**: p. 307-311.

127. Furuyama, H., et al., *Assessment of coronary function in children with a history of Kawasaki disease using (15)O-water positron emission tomography.* Circulation, 2002. **105**(24): p. 2878-84.

128. Hauser, M., et al., *Myocardial blood flow and coronary flow reserve in children with "normal" epicardial coronary arteries after the onset of Kawasaki disease assessed by positron emission tomography.* Pediatr Cardiol, 2004. **25**(2): p. 108-12.

129. Furuyama, H., et al., *Altered myocardial flow reserve and endothelial function late after Kawasaki disease.* J Pediatr, 2003. **142**(2): p. 149-54.

130. Roberts, W., *Editorial: Coronary thrombosis and fatal myocardial ischemia.* Circulation, 1974. **49**(1): p. 1-3.

131. Heusch, G., *Coronary microvascular obstruction: the new frontier in cardioprotection.* Basic Res Cardiol, 2019. **114**(6): p. 45.

132. Muthusami, P., et al., *Myocardial Perfusion, Fibrosis, and Contractility in Children With Kawasaki Disease.* JACC Cardiovasc Imaging, 2018. **11**(12): p. 1922-1924.

133. Bratis, K., et al., *Abnormal myocardial perfusion in Kawasaki disease convalescence.* JACC Cardiovasc Imaging, 2015. **8**(1): p. 106-108.

134. Mori, M., et al., *Meta-analysis of the results of intravenous gamma globulin treatment of coronary artery lesions in Kawasaki disease.* Mod Rheumatol, 2004. **14**(5): p. 361-6.

135. Oates-Whitehead, R.M., et al., *Intravenous immunoglobulin for the treatment of Kawasaki disease in children.* Cochrane Database Syst Rev, 2003(4): p. CD004000.

136. Baumer, J.H., et al., *Salicylate for the treatment of Kawasaki disease in children.* Cochrane Database Syst Rev, 2006(4): p. CD004175.

137. Ohkubo, T., et al., *Reduced shear stress and disturbed flow may lead to coronary aneurysm and thrombus formations.* Pediatr Int, 2007. **49**(1): p. 1-7.

138. Kuramochi, Y., et al., *Hemodynamic factors of thrombus formation in coronary aneurysms associated with Kawasaki disease.* Pediatr Int, 2000. **42**(5): p. 470-5.

139. Sengupta, D., et al., *Image-based modeling of hemodynamics in coronary artery aneurysms caused by Kawasaki disease.* Biomech Model Mechanobiol, 2012. **11**(6): p. 915-32.

140. Sengupta, D., et al., *Thrombotic risk stratification using computational modeling in patients with coronary artery aneurysms following Kawasaki disease.* Biomech Model Mechanobiol, 2014. **13**(6): p. 1261-76.

141. Sugahara, Y., et al., *Warfarin therapy for giant aneurysm prevents myocardial infarction in Kawasaki disease.* Pediatr Cardiol, 2008. **29**(2): p. 398-401.

142. Squizzato, A., et al., *Clopidogrel plus aspirin versus aspirin alone for preventing cardiovascular disease.* Cochrane Database Syst Rev, 2011(1): p. CD005158.

143. Park, J.J., et al., *Effect of beta-Blockers Beyond 3 Years After Acute Myocardial Infarction.* J Am Heart Assoc, 2018. **7**(5).

144. Stone, N.J., et al., *2013 ACC/AHA guideline on the treatment of blood cholesterol to reduce atherosclerotic cardiovascular risk in adults: a report of the American College of Cardiology/American Heart Association Task Force on Practice Guidelines.* Circulation, 2014. **129**(25 Suppl 2): p. S1-45.

145. Antonopoulos, A.S., et al., *Statins as anti-inflammatory agents in atherogenesis: molecular mechanisms and lessons from the recent clinical trials.* Curr Pharm Des, 2012. **18**(11): p. 1519-30.

146. Sikora, J., et al., *Effect of statins on platelet function in patients with hyperlipidemia.* Arch Med Sci, 2013. **9**(4): p. 622-8.

147. Undas, A., K.E. Brummel-Ziedins, and K.G. Mann, *Anticoagulant effects of statins and their clinical implications.* Thromb Haemost, 2014. **111**(3): p. 392-400.

148. Blankier, S., et al., *The role of atorvastatin in regulating the immune response leading to vascular damage in a model of Kawasaki disease.* Clin Exp Immunol, 2011. **164**(2): p. 193-201.

149. Bruni, F., et al., *Effect of atorvastatin on different fibrinolyis mechanisms in hypercholesterolemic subjects.* Int J Cardiol, 2004. **95**(2-3): p. 269-74.

150.   Brownfoot, F.C., Kaitu'u-Lino, T.J., Hannan, N., Hastie, R., Cannon, P., Onda, K., Tong, S., *Statins reduce soluble Flt1, and quench endothelial dysfunction in primary human tissues, but increase soluble endoglin release.* Pregnancy Hypertens, 2015. **5**(1): p. 22-23.

151.   Assmus, B., et al., *HMG-CoA reductase inhibitors reduce senescence and increase proliferation of endothelial progenitor cells via regulation of cell cycle regulatory genes.* Circ Res, 2003. **92**(9): p. 1049-55.

152.   Szmitko, P.E., et al., *Endothelial progenitor cells: new hope for a broken heart.* Circulation, 2003. **107**(24): p. 3093-100.

153.   Llevadot, J., et al., *HMG-CoA reductase inhibitor mobilizes bone marrow--derived endothelial progenitor cells.* J Clin Invest, 2001. **108**(3): p. 399-405.

154.   Weis, M., et al., *Statins have biphasic effects on angiogenesis.* Circulation, 2002. **105**(6): p. 739-45.

155.   Stark, W.W., Jr., et al., *Inhibiting geranylgeranylation blocks growth and promotes apoptosis in pulmonary vascular smooth muscle cells.* Am J Physiol, 1998. **275**(1 Pt 1): p. L55-63.

156.   Gray, C., et al., *Statins promote residual aneurysm sac regression following endovascular aortic aneurysm repair.* Vasc Endovascular Surg, 2014. **48**(2): p. 111-5.

157.   Ferguson, C.D., et al., *Association of statin prescription with small abdominal aortic aneurysm progression.* Am Heart J, 2010. **159**(2): p. 307-13.

158.   Tada, Y., et al., *Statins promote the growth of experimentally induced cerebral aneurysms in estrogen-deficient rats.* Stroke, 2011. **42**(8): p. 2286-93.

159.   Niedra, E., et al., *Atorvastatin safety in Kawasaki disease patients with coronary artery aneurysms.* Pediatr Cardiol, 2014. **35**(1): p. 89-92.

160.   Chahal, N., et al., *Parental anxiety associated with Kawasaki disease in previously healthy children.* J Pediatr Health Care, 2010. **24**(4): p. 250-7.

161.   Banks, L., et al., *Factors associated with low moderate-to-vigorous physical activity levels in pediatric patients with Kawasaki disease.* Clin Pediatr (Phila), 2012. **51**(9): p. 828-34.

162.   [Abstract], B.W.M.f.t.N.A.K.D.R., *North American Kawasaki Disease Registry – Advancing clinical research through collaboration.* Circulation, 2015. **131**: p. A222.

163.   Tierney, E.S.S., McCrindle, B.W., Runeckles, K., Thacker, D., Mackie, A., Colyer, J., Burns, J.C., Mahle, W.T., Warren, A., Raghuveer, G., *Variation among Institutions in Pharmacological Management of Patients with Coronary Artery Aneurysms after Kawasaki Disease [Abstract].* circulation, 2018. **[Accepted]**.

164.   Bluestein, D., et al., *Fluid mechanics of arterial stenosis: relationship to the development of mural thrombus.* Ann Biomed Eng, 1997. **25**(2): p. 344-56.

165.   Shadden, S.C. and S. Hendabadi, *Potential fluid mechanic pathways of platelet activation.* Biomech Model Mechanobiol, 2013. **12**(3): p. 467-74.

166.   Sun, Z. and L. Xu, *Computational fluid dynamics in coronary artery disease.* Comput Med Imaging Graph, 2014. **38**(8): p. 651-63.

167.   Kobayashi, T., et al., *A New Z Score Curve of the Coronary Arterial Internal Diameter Using the Lambda-Mu-Sigma Method in a Pediatric Population.* J Am Soc Echocardiogr, 2016. **29**(8): p. 794-801 e29.

168.   Ronai, C., et al., *Coronary Artery Aneurysm Measurement and Z Score Variability in Kawasaki Disease.* J Am Soc Echocardiogr, 2016. **29**(2): p. 150-7.

169.   Zeng, Z., et al., *Can aspect ratio be used to categorize intra-aneurysmal hemodynamics?--A study of elastase induced aneurysms in rabbit.* J Biomech, 2011. **44**(16): p. 2809-16.

170.   Grande Gutierrez, N., et al., *Hemodynamic variables in aneurysms are associated with thrombotic risk in children with Kawasaki disease.* Int J Cardiol, 2019. **281**: p. 15-21.

171.   Elster, A.D. *Questions and answers in MRI*. [Website] 2017 [cited 2018; Available from: http://mriquestions.com/index.html.

172.   Updegrove, A., et al., *SimVascular: An Open Source Pipeline for Cardiovascular Simulation.* Ann Biomed Eng, 2017. **45**(3): p. 525-541.

173.   Si, H., *TetGen, a Delaunay-based quality tetrahedral mesh generator. .* ACM Transacyion on Mathematical Software (TOMS). 2015. **41**(2): p. A:11.

174.   Fournier, R.L., *Basic transport phenomena in biomedical engineering*. 2012: CRC Press.

175.   Figueroa, C.A., Vignon-Clementel, I.E., Jansen, K.E., Hughes, T.J.R., Taylor, C.A., *A coupled momentum method for modeling blood flow in three-dimensional deformable arteries.* Comput Methods Appl Mech Engrg, 2005. **195**: p. 5685-5706.

176.   Long, C.C., et al., *Fluid-structure interaction simulations of the Fontan procedure using variable wall properties.* Int J Numer Method Biomed Eng, 2012. **28**(5): p. 513-27.

177.   Ramachandra, A.B., A.M. Kahn, and A.L. Marsden, *Patient-Specific Simulations Reveal Significant Differences in Mechanical Stimuli in Venous and Arterial Coronary Grafts.* J Cardiovasc Transl Res, 2016. **9**(4): p. 279-90.

178.   Nichols, W.W. and D.A. McDonald, *McDonald's blood flow in arteries : theoretic, experimental, and clinical principles*. 6th ed. 2011, London: Hodder Arnold. xiv,755 p.

179.   Roccabianca, S., et al., *Quantification of regional differences in aortic stiffness in the aging human.* J Mech Behav Biomed Mater, 2014. **29**: p. 618-34.

180.   Podesser, B.K., et al., *Outer radius-wall thickness ratio, a postmortem quantitative histology in human coronary arteries.* Acta Anat (Basel), 1998. **163**(2): p. 63-8.

181.   Coogan, J.S., J.D. Humphrey, and C.A. Figueroa, *Computational simulations of hemodynamic changes within thoracic, coronary, and cerebral arteries following early wall remodeling in response to distal aortic coarctation.* Biomech Model Mechanobiol, 2013. **12**(1): p. 79-93.

182.   Kim, H.J., et al., *Patient-specific modeling of blood flow and pressure in human coronary arteries.* Ann Biomed Eng, 2010. **38**(10): p. 3195-209.

183.   Bove, E.L., et al., *Toward optimal hemodynamics: computer modeling of the Fontan circuit.* Pediatr Cardiol, 2007. **28**(6): p. 477-81.

184.   Corsini, C., et al., *Multiscale models of the hybrid palliation for hypoplastic left heart syndrome.* J Biomech, 2011. **44**(4): p. 767-70.

185.   Sankaran, S., et al., *Patient-specific multiscale modeling of blood flow for coronary artery bypass graft surgery.* Ann Biomed Eng, 2012. **40**(10): p. 2228-42.

186.   Moghadam, M.E., et al., *Optimization of shunt placement for the Norwood surgery using multi-domain modeling.* J Biomech Eng, 2012. **134**(5): p. 051002.

187.   Tran, J.S., et al., *Automated Tuning for Parameter Identification and Uncertainty Quantification in Multi-scale Coronary Simulations.* Comput Fluids, 2017. **142**: p. 128-138.

188.   Ayachlt, U., *The ParaView Guide: A Parallel Visualization Application*. 2015: Kitware.

189.   Esmaily-Moghadam, M., T.Y. Hsia, and A.L. Marsden, *A non-discrete method for computation of residence time in fluid mechanics simulations.* Phys Fluids (1994), 2013. **25**(11): p. 110802.

190.   B.W. McCrindle, C.M., K. Sexson, P. Jone, M. Mathew, K. Norozi, K.C. Harris, A. Hughes, A. Ferris, F. Dallaire, A.M. Crean and N. Dahdah for the North American Kawasaki Disease Registry., *Medium-term outcomes of coronary artery aneurysms after Kawasaki disease: A study from the North American Kawasaki Disease Registry*

Circulation, 2015. **131**: p. AO58.

191.   Keedy, A., *An overview of intracranial aneurysms.* Mcgill J Med, 2006. **9**(2): p. 141-6.

192.   Dhar, S., et al., *Morphology parameters for intracranial aneurysm rupture risk assessment.* Neurosurgery, 2008. **63**(2): p. 185-96; discussion 196-7.

193.   Hatakeyama, T., H. Shigematsu, and T. Muto, *Risk factors for rupture of abdominal aortic aneurysm based on three-dimensional study.* J Vasc Surg, 2001. **33**(3): p. 453-61.

194.   Leotta, D.F., et al., *Measurement of abdominal aortic aneurysms with three-dimensional ultrasound imaging: preliminary report.* J Vasc Surg, 2001. **33**(4): p. 700-7.

195.   Dionne, A., et al., *Difference Between Persistent Aneurysm, Regressed Aneurysm, and Coronary Dilation in Kawasaki Disease: An Optical Coherence Tomography Study.* Can J Cardiol, 2018. **34**(9): p. 1120-1128.

196.   Tsujii, N., et al., *Late Wall Thickening and Calcification in Patients After Kawasaki Disease.* J Pediatr, 2017. **181**: p. 167-171 e2.

197.   Takahashi, M., W. Mason, and A.B. Lewis, *Regression of Coronary Aneurysms in Patients with Kawasaki Syndrome.* Circulation, 1987. **75**(2): p. 387-394.

198.   Reddy, S.V., Forbes, T.J., Chintala, K., *Cardiovascular involvement in Kawasaki Disease.* Images Paediatr Cardiol, 2005. **7**(2): p. 1-9.

199.   Camera, M., et al., *The Role of Tissue Factor in Atherothrombosis and Coronary Artery Disease: Insights into Platelet Tissue Factor.* Semin Thromb Hemost, 2015. **41**(7): p. 737-46.

200.   Hashimoto, M., et al., *Difference between proximal and distal right coronary flow velocity pattern in humans.* Hiroshima J Med Sci, 1996. **45**(4): p. 105-8.

201.   Cami, E., et al., *Assessment of lesion-specific ischemia using fractional flow reserve (FFR) profiles derived from coronary computed tomography angiography (FFRCT) and invasive pressure measurements (FFRINV): Importance of the site of measurement and implications for patient referral for invasive coronary angiography and percutaneous coronary intervention.* J Cardiovasc Comput Tomogr, 2018.

202.   Abou Sherif, S., et al., *Coronary Artery Aneurysms: A Review of the Epidemiology, Pathophysiology, Diagnosis, and Treatment.* Front Cardiovasc Med, 2017. **4**: p. 24.

203.   Ullah, W.Q., Qamar, K., Butt, S.A., *Wall thickness of major coronary arteries in pakistani population.* Pakistan Armed Forces Med J, 2012. **62**(1).

204.   Aggarwal, A., S. Srivastava, and M. Velmurugan, *Newer perspectives of coronary artery disease in young.* World J Cardiol, 2016. **8**(12): p. 728-734.

205.   Pranjali, R., Sachin, S., *Histology of coronary arteries in relation to coornary stenosis.* J Human Anat, 2018. **2**(2).

206.   Gong, G.W., et al., *Arthritis presenting during the acute phase of Kawasaki disease.* J Pediatr, 2006. **148**(6): p. 800-5.

207.   Blake, G.J. and P.M. Ridker, *Are statins anti-inflammatory?* Curr Control Trials Cardiovasc Med, 2000. **1**(3): p. 161-165.

208.   Brownfoot, F.C., Tu'uhevaha J.K., Hannan, N., Hastie, R., Cannon, P., Onda, K., Tong, S., *[44-OR]: Statins reduce soluble Flt1, and quench endothelial dysfunction in primary human tissues, but increase soluble endoglin release.* Pregnancy Hypertens., 2015. **5**(1): p. 22-23.

209.   Schramm, A., et al., *Targeting NADPH oxidases in vascular pharmacology.* Vascul Pharmacol, 2012. **56**(5-6): p. 216-31.

210.   Huang, S.M., et al., *Effects of statin therapy in children complicated with coronary arterial abnormality late after Kawasaki disease: a pilot study.* Circ J, 2008. **72**(10): p. 1583-7.

211.   Suda, K., et al., *Statin reduces persistent coronary arterial inflammation evaluated by serial (1)(8)fluorodeoxyglucose positron emission tomography imaging long after Kawasaki disease.* Int J Cardiol, 2015. **179**: p. 61-2.

212.   Weis, M., Heeschen, C., Glassford, A.J., Cooke, J.P., *Statins have biphasic effects on angiogenesis.* Circulation, 2002. **105**(6): p. 739-745.

213.   Fukumura, D., Gohongi, T., Kadambi, A., Izumi, Y., Ang, J., *Predominant role of endothelial nitric oxide synthase in vascular endothelial growth factor-induced angiogenesis and vascular permeability.* Proc Natl Acad Sci U S A, 2001. **98**(5): p. 2604-2609.

214.   Doyon, M., et al., *Does atorvastatin induce aortic smooth muscle cell apoptosis in vivo?* Vascul Pharmacol, 2011. **54**(1-2): p. 5-12.

215.   Prasad, K., *Do statins have a role in reduction/prevention of post-PCI restenosis?* Cardiovasc Ther, 2013. **31**(1): p. 12-26.

216.   Liu, Y., et al., *Image quality and radiation dose of dual-source CT cardiac angiography using prospective ECG-triggering technique in pediatric patients with congenital heart disease.* J Cardiothorac Surg, 2016. **11**: p. 47.

217.   Abdolmanafi, A., et al., *Deep feature learning for automatic tissue classification of coronary artery using optical coherence tomography.* Biomed Opt Express, 2017. **8**(2): p. 1203-1220.

218.   Abdolmanafi, A., *Characterization of Coronary Artery Tissues in Kawasaki Disease Using Optical Coherence Tomography (OCT) Imaging.* Abstract presented at the 12th International Kawasaki Disease Symposium, Yokohama, Japan, 2018.